

**BULGARIAN ACADEMY OF SCIENCES  
INSTITUTE OF CHEMICAL ENGINEERING**

---

**Aleksandar Georgiev Georgiev**

**EVALUATION OF MIXED INSTALLATIONS WITH  
ALTERNATIVE ENERGY SOURCES**

**A B S T R A C T**

of a dissertation for the award of a scientific degree "Doctor of  
Science"

Scientific field 4. Natural sciences, mathematics and computer science

Professional field: 4.2. Chemical Sciences

Scientific specialty: Processes and apparatus in the chemical and  
biochemical technology

**Scientific Jury:**

1. Prof. Venko Nikolaev Beshkov, DSc
2. Prof. Georgi Ivanov Valchev, PhD, eng.
3. Prof. Sonia Stoyanova Tabakova, PhD
4. Prof. Ilia Krastev Iliev, PhD, eng.
5. Prof. Aleksei Dimitrov Benderev, PhD
6. Assoc. prof. Tatiana Stefanova Petrova, PhD
7. Assoc. prof. Petar Nikolov Gerginov, PhD

**Sofia 2021**

## *Aleksandar Georgiev*

The dissertation presents an introduction, literature review, goals and objectives, author's research in two chapters, general conclusions, main contributions, bibliography and a list of the author's publications in the full text of the dissertation.

The dissertation contains 345 pages, including 201 figures and 29 tables. The bibliography covers 229 sources. The list of author's publications in full text on the topic presents 36 articles. Of these, 15 are in journals with an impact factor for the year, 11 have been published in specialized international journals or in full in collections of international scientific forums with editor and publisher, and 15 have been published in the last 5 years (2016 - 2020). The author of the dissertation is in first place in 17 of the publications. The presented publications have been cited a total of 244 times.

The author of the dissertation works as a professor at the Institute of Chemical Engineering - BAS (ICE - BAS).

The dissertation was discussed by the Colloquium of ICE-BAS for opening a procedure for defense at a meeting held on 04.11.2021 (Minutes №4/ 4.11.2021) and with a decision of the Scientific council of IEES-BAS from 11.11.2021 (Minutes № 14/ 11.11.2021) a dissertation defense procedure has been opened. At a meeting of the Colloquium of ICE-BAS on 25.11.2021 (Minutes №7/ 25.11.2021) preliminary defense was carried out and with a subsequent decision of the Scientific council of IEES-BAS from 15.12.2021 (Minutes №16/ 15.12.2021) a Scientific Jury was elected consisting of:

1. Prof. Venko Nikolaev Beshkov, DSc (ICE, BAS) (internal member)
2. Prof. Georgi Ivanov Valchev, PhD, eng. (University of Food Technologies, Plovdiv)
3. Prof. Sonia Stoyanova Tabakova, PhD (Institute of Mechanics, BAS)
4. Prof. Ilija Krastev Iliev, PhD, eng. (University of Ruse)
5. Prof. Aleksei Dimitrov Benderev, PhD (Geological institute, BAS)
6. Assoc. prof. Tatiana Stefanova Petrova, PhD (ICE, BAS) (internal member)
7. Assoc. prof. Petar Nikolov Gerginov, PhD (Geological institute, BAS)

### Reserves:

1. Prof. Dragomir Simeonov Yankov, PhD (ICE, BAS) (internal member)
2. Assoc. prof. Angel Kostadinov Terziev, PhD, eng. (TU Sofia)

The defense of the dissertation will take place at 2pm on 11.03.2022 in the Conference room of ICE - BAS, Acad. G. Bonchev Str, bl. 103, Sofia.

**C O N T E N T**

<b>Introduction.....</b>	<b>4</b>
<b>1. Main conclusions from the literature review.....</b>	<b>5</b>
<b>2. Goals and objectives of the dissertation.....</b>	<b>7</b>
<b>3. Components of mixed installations with alternative energy sources (AES) .....</b>	<b>8</b>
<b>3.1. Vacuum solar collector with flat-plate absorber and heat pipe.....</b>	<b>8</b>
<b>3.2. Thermal storages.....</b>	<b>13</b>
<b>3.2.1. Mixed water storage with stratification.....</b>	<b>13</b>
<b>3.2.2. Water storage with four turn pipe windings.....</b>	<b>14</b>
<b>3.2.3. Thermal response test (TRT) of seasonal Underground thermal energy storages (UTES).....</b>	<b>15</b>
<b>3.2.4. Latent thermal storage (LTS) with phase change materials (PCM).....</b>	<b>24</b>
<b>4. Mixed installations with alternative energy sources (AES).....</b>	<b>29</b>
<b>4.1. Solar collectors with water storage.....</b>	<b>29</b>
<b>4.2. Refrigeration installation with built-in solar collectors and thermal storage.....</b>	<b>34</b>
<b>4.3. Borehole thermal energy storage (BTES) with solar collectors.....</b>	<b>35</b>
<b>4.4. Photovoltaic-thermal (PV/T) installations.....</b>	<b>38</b>
<b>4.5. Ground source heat pump (GSHP) system with solar collectors.....</b>	<b>44</b>
<b>4.6. Ground source heat pump (GSHP) installation using phase change materials (PCM).....</b>	<b>57</b>
<b>4.7. Mixed micro-cogeneration system with photovoltaic panels and Stirling engine for local heating.....</b>	<b>60</b>
<b>5. General conclusions.....</b>	<b>61</b>
<b>6. Main contributions.....</b>	<b>63</b>
<b>7. Author’s publications in the full text of the dissertation.....</b>	<b>65</b>

## INTRODUCTION

The dissertation covers a long time period (over 30 years - the earliest attached article was published in 1989). After completing my doctoral dissertation in 1988 I deal exclusively in the field of Renewable Energy Sources (RES), mainly in their thermal engineering part. Since the beginning of the century (2001), this topic has become a top priority in the European Community (EC). A law has been introduced for member states to double over the next 10 years energy production from renewable sources. In 2011 the next EC law was introduced - to increase to 25% the production of energy from renewable sources in the member states (then this quota was changed for different countries, for Bulgaria it was 16%). The trend is in 2050 about 60% of the energy produced in the EC is from renewable sources.

Bulgaria also pays attention to this energy sector. The first solar installations (flat plate solar collectors with their associated storages) were installed and used on the Black Sea coast in the early 80s of last century. Then in Sofia a plant "New Energy Sources" was established, which began production of various systems related to renewable energy. An institute was established at the plant, and some doctoral students in RES started working at the Technical University of Sofia. Some plants started production of elements from these installations (solar collectors were produced in the aluminum plant in Shumen, and in Razgrad began production of various components of these systems). Immediately after the change in 1989 there was a boom in this production (unfortunately unsuccessful because everyone wanted to produce something attractive, but in most cases unrealistic). Fortunately, after Bulgaria's accession to the EC, there was another boom, this time successful and adequate, as solar panels for electricity production and wind generators were widely installed in the country.

To date, renewable energy sources are already quite common and known in Bulgaria. Here, however, comes the question of whether the sources are "New" (as the plant was called), "Renewable" or simply "Alternative". These sources are definitely not "New" because the main one is the Sun. The extent to which each of them is "Renewable" is also a moot point (especially with regard to the installations that serve them). But the "Alternatives" are attractive at the moment, because they include RES, and on the other hand, according to some of their parameters, we can include other materials (not only RES). An elementary example - biomass is not renewable (in terms of disappearing after use), but it is renewable in terms of being available again in the next 1 to 20 years. At the same time, paraffins (as an attractive representative of phase change materials, PCM) are produced from petroleum, i. e. they are not renewable. But they usually have melting/ solidification cycles over 200 times, which ranks them well in the field of renewable energy.

The dissertation is based on articles published in various fields of RES (from solar collectors and installations, to geothermal installations and systems with PCM). Over the years I have worked with many teams (most of them foreign) and in different countries (mostly in Germany and Chile - about 3 years in total). As a result, there are studies of many different mixed installations with RES and their components. Many of them are described in the dissertation and an assessment is made of how effective and advanced-garde they are. Here I must note that the attached bibliography, as well as all the presented experiments and studies are strictly up to date as of the date of publication of the articles. Over the years (and this is more than 30 years) there have been changes, during which certain topics are already quite developed and not as advanced-garde as in the beginning. I draw attention to this fact so that there is no doubt in the evaluation of some of the contributions mentioned at the end of the dissertation.

As almost all presented articles are in Latin (German or English), there is a mixture of Cyrillic and Latin in the indexes. Separately, I have left almost all the figures in their original form (in Bulgarian or English). The same applies to the abbreviations (some of them still have no analogues in the Bulgarian language, while others are perceived by specialists in their original form).

## **1. MAIN CONCLUSIONS FROM THE LITERATURE REVIEW**

The heating system is a unit that consists of several components. The unit contains not only thermal elements - there are also electrical and mechanical parts. Usually the term "mixed installation" refers to at least two types of installations. They contain elements such as phase change materials (PCM), heat pump, solar collectors, water seasonal accumulator and underground thermal energy storage that can be combined with electrical appliances (e.g. photovoltaic/ thermal, PV/T collectors) and a second heat pump in order to improve the energy efficiency of the system.

Based on the presented literature review, the following main conclusions can be made for the individual components, as well as for the different types of mixed installations with alternative energy sources:

- The different types of solar collectors presented in the review (flat-plate solar collectors, vacuum liquid solar collectors, air heating solar collectors and concentrating solar collectors) have different advantages and disadvantages related to both their technical characteristics and their economic realization. The relatively high values of efficiency at high temperature differences allow the efficient use of vacuum solar collectors when reaching high temperatures of the brine;

- Existing thermal storages are divided into devices that store sensible and latent (hidden) heat on the one hand, and thermal storages on a daily or seasonal (3 to 6 months) basis on the other hand. The mixed water storage of sensible

heat with stratification is interesting for practice due to the presence of different temperatures in the height of the accumulator. Underground storages (especially the Borehole Thermal Energy Storage, BTES) play an essential role in seasonal thermal storage, as an important element is not only their design, but also experimental ways to determine the thermal properties of the soil around them and methods for processing of the received data. Latent storages are currently one of the most promising technologies for heat accumulation. Their development is in two directions - the use of appropriate materials and the choice of design that ensures good heat transfer. The different way of modeling, as well as the subsequent simulations lead to a better study of the respective storage;

- The literature review covers solar installations that are used for production of domestic hot water (DHW) and heating. Installations comprising vacuum solar collectors with a heat pipe and a suitable storage may, under certain conditions, reach a temperature of more than 100 °C of the heated fluid;

- The annual period of operation of solar systems is extended if they are connected to the evaporator of a heat pump system. Thus, the so-called solar-assisted heat pump (SAHP) systems are of interest for research and implementation in practice;

- Several types of underground storages are used in practice. The most attractive of them is BTES due to its versatility and independence from the environment. It uses the earth not only as a source of energy, but also as a thermal storage, which is charged e.g. from solar collectors;

- The photovoltaic/ thermal (PV/T) panel is a mixture of photovoltaic cells and a solar thermal collector. This combination reduces the operating temperature of photovoltaic cells and increases their efficiency, and additionally produces thermal energy. Despite the great design diversity of this type of panels, it is necessary to emphasize the detailed study (experiments with precise measurement and proper processing of results) not only those with the most elementary structure, but also PV/T panels with larger efficiency (e. g. PV/T collector with concentrator);

- Ground source heat pump (GSHP) systems are using the ground as a source of heat or cold and transfer the received energy to a higher level through the heat pump for heating or cooling. Such an installation combined with solar collectors can operate in different modes (e. g. charging the water storage or the borehole thermal energy storage, heating buildings using the heat pump powered by the underground storage or solar collectors, and cooling with the heat pump unit). The simulation of the described processes is also of great practical interest;

- There are different types of GSHP systems using PCM - solar domestic hot water system with mixed storage installation, latent thermal storages connected to heat pumps and solar heating systems, mixed heating system with renewable energy sources (RES), combined with latent thermal storage and heat

pump, etc. It is worth noting that the GSHP system using micro-encapsulated PCM is studied, with an emphasis on simulation;

- Cogeneration systems (CHP), which produce both heat and electricity, are attractive on various scales. Micro-cogeneration systems with photovoltaic panels and a Stirling engine for local heating are suitable for powering individual buildings located in rural or remote areas, and the combination of different RES has not yet been well studied.

The above conclusions from the literature review are valid until the publication of the results presented in the dissertation.

## **2. GOALS AND OBJECTIVES OF THE DISSERTATION**

As a result of the literature review and the main conclusions from it, the **main goal** of this paper is defined:

Research and evaluation of different types of mixed installations based on alternative energy sources, as well as their main components.

The following **main tasks** are solved in the dissertation (they are different for the specific components and systems):

### **1. Vacuum solar collector with flat-plate absorber and heat pipe**

- mathematical modeling of a vacuum collector with a flat-plate absorber and a heat pipe;
- programming of the mathematical model;
- performing simulations;
- experimental tests of a vacuum collector with a heat pipe.

### **2. Thermal storages**

- mathematical modeling and testing of a mixed water storage with stratification;
- mathematical modeling of a water storage with four turn pipe windings and performing experiments;
- Thermal response test (TRT) of seasonal Underground thermal energy storages (UTES) including construction of installations, conducting experiments, data processing with different methods, performing simulations;
- study of a latent storage with paraffin as a phase change material (PCM) including design, construction, modeling and simulations.

### **3. Vacuum solar collectors with water thermal storage**

- experimental study of the installation with vacuum solar collectors and water thermal accumulator;
- mathematical modeling;
- programming of the mathematical model;
- comparison of the calculated with the experimental data.

### **4. Refrigeration installation with built-in solar collectors and thermal storage**

- creation of methods for calculating the main thermal parameters of the system;

- performing sample calculations.

#### **5. Borehole thermal energy storage (BTES) with solar collectors**

- design and construction of the BTES installation;
- experimental study during charging and discharging;
- performing simulations.

#### **6. Photovoltaic-thermal (PV/T) installations**

- construction of PV/T installations;
- conducting experiments with PV/T installations;
- processing of the experimental results.

#### **7. Ground source heat pump (GSHP) system with solar collectors**

- construction of GSHP system with solar collectors;
- creation of investigation methods;
- conducting experiments;
- TRNSYS simulations of a house powered by GSHP with solar collectors.

#### **8. Ground source heat pump (GSHP) installation using phase change materials (PCM)**

- creation of methodology;
- modeling;
- conducting simulations.

#### **9. Mixed micro-cogeneration system with photovoltaic panels and Stirling engine for local heating**

- construction of an experimental system;
- conducting experiments

### **3. COMPONENTS OF MIXED INSTALLATIONS WITH ALTERNATIVE ENERGY SOURCES (AES)**

#### **3.1. VACUUM SOLAR COLLECTOR WITH FLAT-PLATE ABSORBER AND HEAT PIPE**

##### **3.1.1. Characteristics of a vacuum collector with a flat-plate absorber and heat pipe**

We consider the calculation of a vacuum solar collector with a heat pipe. The differential equation, which is the basis of the calculations, applies to both flat collectors and vacuum solar collectors.

Compared to a flat-plate collector, the collector with heat pipe has an additional heat exchanger - the condenser of the heat pipe. In addition, it is difficult to determine the heat transfer coefficients during boiling and condensation in the heat pipe. Difficulties also arise in the iterative determination of the temperature of the glass tube  $t_{mn}$ , the absorber temperature  $t_{a6}$  and the temperature of the working fluid in the heat pipe  $t_{pc}$ .



## *Evaluation of mixed installations with alternative energy sources*

The calculation of the solar radiation in the plane of the collector is based on the change of the total solar radiation  $I_{\text{хор, об}}$  and the diffuse radiation  $I_{\text{хор, диф}}$  on a horizontal plane.

### **3.1.1.1. Vacuum solar collector with heat pipe KL VR 140**

The collector type KL VR 140 is an example of a vacuum solar collector with a heat pipe. The conversion of radiation into heat energy takes place through a black absorbent surface, which is located in a glass tube from which air is drawn. The surface of the absorber consists of copper with a selective coating of black chrome. A heat pipe is welded to the absorber. In this heat pipe the absorbed heat is transferred to the water/ glycol mixture in the circuit of the solar collectors due to the evaporation-condensation process.

The evaporation zone extends to the end of the absorber. Between the condenser and the absorber is the adiabatic zone. The vacuum solar collectors are assembled in modules of 20 to 30 pieces (Fig.3.1). The condensers are located in a duct, where they flow from the water/ glycol mixture and thus give off the heat generated by the sun.

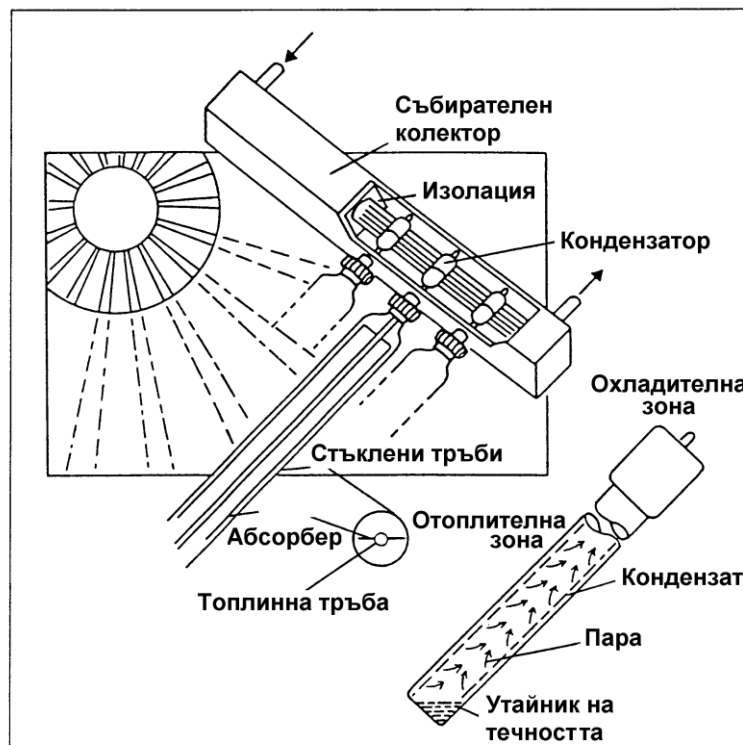


**Fig.3.1.** Sketch of a vacuum collector block

### **3.1.1.2. Differential equation**

The balance equation for a vacuum solar collector with a heat pipe and a flat absorber in the glass tube and a diffuse back reflector is given by the following equation:

$$(3.1) \quad C_{\text{ef}} \frac{\partial t_{\text{фл}}}{\partial \tau} + C_{\text{фл}} \cdot v_{\text{фл}} \frac{\partial t_{\text{фл}}}{\partial x} + \frac{t_{\text{фл}}}{R_{\text{о6}}} = (\tau\alpha)_{\text{ef}} I_{\text{ck,о6}}(\tau) + \frac{t_{\text{ок}}(\tau)}{R_{\text{о6}}}.$$

The solution of this differential equation gives us the temperature of the heated fluid  $t_{\text{фл}}$  along the collector length  $x$  and as a function of time  $\tau$ . Equation (3.1) shows that the effective heat capacity of the collector  $C_{\text{ef}}$ , the heat capacity of the collector fluid  $C_{\text{фл}}$ , the fluid velocity  $v_{\text{фл}}$  and the effective transmittance-absorptance product  $(\tau\alpha)_{\text{ef}}$  are required to determine the fluid temperature. In addition, we must have the change in the total solar radiation in the collector plane  $I_{\text{ck,о6}}$  and the ambient temperature  $t_{\text{ок}}$  as a function of time  $\tau$ . At each time step, the  $(\tau\alpha)_{\text{ef}}$  and the total heat transfer resistance  $R_{\text{о6}}$  are calculated.

### ***3.1.1.3. Sample calculations with a separate block of collectors***

The derived mathematical model was used in the computer program WRVK (in FORTRAN programming language). With the help of the WRVK program, a collector unit manufactured by Klöckner company was theoretically investigated. The technical data of the collector unit were used in the calculation. The following angles are accepted: slope angle  $s = 45^\circ$ , azimuthal angle of the collector block  $\gamma = -29^\circ$  and latitude  $\varphi = 50,87^\circ$  (Siegen, Germany). Water was chosen as the working fluid in the collector circuit, and the thermal properties were adopted at a water temperature of about  $70^\circ\text{C}$ . As the information on the working fluid was quite general (the family of alcohols), its parameters were accepted as the average of several types of alcohol.

The values of the ambient temperature  $t_{\text{ок}}$ , the reflectivity of the back reflector  $\rho_{\text{sp}}$ , the wind speed  $v_{\text{B}}$ , the solar radiation in the collector plane  $I_{\text{ck,о6}}$ , the serial number of the day of the year  $n$ , the inlet temperature of the fluid  $t_{\text{ck,BX}}$  and the mass flow rate of the collector  $\dot{m}_{\text{ck}}$  change in the calculations.

### **Conclusions to Chapter 3.1.1**

A theoretical vacuum solar collector with a heat pipe and a flat absorber was studied. With the help of the created methodology the outlet temperature, the efficiency of the collector and the useful heat flow rate of the collector can be calculated at set values of the input parameters. The following conclusions can be made on the basis of the calculations of some parameters of the collectors with the computer program WRVK:

- The choice of back reflector behind the collectors is very important - a difference of 0,7 in the reflectivity of the back reflector leads to a variation in efficiency by 8 to 10%;

- The efficiency decreases at higher values of the total solar radiation for higher values of the complex factor;

## *Evaluation of mixed installations with alternative energy sources*

- At high temperature differences the efficiency decreases in relation to lower total solar radiation;
- Relatively high values of efficiency at high temperature differences allow the effective use of this type of collector when reaching high temperatures of the saline solution;
- The efficiency of higher total solar radiation increases with increasing mass flow rate of the fluid;
- The density of the useful heat flow rate increases with decreasing difference between the inlet and ambient temperatures  $(t_{\text{ck,BX}} - t_{\text{ok}})$  and with increasing total radiation;
- The volume flow rate  $\dot{v}_{\text{ck}}$  decreases with increasing differences between the outlet and inlet temperatures  $(t_{\text{ck,ИЗХ}} - t_{\text{ck,ВХ}})$  and decreasing total radiation  $I_{\text{ck,о6}}$ .

### **3.1.2. Experimental study of a vacuum collector with a heat pipe**

An experimental study of a vacuum collector with a heat pipe was performed. The active experiment was not used in the study, as the collectors were studied naturally, and the possible measurement days were not sufficient. However, the experimental results were used to create statistical models that describe the collector efficiency  $\eta_{\text{ck}}$  and the useful heat flow rate density  $\dot{q}_{\text{ck}}$ .

During the experiment, the inlet  $t_{\text{ck,BX}}$  and outlet collector temperature  $t_{\text{ck,ИЗХ}}$ , the volume flow rate of a separate block of collectors  $\dot{V}_{\text{ck}}$  (30 vacuum solar collectors) and the meteorological values - ambient temperature  $t_{\text{ok}}$ , wind speed  $v_{\text{B}}$  and total solar radiation in the collector plane were measured  $I_{\text{ck,о6}}$  (Fig.3.2).

Based on the available experimental results, several statistical models were created. The first model (3.2) presents the collector efficiency  $\eta_{\text{ck}}$  as a function of the complex factor  $K = (t_{\text{ck,BX}} - t_{\text{ok}})/I_{\text{ck,о6}}$  at different total solar radiation  $I_{\text{ck,о6}}$  in the collector plane.

$$(3.2) \quad \eta_{\text{c}} = -0,31852 + 1,0195.K + 0,31795 \cdot 10^{-2} \cdot I_{\text{ck,о6}} - 0,78993 \cdot 10^{-2} \cdot K \cdot I_{\text{ck,о6}} + 1,815 \cdot K^2 - 0,22685 \cdot 10^{-5} \cdot I_{\text{ck,о6}}^2.$$

The next statistical model (3.3) presents the collector efficiency  $\eta_{\text{ck}}$  as a function of the temperature difference  $\Delta t = (t_{\text{ck,BX}} - t_{\text{ok}})$  at different total solar radiation in the collector plane.

$$(3.3) \quad \eta_{\text{ck}} = 0,055933 - 0,96751 \cdot 10^{-2} \cdot \Delta t + 0,15987 \cdot 10^{-2} \cdot I_{\text{ck,о6}} - 0,81596 \cdot 10^{-5} \cdot \Delta t \cdot I_{\text{ck,о6}} + 0,13228 \cdot 10^{-3} \cdot \Delta t^2 - 0,63772 \cdot 10^{-6} \cdot I_{\text{ck,о6}}^2.$$

The efficiency of the collector  $\eta_{\text{ck}}$  is a function of the total solar radiation in the collector plane  $I_{\text{ck,о6}}$  at three different flow rates  $\dot{m}_{\text{ck}}$ :

$$(3.4) \quad \eta_{ck} = -0,12506 - 1,187 \cdot \dot{m}_{ck} + 0,18257 \cdot 10^{-2} \cdot I_{ck,об} + 0,24746 \cdot 10^{-2} \cdot \dot{m}_{ck} \cdot I_{ck,об} + 9,8986 \cdot \dot{m}_{ck}^2 - 0,12308 \cdot 10^{-5} \cdot I_{ck,об}^2.$$

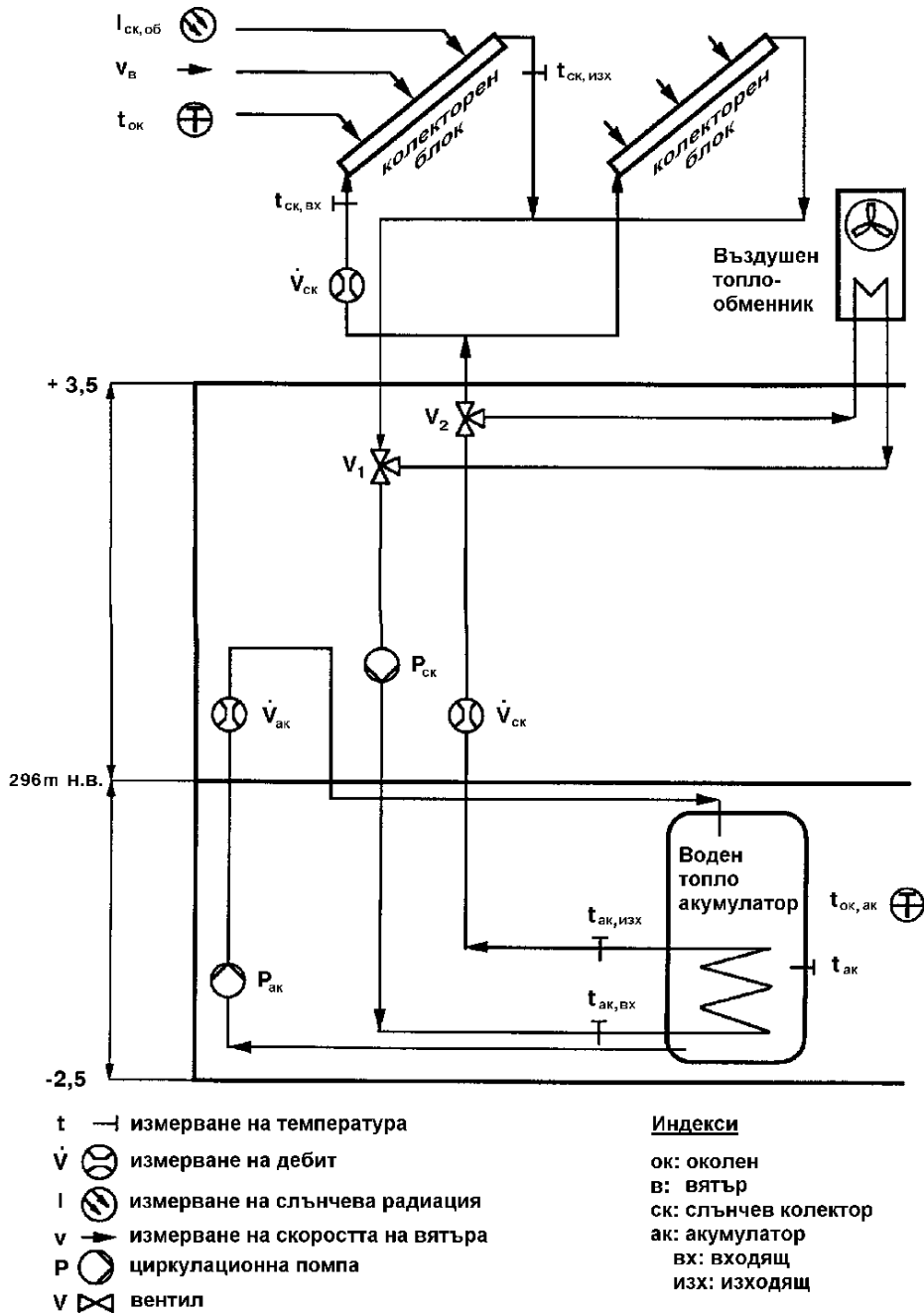


Fig.3.2. Layout and measurement plan of the test facility “vacuum solar collectors - warm water storage”

The last model (3.5) gives us the relationship between the density of the useful heat flow rate  $\dot{q}_{ck}$  and the total solar radiation in the collector plane  $I_{ck,об}$  at different temperature differences  $\Delta t = (t_{ck,вх} - t_{ок})$ .

$$(3.5) \quad \dot{q}_{ck} = -89,581 - 1,6968 \cdot \Delta t + 0,76553 \cdot I_{ck,06} - \\ - 0,93025 \cdot 10^{-2} \cdot \Delta t \cdot I_{ck,06} + 0,54337 \cdot 10^{-1} \cdot \Delta t^2 + 0,24139 \cdot 10^{-3} \cdot I_{ck,06}^2.$$

The factors involved in equations (3.2 to 3.5) are in the following range:

$$K \in [0,01; 0,15] \text{ m}^2\text{K/W};$$

$$I_{ck,06} \in [200; 900] \text{ W/m}^2;$$

$$\Delta t \in [5; 60] \text{ }^\circ\text{C};$$

$$\dot{m}_{ck} \in [0,01; 0,11] \text{ kg/s}.$$

### **Conclusions to Chapter 3.1.2**

Four statistical models were created, describing a vacuum solar collector with a heat pipe and a flat absorber, studied experimentally. The following conclusions can be drawn from the data obtained:

- This type of solar collectors can be used at high temperatures - at a temperature difference  $\Delta t = (t_{ck,BX} - t_{ok}) = 50 \text{ }^\circ\text{C}$  we still have the efficiency of the collector  $\eta_{ck} = 0,5$  (at  $I_{ck,06} = 700 \text{ W/m}^2$ );

- At higher flow rate  $\dot{m}_{ck}$  the efficiency of the collector increases.

## **3.2. THERMAL STORAGE**

### **3.2.1. Mixed water storage with stratification**

To calculate the temperature of the fluid in the individual layers of the mixed water storage with stratification, a program block AKIM in algorithmic language FORTRAN-77 has been created. It is based on a model of simple differential equations.

The following input data is set during the program execution:

1. Constructive:

- thickness of the insulation layer - 0,1 m;

- number of layers - 10;

- storage volume - 0,32 m<sup>3</sup>;

- full surface of the storage - 2,93 m<sup>2</sup>.

2. Thermal (thermal conductivity):

- on the first attempt - 0,630 W/mK;

- on the second attempt - 0,615 W/mK.

3. Mass flow rates through the storage on the charge and discharge side:

- on the first attempt - 0,79 kg/s;

- on the second attempt - 0,96 kg/s.

4. Initial fluid temperature in the layers of the storage: 18 °C;

5. Initial ambient temperature:

- on first attempt - 22 °C;

- on second attempt - 20 °C.

As a result of the operation of the program, the temperatures of the fluid in the different layers of the storage at any time, as well as the inlet storage temperatures are obtained. The standard DVERK subroutine from the ISML package was used to solve the system of differential equations.

The verification of the reliability of the model was made with the help of natural experiments of water mixed storage AB-320, included in the structural scheme of the energy conversion system solar collectors - heat pump - consumer.

### **Conclusions to Chapter 3.2.1**

The use of the AKIM program block, based on the verified mathematical model, allows to simulate the processes in liquid mixed storages of different sizes when there are no experimental data. The number of set layers can be arbitrary. The results obtained will correspond with sufficient reliability to the actual ones.

### **3.2.2. Water storage with four turn pipe windings**

The TBS-Isocal SEB 600 storage is an example of a water storage with four turn pipe windings. The accumulator consists of an insulated, vertically arranged cylindrical tank containing two heat transfer coils.

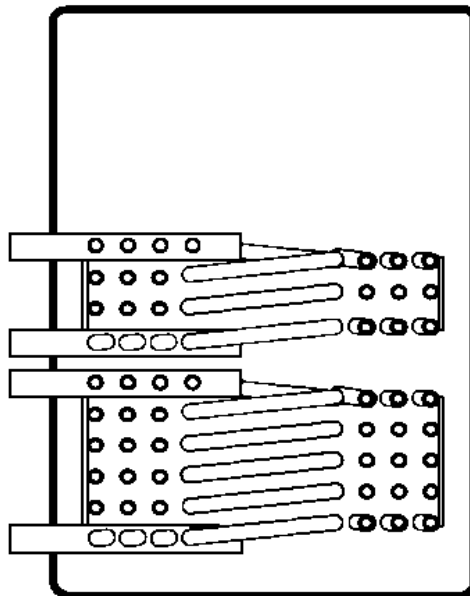


**Fig.3.3.** Scheme of a water storage with four turn pipe windings

A detailed methodology for the mathematical description of a water thermal storage has been created. Two differential equations describe the change in the outlet fluid temperature from the coil and the temperature of the working fluid in the storage as a function of time  $\tau$ . The solution of the differential equations leads to the determination of these two temperatures.

The energy balance for a homogeneous storage without stratification (Fig.3.3) is set by the following equation (if the heat exchange from the upper to the lower layer is neglected):

$$(3.6) \quad \frac{\partial(m_{ak} \cdot h_{ak})}{\partial \tau} = \dot{Q}_{ak} + \dot{Q}_{cr} + \dot{Q}_{tp},$$

where  $\dot{Q}_{cr}$  and  $\dot{Q}_{tp}$  are outlet, and  $\dot{Q}_{ak}$  - inlet heat flow rates for the storage.

$m_{ak}$  - storage fluid mass, kg;

$h_{ak}$  - specific storage fluid enthalpy, J/kg;

The computer program "Speicher" of Fortran-77 was created in order to describe the ongoing processes in the storage. With this program, calculations were made to determine the outlet brine storage temperature  $t_{ak,изх}$  and the temperature of the fluid in the storage  $t_{ak}$ . The calculated values were then compared with the experimental results for 13.10.1992.

The calculations made with the model are compared with the experimental results of the same storage. Comparisons show a good match.

### **Conclusions to Chapter 3.2.2**

The outlet fluid storage temperature  $t_{ak,изх}$  and the fluid temperature in the storage  $t_{ak}$  can be calculated using the presented methodology if values of the inlet fluid storage temperature  $t_{ak,вх}$  are available.

The following conclusions from the study are required:

- The calculation of the fluid temperature in the storage  $t_{ak}$  and the outlet fluid storage temperature  $t_{ak,изх}$  over time with the computer unit "Speicher" shows a good match of the calculated and measured values;
- The proposed model is valid for a water storage with four turn pipe windings with the possibility to use other operating media.

### **3.2.3. Thermal response test (TRT) of seasonal Underground thermal energy storages (UTES)**

#### **3.2.3.1. Installation for TRT**

##### *3.2.3.1.1. Built stationary installation in Chile*

The installation was constructed on the territory of the experimental field "Solar Energy Laboratory" of the Technical University Federico Santa Maria (UTFSM), Quilpue. The schematic diagram of the setup is shown in Fig.3.4.

In 2002 three perforations were made along a line to a depth of about 22 m. The soil at the site consists of three main layers. The central perforation is a borehole with a depth of 16,9 m and a diameter of 15 cm. The borehole was subsequently grouted with a 12% bentonite mixture (commercial mane Max Gel, produced in Federal Summit, Houston, TX). In the center of the BHE four

thermocouples of type K (Chromel/Alumel) were mounted at depths of 16,9, 10,7, 3,24 and 0,25 m. Two additional perforations were realized, one 0,4 m to the left of the BHE, the other 0,8m to its right. Thermocouples of type K were also installed in these perforations at depths of 20,5, 13,67, 6,84 and 0,25 m. These perforations were filled up again with the same soil.

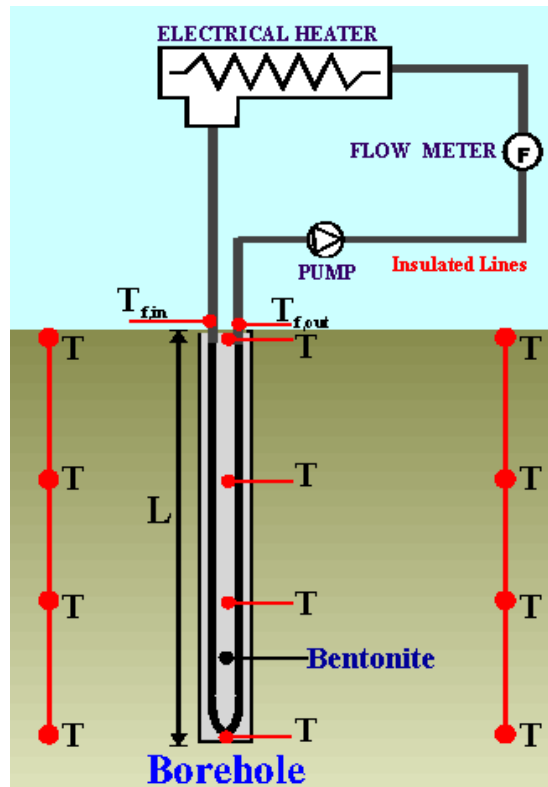


**Fig.3.4.** Scheme of the test installation situated in the Solar Energy Laboratory of the UTFSM, Valparaiso, Chile

### *3.2.3.1.2. Mobile installation with electric heater for conducting TRT in Bulgaria*

The scheme of the equipment of this system is given in Fig.3.5. The main components of the system are the circulation pump, buffer tank, electric boiler for water heating, thermometer, manometer, heat meter and sensors for monitoring the parameters of the heat carrier (water).

### *3.2.3.1.3. Mobile installation with heat pump for conducting TRT in Spain*

Two different methods have been developed: one using electric heating elements and another using a reversible heat pump (heat can be supplied to and from the ground here).

The mobile TRT installation, implemented at the Polytechnic University of Valencia (UPV), contains a reversible heat pump. This is a new generation in the implementation of TRT – it can work in both heating (extraction of energy from the ground) and cooling (injection of energy to earth).



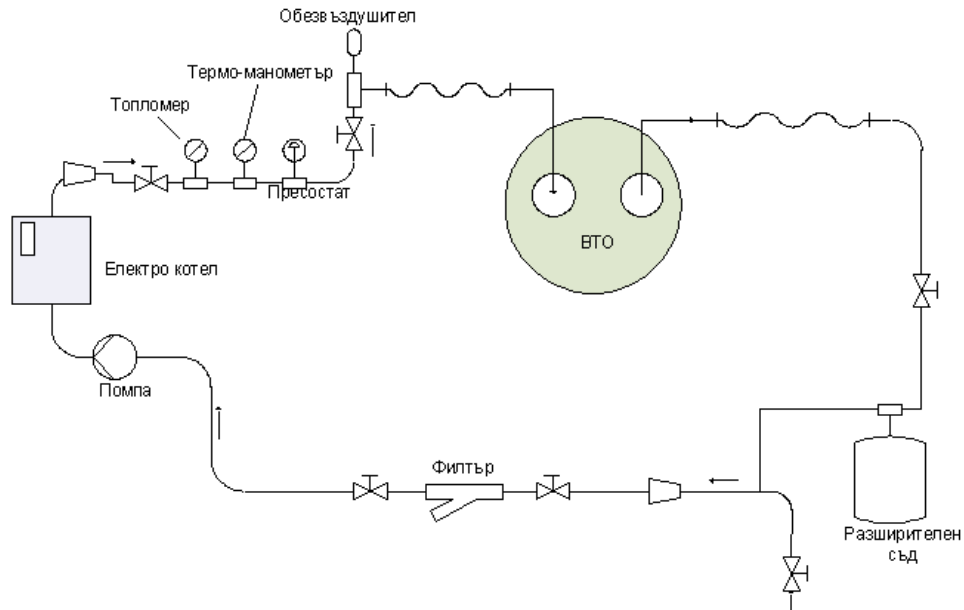


**Fig.3.5.** Schematic diagram of the installation for TRT conducting in Plovdiv, Bulgaria

### **Conclusions to Chapter 3.2.3.1.3**

The mechanical part and the control system from an experimental platform for conducting TRT test, based on the concept of Henk Witte from Holland Groenholland, were presented. We can make the following main conclusions after the work done:

- The main difference compared to most other systems is that the experimental apparatus described here maintains a fixed temperature difference between the BHE input and output;
- Scientists from some countries (e. g. Sweden), who used an electric heater before in the installation, prefer and later built (in 2004) a mobile experimental platform with a heat pump;
- The Line source model (LSM), which is an easy and convenient method for estimating the thermal properties of the earth, needs a very stable heat output, brought to the BHE (in this case provided by the experimental platform described above).

### **3.2.3.2. Thermal response tests (TRTs)**

#### **3.2.3.2.1. Thermal response test conducted in Chile**

The TRT was carried out over 9 days from 24 June to 3 July 2003. The temperatures measured were - ambient temperature, inlet and outlet borehole temperatures. Additionally, although the flow rate was fixed at the constant value of 3,17 l/min, it was periodically measured and controlled. The electrical power was regulated and maintained constant at about 1000 W. The electrical power of the circulating pump was about 350 W.

Fig.3.6 depicts the time evolution of the variables considered in the data evaluation. The fluctuations in thermal power injected are clearly visible. Some

of the main features exhibited correlate with ambient temperature fluctuation in what is called as “ambient coupling”.

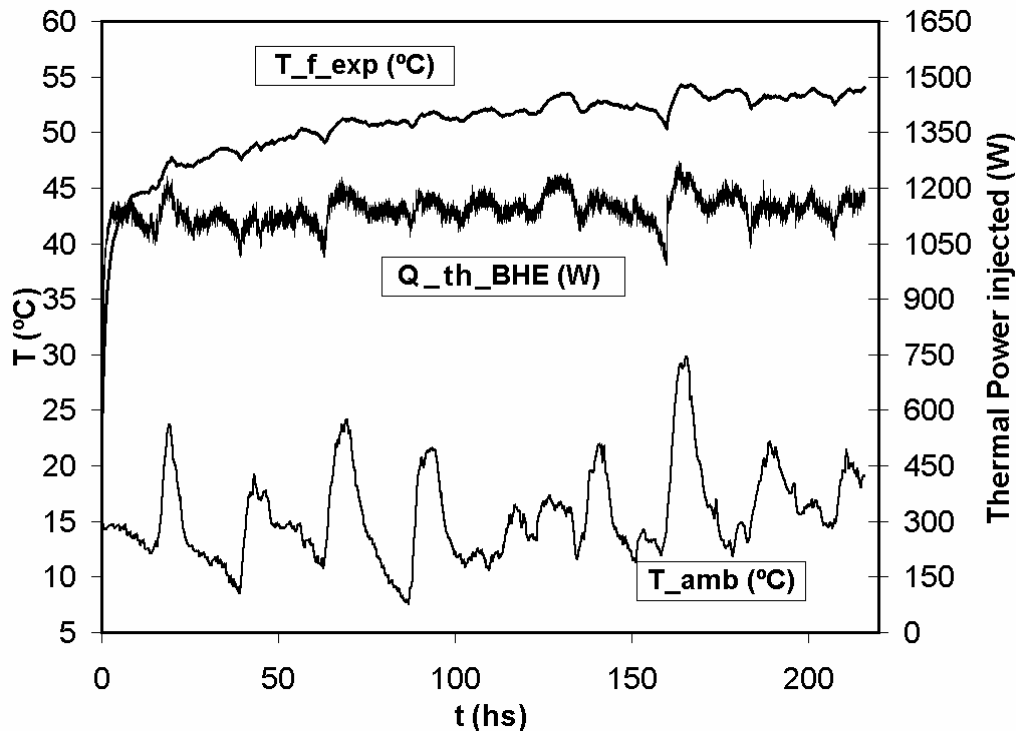


**Fig.3.6.** Time response of the system. Only variables considered in the data evaluation are shown

#### 3.2.3.2.2. Thermal response tests conducted in Bulgaria

Several different TRTs have been built on the territory of TU - Sofia, Plovdiv branch. The first test place was chosen in the yard of block 3 of the Technical University in Sofia, Plovdiv branch. A 180 mm diameter hole was made at a depth of 42 m in November 2008.

The first TRT, 10 days long, was carried out from the 11th to the 21st of January 2009. The measured parameters were the ambient temperature, the inlet and outlet fluid temperatures of the borehole and the temperatures of the BHE at different depths. The flow rate was measured and controlled at the constant value of 6,45 l/min. The electrical power was regulated and maintained constant at about 1500 W. The electrical power of the circulating pump was about 100 W. The water pressure in the installation was maintained at about  $2,2 \cdot 10^5$  Pa. The measuring time step was 60 s. The mean undisturbed ground temperature  $T_{0,m}$  was determined by pumping the heat carrier fluid out of the borehole pipes and measuring its outlet temperature over a time of 10s.  $T_{0,m}$  is then calculated as the mean of the measurement data. In the presented experiments  $T_{0,m}$  has been established to be 16,3 $^{\circ}\text{C}$ .

All data is controlled automatically by a specially designed control system installed on the laboratory trailer. The system is fully automatic and stores all

measured data in text files. In the experiments the aim of a constant heat flow was realized by a constant frequency control of the circulation pump and boiler.

*3.2.3.2.3. Creating a cadastral map in different locations in Bulgaria*

The idea of the team under the leadership of Prof. Aleksandar Georgiev from TU Sofia, Plovdiv branch is to prepare a cadaster of terrestrial thermal properties in Bulgaria. Due to the geological structure, different values can be obtained at different locations. At least 28 thermal response tests must be performed (there are 27 regional centers in Bulgaria with a population of between 60,000 and 400,000 citizens). In addition, more TRTs need to be done in the capital Sofia alone, which has about 2 million citizens. The average values of the thermal parameters collected in the cadaster of terrestrial thermal properties will help the specialists in the field during the preparation of the respective geothermal projects.

**3.2.3.3. Methods for data processing by TRT**

*3.2.3.3.1. Line Source Model (LSM)*

The "Line Source Model" is the most commonly used method for estimating TRT. Below we present the evaluation of several tests conducted in different countries.

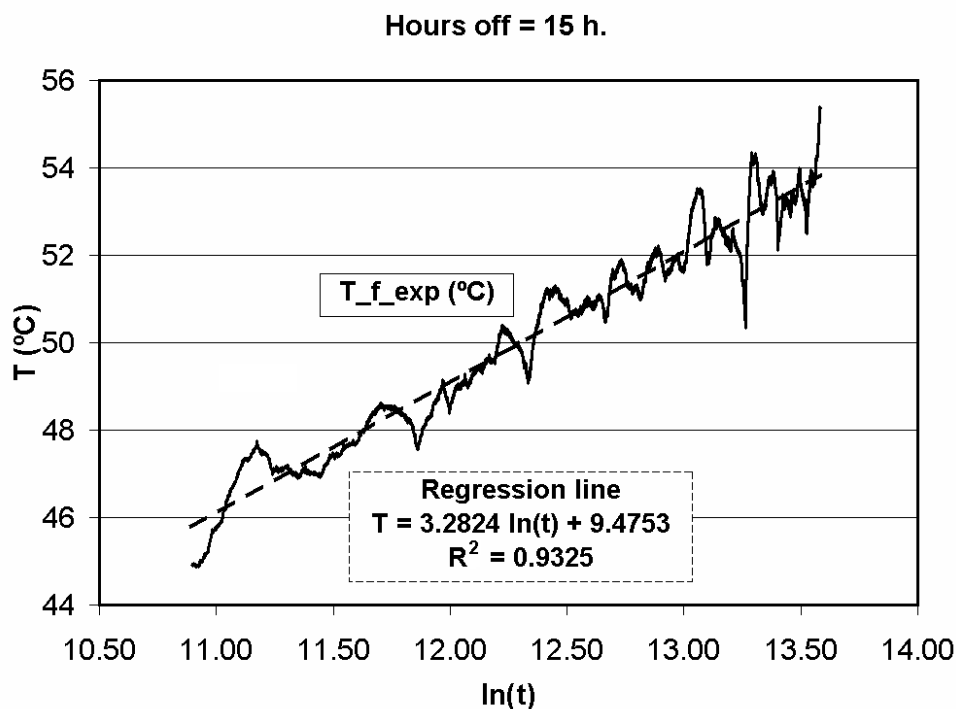


**Fig.3.7.** Logarithmic time plot of the mean fluid temperature

**Evaluation of TRT in Chile**

The thermal conductivity is related to the slope of the obtained line in a logarithmic graph for the time of the mean fluid temperature in the BHE

(Fig.3.7). The resulting values for ground thermal conductivity and BHE thermal resistance are 1,8 W/mK and 0,3 mK/W, respectively.

### Evaluation of TRT in Bulgaria

*Starting point and duration of the analysis of the experiment.* Usually the data corresponding to the first 7 to 24 hours of the experiment are not taken into account in the analysis. Fig. 3.8 (block 3, Technical University of Sofia, Plovdiv branch) shows the average temperature vs the logarithmic time dependence, as well as the slope of the connected regression line (the accepted starting point is 15h).

The thermal conductivity  $\lambda$  is related to the slope of the resulting line. The values obtained during the tests for  $\lambda$  are 1,38 W/mK and for  $R_b$  - 0,314 mK/W (block 3).

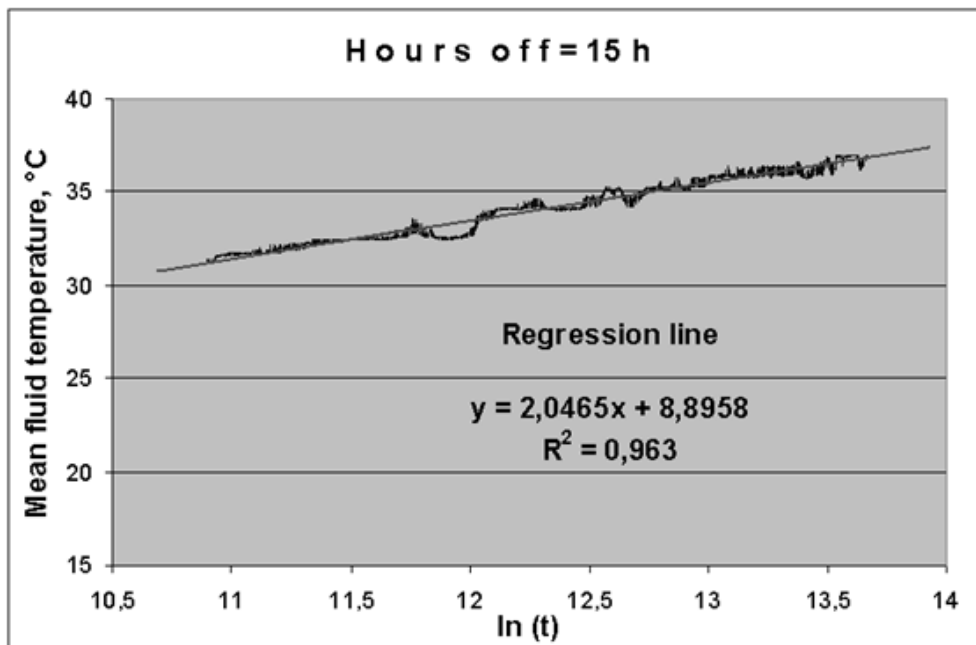


Fig.3.8. Logarithmic time plot of the mean temperature for the entire test length (excluding the first 15 hours)

A comparison was made with the results of various experiments conducted elsewhere in the world. It shows that the values of thermal conductivity and thermal resistance of the BHE obtained from tests in Plovdiv are comparable to the values obtained from other tests.

#### 3.2.3.3.2. Two-variable parameter fitting (TPF)

The "Two-variable parameter fitting" method was used to evaluate the experiment in Chile. Fig.3.9 is a plot of the resulting non-linear fitting curve superimposed to the experimental data (chi square is defined as the sum of the squares of the deviations of the theoretical curve from the experimental points). The inset presents the summary of results with the values of the two variable parameters,  $\lambda = 1,749$  W/mK и  $R_b = 0,299$  mK/W.

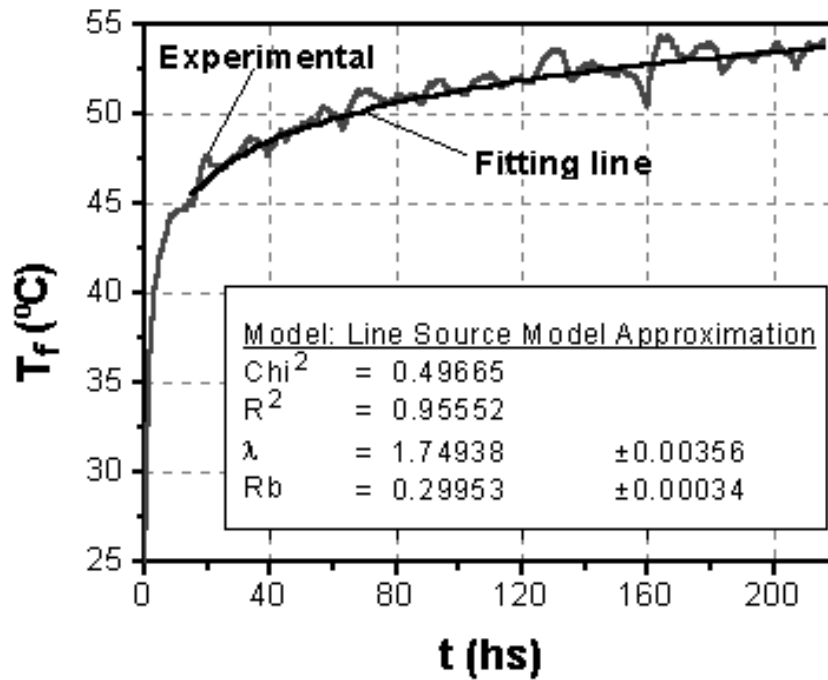


Fig.3.9. Data obtained using the “Two-variable parameter fitting” method

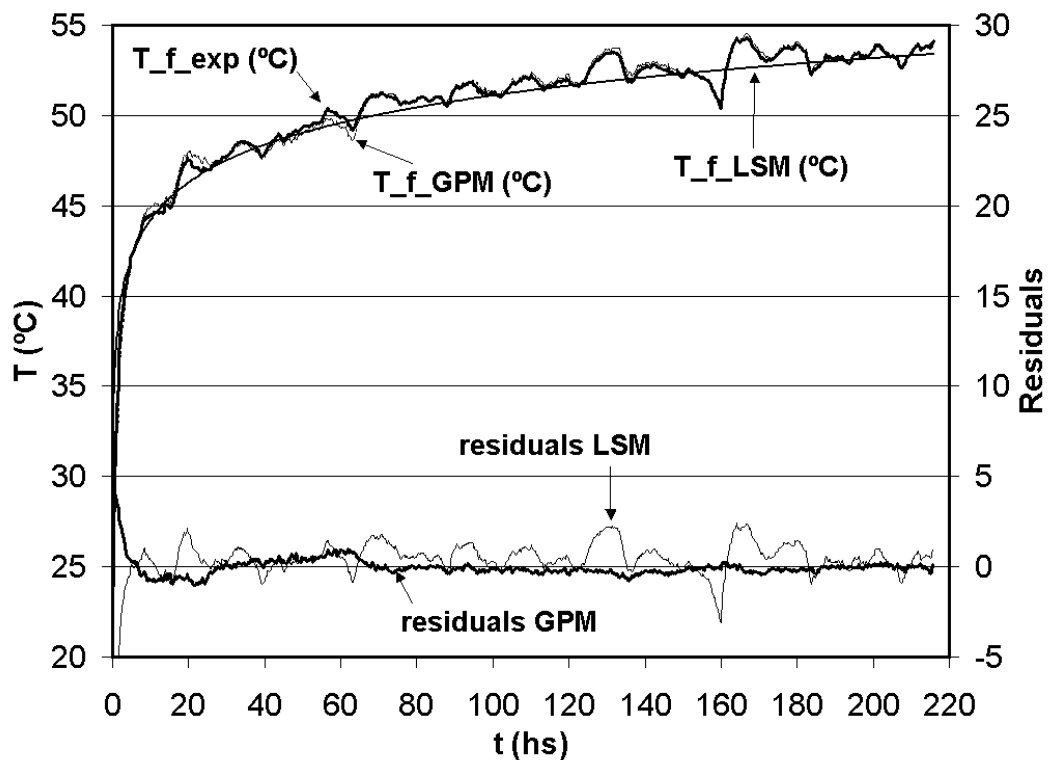


Fig.3.10. System response using  $\lambda$  и  $R_b$  values calculated by GPM program and the LSM method

### 3.2.3.3.3. Geothermal properties measurement (GPM)

A third method, the so-called "Geothermal properties measurement (GPM)", was used to evaluate the experiment in Chile. The results of the analysis using the GPM software are presented in Fig.3.10. The mean fluid

temperature predicted by LSM is superimposed. Owing to the transient nature of the model, the entire data set is used in the analysis. The residuals (absolute errors) between predictions and experimental points are shown in the lower part of the graph with GPM values very close to zero. Relative large absolute errors can be observed during early stages of the test (between 0 and 10 h) possibly due to differences between real BHE response and that predicted by the model. Resulting values for the thermal conductivity and the borehole thermal resistance are 2,35 W/(mK) and 0,32 mK/W, respectively.

The values of ground thermal conductivity  $\lambda$  and BHE thermal resistance  $R_b$ , obtained on the basis of the three methods "Line source model", "Two-variable parameter fitting" and "Geothermal properties measurement", were compared on the basis of data obtained from the TRT in Chile. and are presented in Table 3.1.

**Table.3.1.** Comparison between results using different evaluation methods

Evaluation method	$\lambda$ , W/mK	$R_b$ , mK/ W
Line source model	1,8	0,3
Two-variable parameter fitting	1,749	0,299
Geothermal properties measurement	2,35	0,32

**Conclusions to Chapters 3.2.3.3.1-3.2.3.3.3 (TRT in Chile)**

Based on the results described above, we draw the following conclusions:

- The effective values of 1,8 W/mK and 0,3 mK/W were determined for the thermal conductivity and borehole thermal resistance respectively;
- The application of the classical slope determination and/ or „Two-variable parameter fitting“ can be used as a fast and reliable tool for data evaluation;
- The accuracy of the evaluation depends on the care taken when performing the test. Important aspects are reliable temperature measurements, constant power supply, a proper determination of undisturbed underground temperature and to weather-proof the system as much as possible;
- The value of the thermal conductivity was quite insensitive to the hours-off condition.

**3.2.3.4. TRT simulations**

**3.2.3.4.1. Simulations of TRT in Chile with the TRNSYS program**

The Thermal response test was further studied using TRNSYS TYPE 141 VERTICAL GROUND HEAT EXCHANGER. This subroutine models a vertical heat exchanger that interacts thermally with the ground. The program assumes that the boreholes are placed uniformly within a cylindrical storage volume of ground. There is convective heat transfer within the pipes, and conductive heat transfer to the storage volume. For our particular case of one

BHE, the volume of the storage region was defined as a cylinder of 1 m radius and depth equal to that of the actual BHE. Although TYPE 141 allows several ground layers to be considered, only one layer was assumed for the simulation.

The program was fed with measured data on BHE inlet and outlet fluid temperature as well as ambient temperature. It might be pointed out that outlet fluid temperature was exclusively used for comparison with predicted outlet temperature in graphical presentation of results. Fig.3.11 presents the results of the TRNSYS simulation. The agreement between experimental and TRNSYS simulated outlet temperature is remarkable. The graph also shows energy rates through the boundaries of the storage region and the evolution of the mean storage temperature.

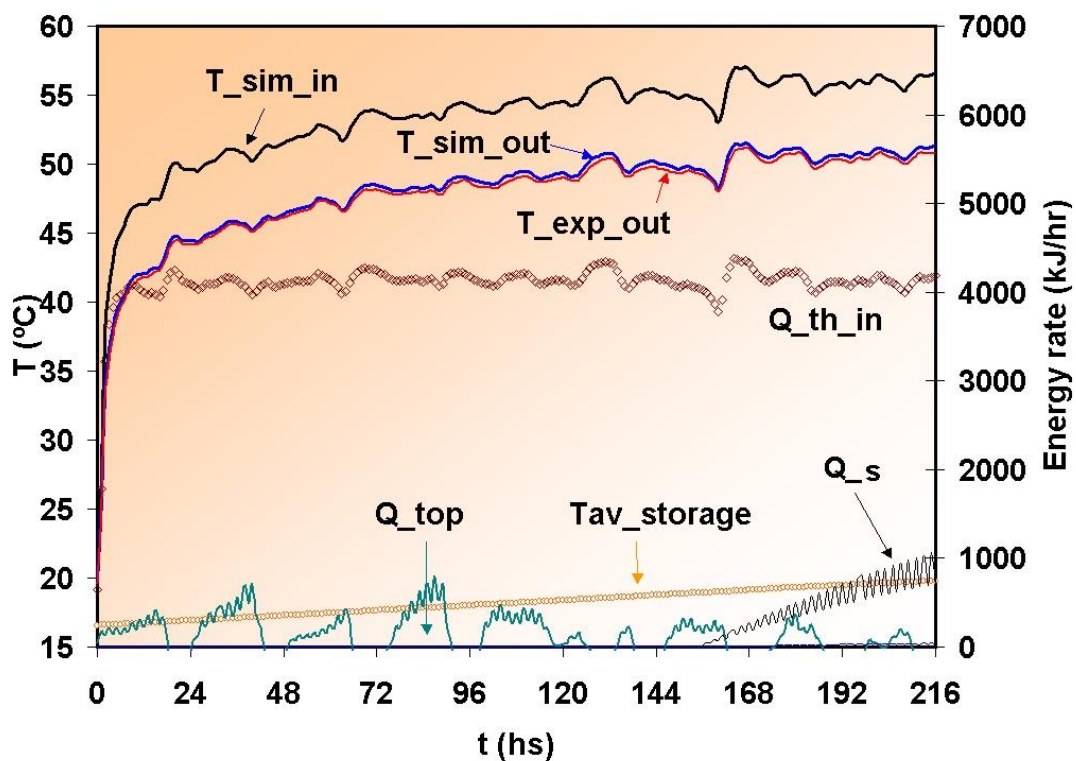


**Fig.3.11.** Comparison of experimental data with simulations made with TRNSYS TYPE 141

#### *3.2.3.4.2. Numerical simulations of TRT in Bulgaria*

Based on the results of the numerical simulation, which is more reliable tool compared to the analytical methods, it is possible to evaluate the temperature field around the borehole heat exchanger (BHE), Fig.3.12. Moreover, the numerical model easily accounts for different heat injection rates by specifying the water temperature at the inlet of the BHE to simulate the process, for instance charging or discharging of the BTES system for a desired time duration. Moreover, the number of the boreholes can be increased up to the desired number of BHE depending on the thermal demand for the users, thus, creating a large scale borehole thermal energy storage.

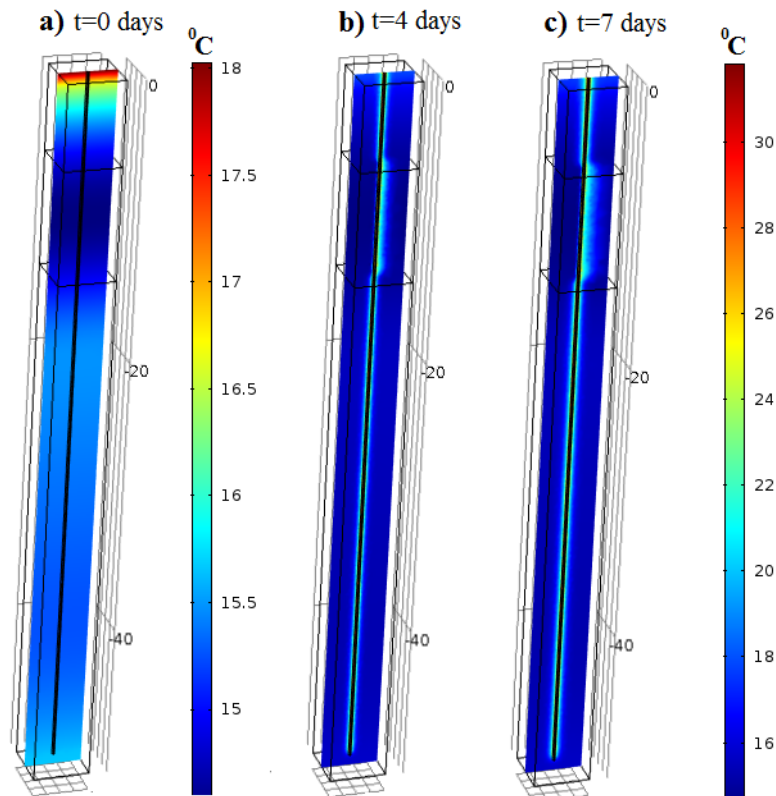


**Fig.3.12.** Temperature distribution at a) the beginning, b) after 4 days and c) after 7 days for the TRT simulation

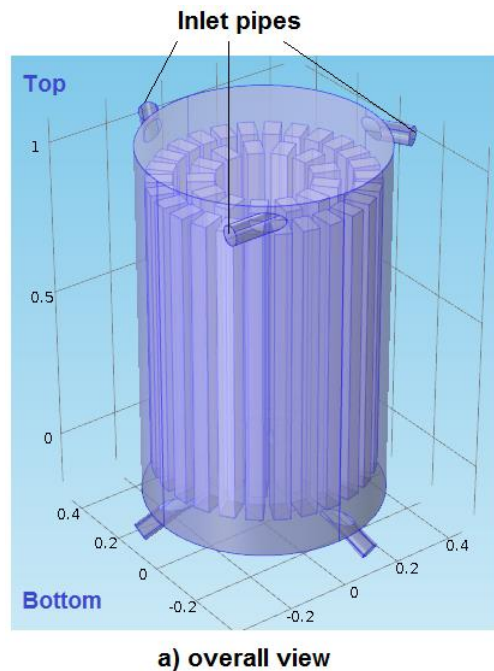


**Fig.3.13.** Construction of the latent thermal storage

### 3.2.4. Latent thermal storage (LTS) with phase change materials (PCM)

#### 3.2.4.1. Construction of a storage with PCM

Prof. A. Georgiev and his team from the Technical University of Sofia, Plovdiv Branch, designed and developed latent thermal storage (Fig.3.13). PCM



containers have rectangular cross section with dimensions 950 x 80 x 50 mm. They are placed into the vertical cylinder tank (storage) with 1 m height and 0,3 m radius. The tank and containers are made of stainless steel grade AISI 304L. Number of PCM containers are 39 and they are located coaxially in the storage. There are two concentric circles: external circle contains 26 containers and the inner circle has 13 containers. All the containers are fixed with brackets to the lower and upper parts of the storage tank in order to make them stable during charging and discharging regimes. There are three inlet pipes in the upper side of the storage where the heat carrier fluid flows into the storage. In the base of the storage other three pipes are connected to the storage to discharge the heat carrier fluid from the storage. The storage is insulated by wrapping with glass wool from the outside.

As a phase change material for the latent heat storage, we used paraffins. Paraffin is considered as effective heat storage material because of its large latent heat of melting (200 kJ/kg or 150 MJ/m<sup>3</sup>), thermal stability, negligible subcooling, non-toxic, and low price. The selection for a specific installation depends mainly on the following main properties: density, kg/m<sup>3</sup>; melting point, °C; specific heat capacity, J/kgK; specific latent heat of fusion, kJ/kg; thermal conductivity, W/mK and volume change, %.

### **3.2.4.2. Numerical modeling of a storage with PCM**

#### **3.2.4.2.1. Numerical modeling of latent thermal storage by means of finite element method based on Comsol multiphysics**

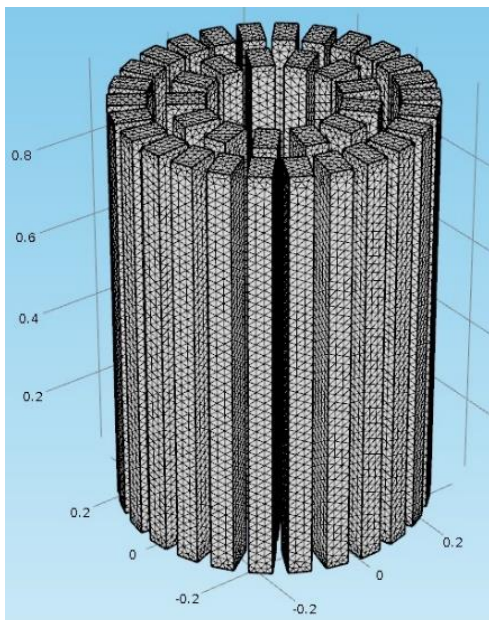


**Fig.3.14.** Meshing of the containers with PCM

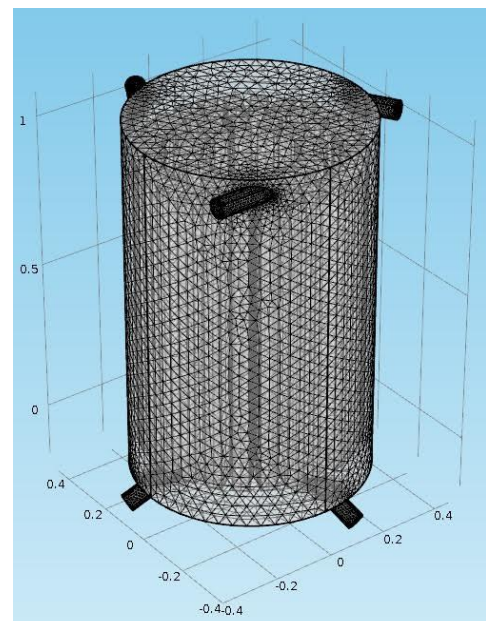


**Fig.3.15.** Meshing of the latent thermal storage

Simulation is conducted in three dimensional space in a time dependent manner by means of finite element method based on Comsol multiphysics. The

geometry used to perform the simulation of charging and discharging of latent storage is presented in Fig.3.13. The containers which contain PCM (e.g. paraffins) are thermally insulated at the top and bottom. Moreover, it is assumed that the volume of the PCM does not change during phase transition. Such assumption, allows to introduce simpler mathematical models, although, according to the experimental investigations, paraffins change their volume during melting or solidification. Moreover, to avoid intensive numerical calculations, the containers are considered as highly conductive layers. Meshing of PCM containers are shown in Fig3.14, and Fig.3.15 shows the meshing of the storage with the containers.

*3.2.4.2.2. Numerical modeling of latent thermal storage by means of the enthalpy porosity technique used in ANSYS Fluent*

The aim of the present work is to develop a fast numerical method for prediction of the thermal behaviour of PCM enclosed in a container with a specific geometry, designed as an active element in a test thermal accumulator at the Technical University Sofia, Plovdiv Branch, Fig.3.16. The working fluid is water entering from three tangential inlet pipes at the top of the tank and leaving from three tangential outlet pipes at the bottom. This device is a part of an experimental thermal solar installation with thermal storage. The typical HTF inlet temperature of the working fluid is 65 °C (from the solar collector) in charging mode, and 15°C (tap water) in discharging mode.

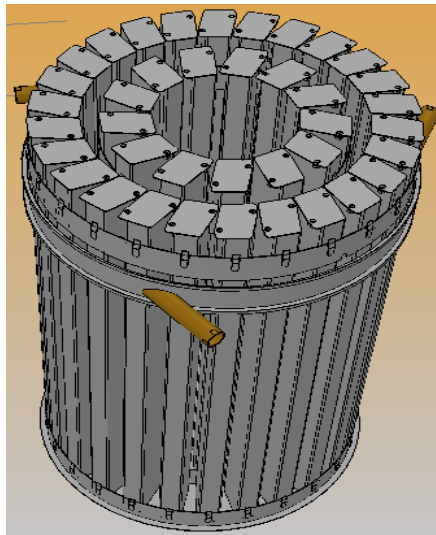


**Fig.3.16.** Inner construction of the latent thermal storage of the experimental thermal solar installation

The purpose of the present numerical simulation is to assess prior to the physical experiment the effect on the phase change process of the following factors: external temperature, convection coefficient of the working fluid and natural convection inside the container.

### **3.2.4.3. Simulations of a storage with PCM**

#### **3.2.4.3.1. Simulations of latent thermal storage by means of finite element method based on Comsol multiphysics**

Three-dimensional transient heat transfer simulations with phase change were performed. The duration of both the charging and discharging simulations lasts three hours, as this is sufficient to perform a heat transfer analysis in the storage.

In Fig.3.17 simulation results are illustrated for the case *a* where only one inlet and one outlet pipe was used for charging process. Moreover, paraffin E46 was considered as PCM in the simulation since it has more thermal stability than other two. Velocity of the heat carrier fluid at the inlet pipe was 0,1 m/s and through the inlet pipe the fluid transferred into the storage 1kJ thermal energy at every second. It can be seen from Fig.3.17a that thermal energy came from the inlet pipe starts to charge the PCM containers which are opposite to the inlet pipe. This is true since heat carrier fluid flows to that area first but after circulation over the PCM containers most part of the fluid flows downward through the center of the storage thus charging coaxially located PCM containers of the inner circle. Main streamlines where actively heat transfer process occurred are shown in Fig.3.17b. After 180 min still temperature distribution inside the storage was uneven and the PCM containers were not fully charged yet - Fig.3.17c.

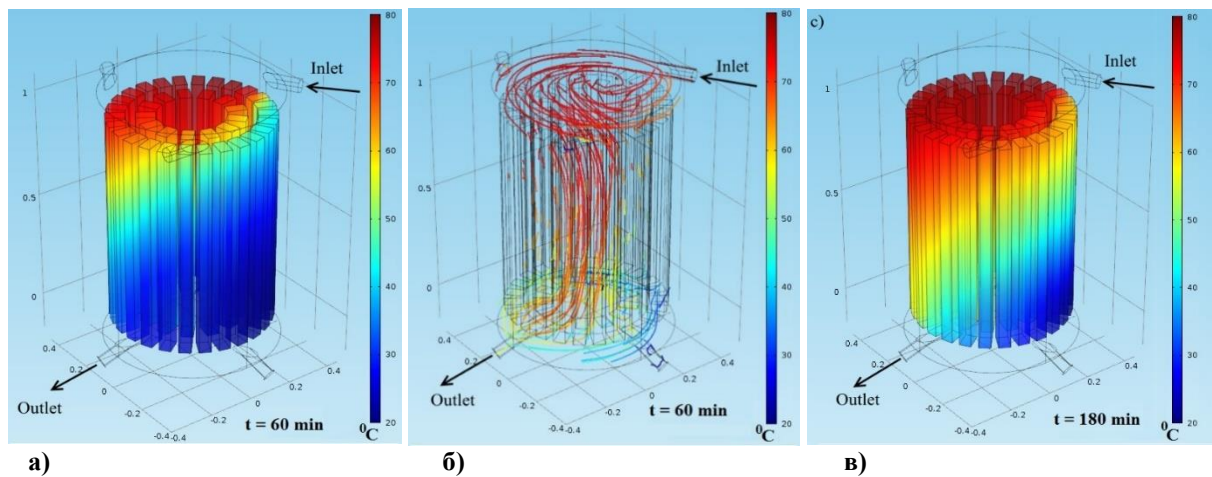


**Fig.3.17.** Charging process with single inlet and outlet pipes: a) Thermal energy distribution in the PCM containers after 60 min; b) Heat carrier fluid flow streamlines with thermal effect at 60 min; c) Thermal energy distribution in the PCM containers at 180 min

#### **Conclusions to Chapter 3.2.4.3.1**

The following conclusions can be made based on the conducted modeling and simulation:

- Three cases were studied in terms of numerical simulation.
- From the results, it can be concluded that two inlet and two outlet pipes are enough to charge or discharge such latent storage in enough short time, that is, three hours.

- Moreover, the PCM containers which are in the inner circle charged first in a short time and outer circle containers were charged after that. It can be concluded that outer circle PCM containers are very close to the storage tank walls, therefore, those areas does not allow fluid flow and heat transfer processes to be intensive.

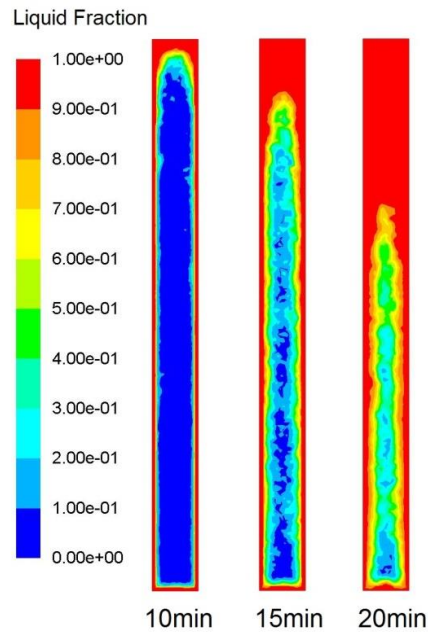


**Fig.3.18.** Contours of liquid fraction in the middle-width plane parallel to the 80 mm face, in charging at  $T_{\text{wall}} = 80 \text{ }^{\circ}\text{C}$

#### *3.2.4.3.2. Simulation of latent thermal storage by means of the enthalpy porosity technique used in ANSYS Fluent*

Macro-encapsulated E53 paraffin in a stainless steel container was considered as an active unit for thermal energy storage. The simulation studied the thermal behaviour of the unit at various temperatures of the external surfaces of the container,  $T_{\text{wall}}=15 \text{ }^{\circ}\text{C}$  for discharging mode,  $T_{\text{wall}}= 65 \text{ }^{\circ}\text{C}$  and  $80 \text{ }^{\circ}\text{C}$  for charging mode. All the surfaces were at constant temperature. Fig.3.18 shows the contour plots of the liquid fraction at 10, 15 and 20 min of the charging process in the middle-width plane parallel to the 80 mm face of the container. After 20 min charging the liquid fraction is 88%, and due to the buoyant forces the paraffin is stratified, liquid at the top, solid at the bottom.

#### **Conclusions to Chapter 3.2.4.3.2**

A time efficient method using the ANSYS Fluent techniques for prediction of phase change processes has been tested. The present simulation has obtained the flow pattern and temperature distribution in macro encapsulated paraffin inside a rectangular container with specific dimensions designed as an active unit in a test heat accumulator of a thermal solar system. The following conclusions are valid in this case:

- The model demonstrates the effects on the melting/ solidification process of the external temperature, the thermal conduction of the working fluid and the natural convection inside the PCM.

- The calculated results correspond to the observations in the literature about the factors affecting PCM encapsulation.

- The simulations add information for better understanding and more precise prediction of the phase change process, which is necessary for the design of thermal energy storage systems.

## **4. MIXED INSTALLATIONS WITH ALTERNATIVE ENERGY SOURCES (AES)**

### **4.1. SOLAR COLLECTORS WITH WATER STORAGE**

#### **4.1.1. Experimental study of an installation with vacuum solar collectors and a water thermal storage**

An installation consisting of vacuum solar collectors with heat pipes and a flat absorber, as well as a water thermal storage with four turn pipe windings was studied. The experimental structure and the measurement plan of the system of this installation are presented (Fig.3.2). As a function of time, meteorological values, temperatures (before and after the components of the installation) and flow rates through the collectors and through the storage were measured. The measurements were performed with water and Thermofrost P in the collector circuit, and with water in the storage.

##### **4.1.1.1. Experimental structure and measurement plan of the system**

The measurement plan in Fig.3.2 shows that the balancing of the tested system requires the coverage of the following groups of quantities:

- Meteorological values: intensity of total solar radiation in the plane of the solar collectors  $I_{\text{ск,об}}$ , W/m<sup>2</sup>; ambient temperature  $t_{\text{ок}}$ , °C; wind speed  $v_{\text{в}}$ , m/s;

- Temperatures, especially before and after the components of the installation;

- Flow rates as a function of time.

The measurement plan of the installation (Fig.3.2) indicates the places where temperatures are measured with thermocouples type L (Fe-CuNi).

##### **4.1.1.2. Investigation of all solar collector units and the water thermal storage**

The study of all 16 blocks of solar collectors (480 vacuum solar collectors) and the water thermal storage was conducted simultaneously. For 6 days the inlet and outlet fluid temperature  $t_{\text{ак,вх}}$  и  $t_{\text{ак,изх}}$  in the storage circuit and, the temperature of the fluid in the storage  $t_{\text{ак}}$ , the flow rate in the collector circuit



$\dot{V}_{\text{ck,ob}}$ , the flow rate in the storage circuit  $\dot{V}_{\text{ak}}$  and the meteorological data (ambient temperature  $t_{\text{ok}}$ , total radiation in the solar plane  $I_{\text{ck,ob}}$  and wind speed  $v_{\text{B}}$ ). The measurements were performed with water and Thermofrost P in the collector circuit.

The change curves of  $t_{\text{ak,изх}}$ ,  $t_{\text{ak,вх}}$ ,  $I_{\text{ck,об}}$ ,  $t_{\text{ок}}$ , as well as  $v_{\text{B}}$  и  $\dot{V}_{\text{ck,об}}$  are presented in Fig.4.1 for 13.10.1992 (working fluid is Thermofrost P).

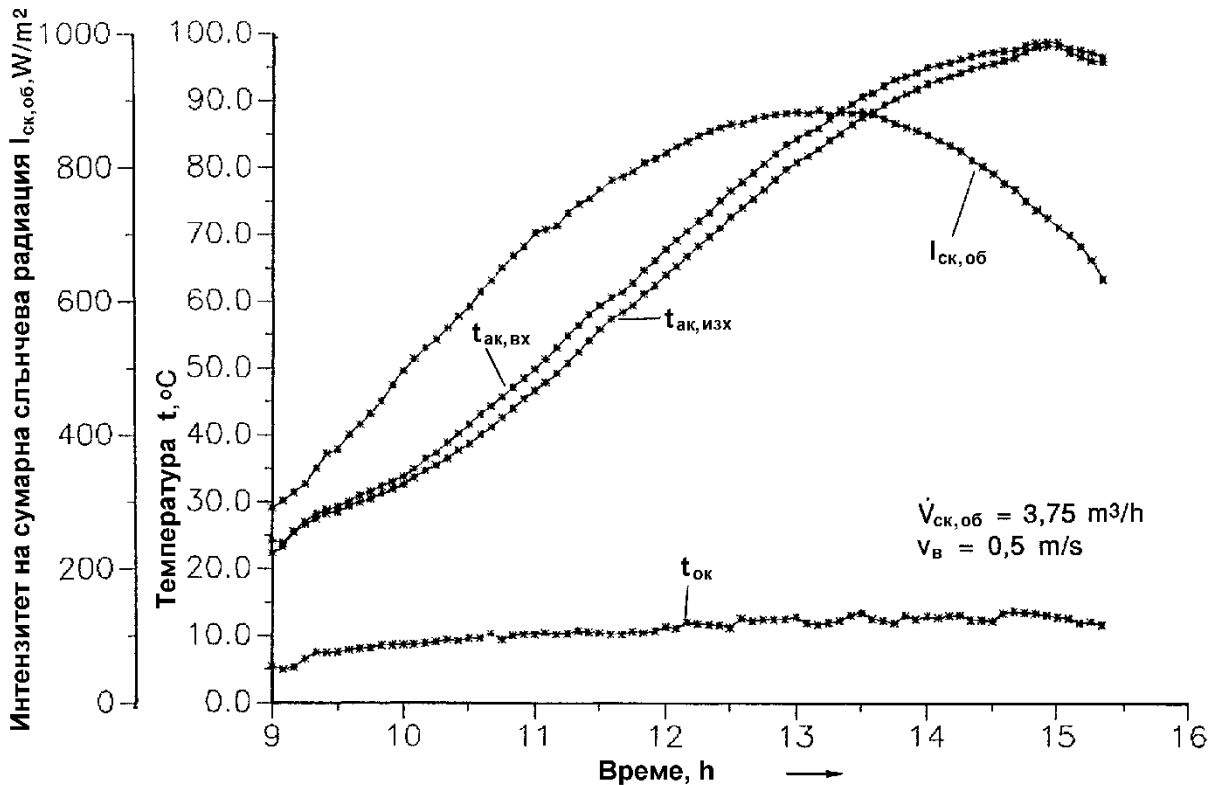


**Fig.4.1.** Meteorological data from the measurement of  $t_{\text{ок}}$  and  $I_{\text{ck,об}}$ , and of the inlet and outlet fluid storage temperature in the general collector circuit  $t_{\text{ак,вх}}$  and  $t_{\text{ак,изх}}$  for 13.10.1992 (with Termofrost P as collector working fluid)

#### 4.1.2. Mathematical modeling of an installation with vacuum solar collectors with heat pipe and water thermal storage

The mathematical simulation is based on 2 mathematical models - the detailed determination of the outlet solar collector temperature is discussed in *item 3.1.1*, and the determination of the fluid storage temperature  $t_{\text{ак}}$  with a four turn pipe windings is described in detail in *item 3.2.2*.

As a result, the inlet fluid collector temperature  $t_{\text{ck,вх}}$ , the outlet fluid collector temperature  $t_{\text{ck,изх}}$  and the inlet fluid storage temperature in the collector circuit  $t_{\text{ак,вх}}$ , as well as the fluid storage temperature  $t_{\text{ак}}$ . The

temperature  $t_{ак}$  is the inlet temperature for the generator of a refrigeration system.

#### **4.1.2.1. Mathematical model**

Based on the mathematical models for vacuum solar collector with heat pipe, described in detail in *item 3.1.1*.

$$(3.1) \quad C_{эф} \frac{\partial t_{фл}}{\partial \tau} + C_{фл} \cdot v_{фл} \frac{\partial t_{фл}}{\partial x} + \frac{t_{фл}}{R_{об}} = (\tau\alpha)_{эф} I_{ск,об}(\tau) + \frac{t_{ок}(\tau)}{R_{об}}$$

and for a water thermal storage, described in detail in *item 3.2.2*

$$(3.6) \quad \frac{\partial(m_{ак} \cdot h_{ак})}{\partial \tau} = \dot{Q}_{ак} + \dot{Q}_{ст} + \dot{Q}_{тр}$$

a general mathematical model can be created, with the help of which the parameters of the system of vacuum solar collectors - water thermal storage can be calculated (Fig.3.2).

The outlet fluid storage temperature  $t_{ак,изх}$  and the fluid storage temperature  $t_{ак}$  are considered as initial temperatures. Then the change in time of the temperatures is determined with the help of a general mathematical model in the combined system of solar collectors - storage, and the change in time is set for the total solar radiation  $I_{хор,об}$  and diffuse solar radiation  $I_{хор,диф}$  on a horizontal plane, ambient temperature  $t_{ок}$ , ambient storage temperature  $t_{ок,ак}$  and wind speed  $v_{в}$ . This calculation is repeated in the next time steps.

#### **4.1.2.2. Computer program SKSP**

The created computer program SKSP describes the phenomena that occur in the general system of solar collectors - water thermal storage. It consists of 8 sub-programs and is a joint program for the WRVK and Speicher programs.

At the beginning, the system parameters (solar collectors, storage) and the operating parameters  $\dot{V}_{ск,об}$  и  $\dot{V}_{ак}$  are entered. Then enter the initial values of  $t_{ак,изх}$  и  $t_{ак}$ , the coefficients for calculating the total radiation  $I_{хор,об}$  and diffuse radiation  $I_{хор,диф}$  on a horizontal surface, wind speed  $v_{в}$ , ambient temperature  $t_{ок}$  and ambient storage temperature  $t_{ок,ак}$ , as well as the initial values of the inlet fluid collector temperature  $t_{ск,вх}$ , the temperature  $t_{обз}$ , the temperature of the absorber  $t_{аб}$ , the temperature of the transparent coating  $t_{ин}$ , the inlet fluid storage temperature  $t_{ак,вх}$  and the heat transfer coefficient  $U_{то}$ .

Then all time-independent parameters are calculated. Based on the equations for heat losses in the pipe between  $t_{ак,изх}$  и  $t_{ск,вх}$  iteratively is

determined the inlet fluid collector temperature  $t_{\text{СК,ВХ}}$ , using subroutines to determine the wind speed  $v_{\text{В}}$ , ambient temperature  $t_{\text{ОК}}$ , ambient storage temperature  $t_{\text{ОК,АК}}$  and the outlet fluid storage temperature  $t_{\text{АК,ИЗХ}}$ .

If determined  $t_{\text{СК,ВХ}}$ , the calculation of the outlet fluid collector temperature  $t_{\text{СК,ИЗХ}}$  follows with the help of the subprograms FGS8 and PINT and the subprograms for the calculation of the total radiation  $I_{\text{ХОП,ОБ}}$  and the diffuse radiation  $I_{\text{ХОП,ДИФ}}$ , where the temperatures  $t_{\text{АБ}}$ ,  $t_{\text{МП}}$  and  $t_{\text{ОБЗ}}$  are determined iteratively. Using the heat loss equations in the pipe between temperature  $t_{\text{СК,ИЗХ}}$  and temperature  $t_{\text{АК,ВХ}}$ , the temperature  $t_{\text{АК,ВХ}}$  is calculated iteratively. Once we have  $t_{\text{АК,ВХ}}$ , we can determine the fluid storage temperature  $t_{\text{АК}}$ .

With the help of the computer program SKSP the general collector system was theoretically studied, where the outlet fluid collector temperature  $t_{\text{СК,ИЗХ}}$  and the fluid storage temperature  $t_{\text{АК}}$  were calculated, as it is an input parameter for the next part of the refrigeration system. The experimental data of the temperature  $t_{\text{АК}}$  were compared with the corresponding calculated values.

#### ***4.1.2.3. Comparison of the calculated with the experimental data of the general collector installation***

With the help of the computer program SKSP, the total collector installation was theoretically investigated and the outlet fluid collector temperature  $t_{\text{СК,ИЗХ}}$  and the fluid storage temperature  $t_{\text{АК}}$  were calculated. The following design data of vacuum solar collector KLVR 140 were used in the calculations: collector slope angle to the horizontal plane  $s = 45^\circ$ , number of collectors  $n_{\text{СК}} = 480$ , latitude  $\varphi = 50,87^\circ$  (for the city of Siegen), azimuthal angle of the collector  $\gamma = -29^\circ$ , reflectivity of the back reflector  $\rho_{\text{ЗР}} = 0,1$ .

The selected experimental atmospheric data are for 13.10.92 (working fluid is Thermofrost P). The values of the physical parameters of the working fluid (specific heat capacity, thermal conductivity, kinematic viscosity, Prandtl number, and density, respectively) are assumed to be constant throughout the day:  $c_{\text{ФЛ}} = 3910 \text{ J / kgK}$ ;  $\lambda_{\text{ФЛ}} = 0,445 \text{ W / mK}$ ;  $\nu_{\text{ФЛ}} = 1364 \cdot 10^{-9} \text{ m}^2 / \text{s}$ ;  $\text{Pr}_{\text{ФЛ}} = 12,1$  и  $\rho_{\text{ФЛ}} = 1010 \text{ kg / m}^3$ .

The average ambient storage temperature  $t_{\text{ОК,АК}} = 19,5^\circ\text{C}$  (laboratory and basement) was chosen. The initial fluid storage temperature was  $t_{\text{АК,НАЧ}} = 28,6^\circ\text{C}$ , and the volumetric fluid flow rates in the collector circuit and through the storage -  $\dot{V}_{\text{СК,ОБ}} = 3,75 \text{ m}^3 / \text{h}$ ,  $\dot{V}_{\text{АК}} = 2,05 \text{ m}^3 / \text{h}$ , respectively.



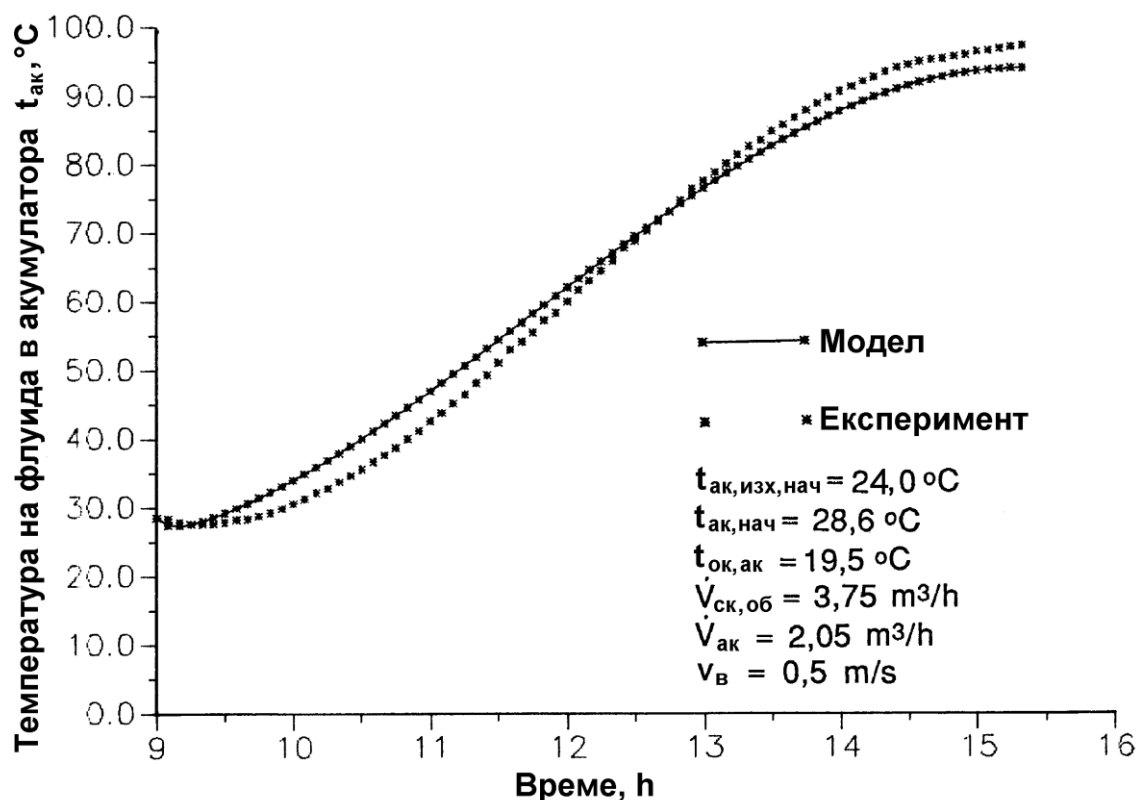


**Fig.4.2.** Comparison of the storage temperature  $t_{ак}$  measured and calculated while charging the storage on 13.10.1992 (with Termofrost P as collector working fluid)

Only 2 initial values support the calculation - the outlet fluid storage temperature  $t_{ак, изх, нач} = 24^\circ\text{C}$  on 13.10.1992, and the storage temperature  $t_{ак, нач} = 28,6^\circ\text{C}$ . The inlet and outlet temperatures of the installation were calculated under the influence of the meteorological data at each step (5 min) in the SKSP program. The experimental results and the corresponding calculated values of the storage temperature  $t_{ак}$  are compared and shown in Fig.4.2.

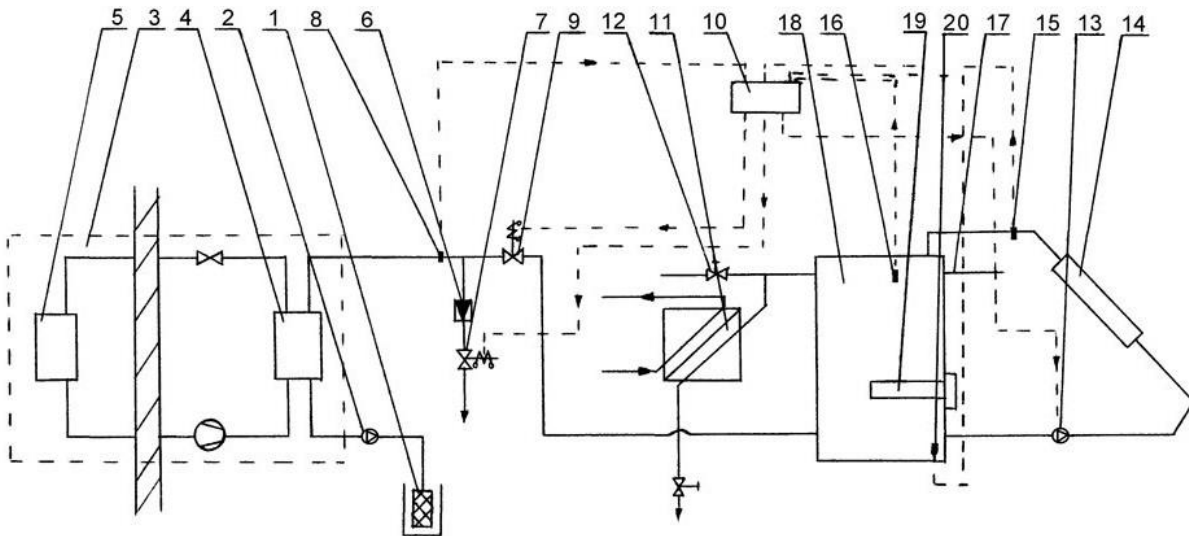
#### **Conclusions to Chapter 4.1**

The conclusions from the theoretical and experimental study of an installation with vacuum solar collectors and a water thermal storage are the following:

- The coincidence of the measured and calculated temperature in the storage (Fig.4.2) is very good. The differences between the model and the experiment in the storage temperatures are due to the fact that the pipes between the storage and the solar collectors were not insulated during the experiment;
- The proposed model can be used to calculate the temperature change of such installations operating at very high fluid temperatures (more than  $90 \text{ } ^\circ\text{C}$ ).

## 4.2. REFRIGERATION INSTALLATION WITH BUILT-IN SOLAR COLLECTORS AND THERMAL STORAGE

Refrigeration systems usually use the cold generated by the evaporator, and the heat from the condenser, which is low-potential energy, is discharged into the environment. Here we consider one of the ways to utilize this energy in a refrigeration unit with a water-cooled condenser (Fig.4.3), as the system also has built-in solar collectors.



1 - water source; 2, 13 - circulation pump; 3 - refrigeration unit; 4 - condenser; 5 - evaporator; 6 - non-return valve; 7, 9 - solenoid valve; 8, 15, 16, 20 - thermosensor; 10 - control unit; 11 - heat exchanger for domestic and technological needs with drinking qualities; 12 - hot water; 14 - solar collectors; 17 - overflow; 18 - storage; 19 - electric heater.

**Fig.4.3.** Scheme of a refrigeration installation with solar collectors and thermal storage

The water heated in the condenser **4** goes to the thermal storage **18**. From there the water is heated by means of flat-plate solar collectors **14** to a higher temperature level. Depending on the quality of the desired water, a heat exchanger **11** can be used to heat water for domestic and technological needs with drinking qualities or to draw hot water from **12**.

The use of this installation for hot water production can take place in the months from April to October. Then water is used as a heat carrier in the solar collectors. A further increase in the efficiency of the installation can be achieved if it is also used in winter. Then it will be necessary to place an additional heat exchanger between the storage and the collectors, forming a new circulation circuit through the collectors. Glycolic solutions should be used instead of water as the working substance in the "solar circle" due to sub-zero ambient temperatures.

The water storage is equipped with an electric heater **19** in order to heat the water to the required temperature in cloudy weather and in winter. This

maintains the desired temperature level, turning on the heater from 22 to 6 hours, when the value of electricity is lowest.

When the refrigeration unit and the solar collectors are running, but there is no hot water consumption, the excess water flows out through the overflow **17**. When the heat pump compressor is switched off, the temperature level in the storage is maintained by the circulation of water through the solar collectors.

In case of insufficient solar radiation, the solar collectors are switched off, because otherwise they will work as coolers. The solenoid valve **9** stops the flow of water to the storage when the temperature of the water after the condenser is lower than that in the storage. Then the solenoid valve **7** opens and the water drains into the sewer.

A control unit **10** is provided to control the whole system. The input effects for it are the pulses received from the thermal sensors **8**, **15** and **16**, which read the water temperature after the condenser, at the outlet of the solar collectors and in the storage. The output effects are directed to the solenoid valves **7**, **9** and the circulation pump **13** to maintain the required modes.

#### **Conclusions to Chapter 4.2**

This scheme is especially suitable for implementation in the food, pharmaceutical, biotechnology and other industries, which require both consumption of cold and heat.

### **4.3. BOREHOLE THERMAL ENERGY STORAGE (BTES) WITH SOLAR COLLECTORS**

#### **4.3.1. Construction of the BTES installation**

The construction of the borehole thermal energy storage (BTES) in TU (UTFSM), Valparaiso, Chile is described in detail in *item 3.2.3.1.1* (Fig.3.4).

##### ***4.3.1.1. Preparing the installation for charging mode***

The reconstruction of the installation started immediately after the completion of the Thermal response test (TRT). Three solar collectors were connected to the BTES (Fig.4.4). Their total active area is about 4,4 m<sup>2</sup> (the size of the collector is 1,05 m x 1,40 m). The distance between the collectors and BTES is about 2 m.

Two additional bypass valves  $V_2$  and  $V_3$  (Fig.4.4) were installed to allow the installation to operate in two different modes depending on the type of power source used - TRT mode, if the power supply is only from the electric heater (valve  $V_1$  is open, valves  $V_2$  and  $V_3$  are closed), solar mode - if BTES is charged by solar energy (valve  $V_1$  is closed, valves  $V_2$  and  $V_3$  are open).

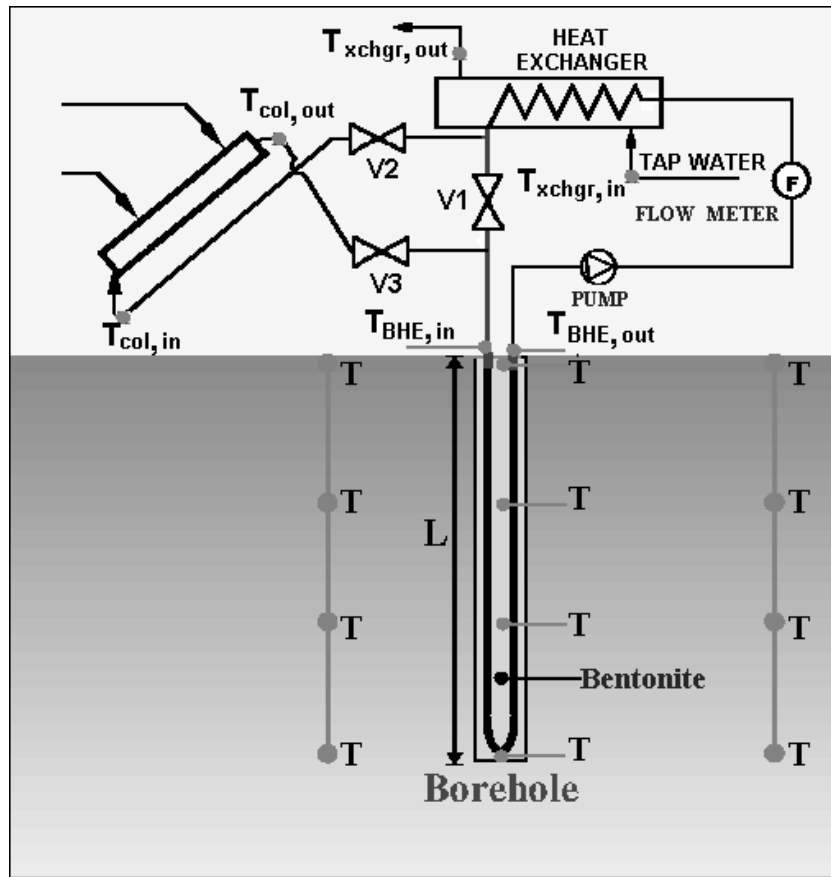


Fig.4.4. Scheme of the reconstructed test installation

#### 4.3.1.2. . Preparing the installation for discharging mode

After the loading cycle, a new modification of the hydraulic system was made. One circuit of a water-to-water cross heat exchanger (car radiator) was connected to the BTES circuit instead of the solar collectors, and the other circuit is supplied by the water network.

The water from the network circulates through the radiator, becoming a cold circuit of the heat exchanger, and the water from the BTES circulates between the radiator and the walls of the housing, thus becoming a hot circuit.

### 4.3.2. Experiment

#### 4.3.2.1. Charging phase

The installation was remodeled after realizing the TRT and was used to charge the ground by means of solar energy (charging mode, natural experiment). The test was conducted in the course of 29 days - from 18th of August to 16th of September 2003. Borehole inlet and outlet temperatures, collector inlet and outlet temperatures and ambient temperature were measured and recorded at a 1 min frequency in the course of the experiment. Although the flow rate was fixed at the constant value of 3,17 l/min, it was periodically measured and controlled. Temperature probes of the differential controller were

located to sense collector outlet and borehole inlet temperatures. Setup points were 5 and 2 °C for Pump-On/Off, respectively.

#### **4.3.2.2. Discharging phase**

After the charging cycle a heat exchanger was installed to extract heat from the ground in a discharging mode. The experiment started on the 17th of September and ended on the 30th of September 2003. Ambient temperature, borehole inlet and outlet temperature (connected to the warm loop of the heat exchanger) and inlet and outlet temperature to the cold loop of the heat exchanger were measured and recorded during this phase. Flow rates measured on the warm and cold circuits of heat exchanger were 3,17 and 1,6 l/min, respectively.

#### **4.3.3. TRNSYS simulation of the processes in the BTES**

The analysis of the experimental data was done by means of TRNSYS DST module (TYPE 141). One of the parameters required by the DST algorithm is the BTES store volume. In this regard, a virtual cylindrical volume surrounding the BHE with a depth equal to that of the BHE and 4 m in diameter was defined. A text data file with measured ambient temperature, collector inlet and outlet temperatures, BHE inlet and outlet temperatures and solar radiation was used as input to the TRNSYS code.

Fig.4.5 depicts the time evolution of accumulated energies for the entire length of the charging phase. It is seen that the available solar radiation accumulated at the end of the charging phase reached almost 2750 MJ. Solar collectors delivered around 70% of the available solar radiation and in turn only around 50% of this energy was injected to the heat storage. Furthermore, a good concurrence is seen to exist between simulated and experimental accumulated injected energies. The difference is due to the constant pumping condition that makes the heat injection cycle more efficient.

#### **Conclusions to Chapter 4.3**

The data from a charging/ discharging experiment of a shallow borehole heat exchanger (BHE) has been presented and analyzed. Simulations using TRNSYS Type 141 has been applied as well in order to better understand some of the features exhibited by thermal behavior of the system.

The main conclusions are as follows:

##### **Charging phase:**

- Thermal insulation on top of the store proved to cut down heat losses through the upper boundary by ~80%;
- Simulation runs showed that side losses first appear after around 72 h and are expected to escalate as high as 46% of the total injected thermal energy by end of the charging period.

##### **Discharging phase:**

- The experimental average store temperature decay during discharging (calculated using temperature measurements from probes in the soil at 0,5 m and 1 m distance from the BHE) agree in magnitude and shape with simulated average store temperature obtained from TRNSYS simulations.

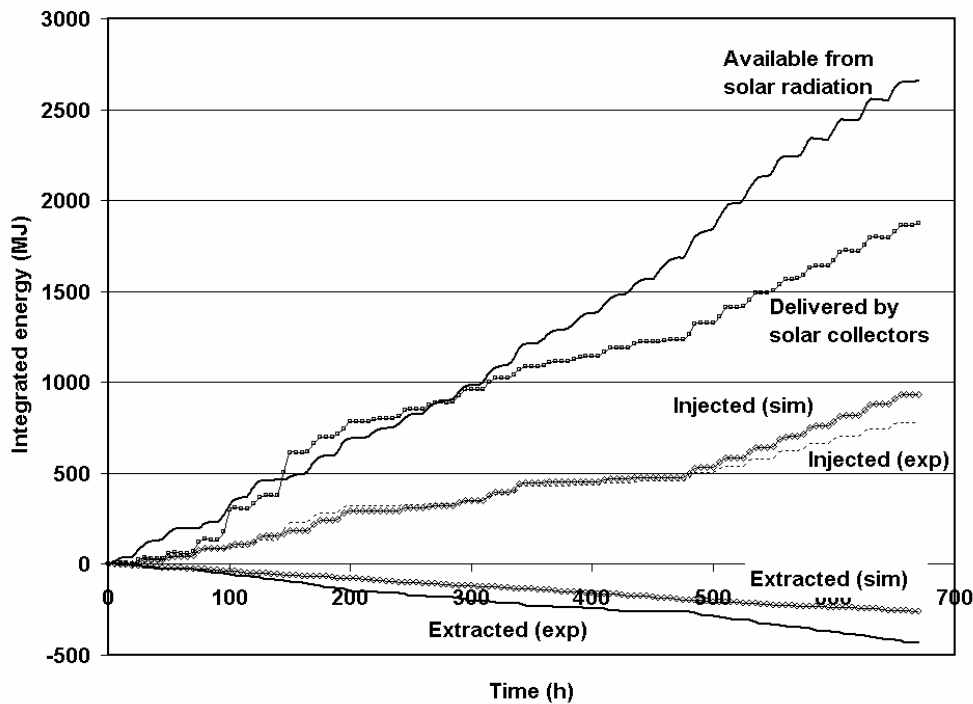


**Fig.4.5.** Time evolution of energies in the system; solar energy available, delivered by collectors

## 4.4. PHOTOVOLTAIC-THERMAL (PV/T) INSTALLATIONS

### 4.4.1. Constructions of PV/T installations

#### 4.4.1.1. PV/T installation in TU Sofia, Plovdiv branch

The installation is for experimental study of a flat PV/T collector cooled with water. Two standard thin-film photovoltaic panels were tested through it. One of them was transformed into a combined PV/T collector with little investment and effort.

An installation for testing of photovoltaic (PV) solar panels was created in the spring of 2010 at the Technical University of Sofia, branch Plovdiv (Fig.4.6). Main parts of the installation are a combined PV/T solar panel **1** and ordinary photovoltaic solar panel **12**. The pump **2** is used to move the cooling fluid through the combined panel **1** and the thermostat tank **3** - it is used to maintain a constant temperature through the PV/T panels. PT100 Signal Conditioner **5** is used to measure the temperature. The signal is sent then to a data logger **6** and treated by means of a Laptop or personal computer **7**. An integrated solarimeter/ anemometer **8** is used to measure the global solar radiation and the wind velocity. The pyrheliometer **9** is measuring the direct

solar radiation by means of the sun following system (sun tracker) **10** and the direct solar radiation measurement unit **11**. The current/ voltage signal conditioners **13** are utilized to measure the gained electrical power from the sun.

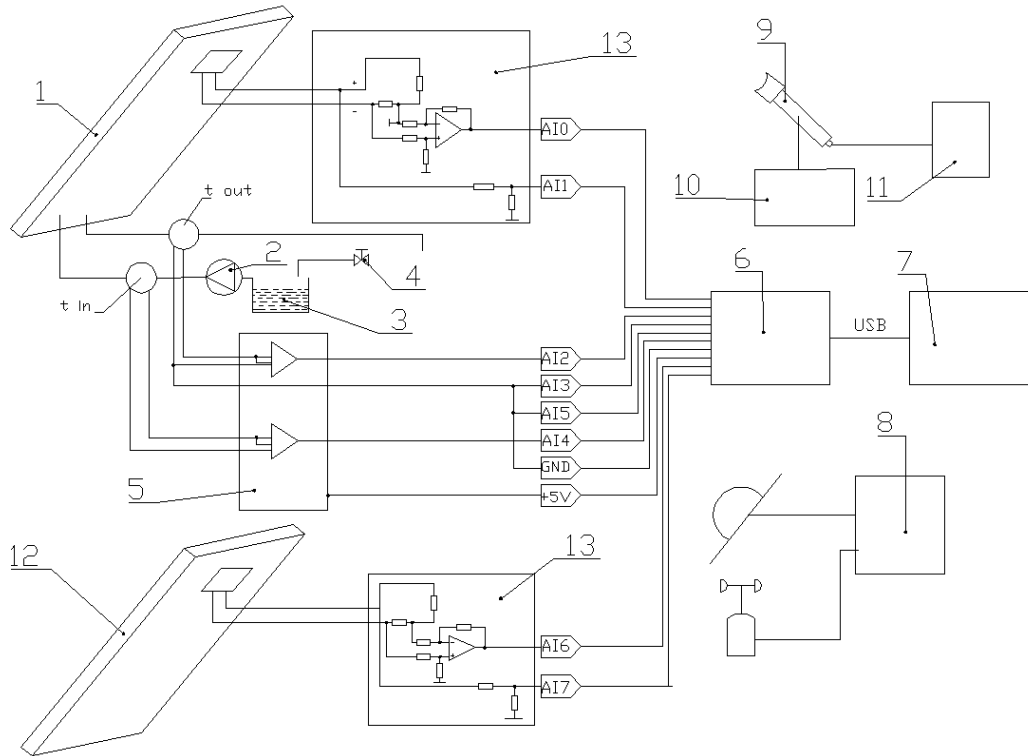
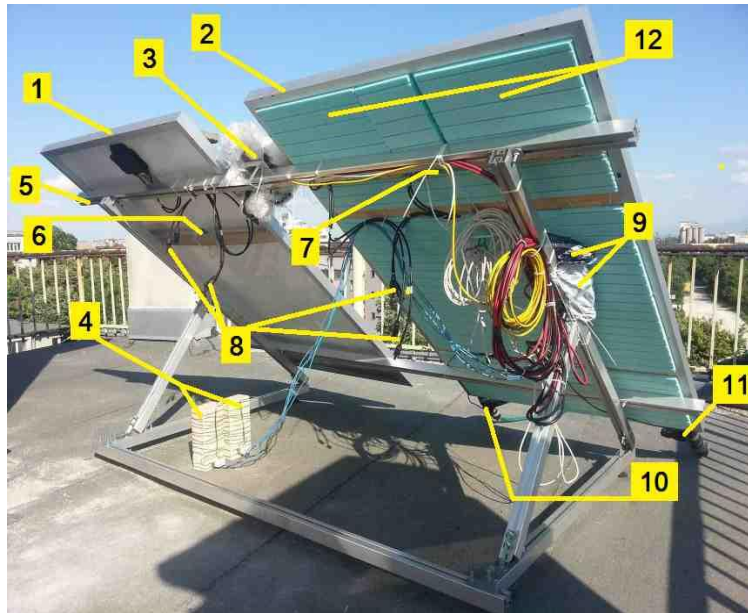


**Fig.4.6.** Installation setup

#### **4.4.1.2. PV/T installation in PU „Paisii Hilendarski“, Plovdiv**

In 2017, a solar thermal system combined with photovoltaic panels was designed at the „Paisii Hilendarski“ University of Plovdiv. The system consists of two main subsystems: thermal part and electrical part.

PV/T panel construction was studied as part of the thermal subsystem (1). Experimental studies have been performed to determine its effectiveness and to compare the characteristics with other existing samples. Two identical 250 Wp polycrystalline photovoltaic modules, manufactured by Crane, were mounted together on an aluminum base as the solar part of the installation (Fig.4.7). Both panels were placed to the south and facing the sun at a 40° angle. A Kipp & Zonen CMP6 pyranometer is mounted in the same plane of the frame. One of the photovoltaic panels was reconstructed as PV/T-type. Pt100 class-A temperature sensors were used to measure the inlet and outlet fluid temperature of the PV/T panels.



1-PV panel; 2-PV/T panel; 3-Pyranometer CMP6; 4-Loads; 5. Metal stand; 6- PV panel cell temperature sensor; 7-PV/T panel cell temperature sensor; 8- Power cable terminals; 9- Expansion card and DAQ board; 10- Outlet fluid temperature sensor; 11-Inlet fluid temperature sensor; 12-PV/T panel thermal insulation layer

**Fig.4.7.** PV and PV/T panel experimental setup

#### ***4.4.1.3. Concentrating CPV/T system with heat pump at the University of Muğla Sıtkı Koçman University in Muğla/Turkey***

To increase the radiation incident on PV and the electrical efficiency of PV, solar radiation is focused on PV with mirrors. This system is called a concentrating photovoltaic module (CPV). PV and CPV systems have a problem with overheating. Overheating reduces the electrical efficiency. For this reason, it must be cooled. PV and CPV systems that are cooled by some fluid are called PV/T and CPV/T. Many fluids can be used as a working fluid. In this study, a refrigerant passing through the heat pump evaporator or water was used to cool the PV cells. The experimental installation of concentrating photovoltaic-thermal (CPV/T) was established at Mugla Sitki Kochman University in Mugla, Turkey. Its structure is shown in Fig.4.8.

Thirty-one mirrors were placed in solar concentrators to focus solar radiation on PV cells. A triangular metal frame was placed on the solar concentrator. The PV modules are located on both surfaces of a triangular frame. Six PV cells are connected in series on both surfaces. The third surface is painted in a matte color to absorb radiation. The evaporator of the heat pump (HP) is located behind the PV module. Temperature measurements were taken from eight points on the back surface of the CPV/T system. R134a was used as a refrigerant in the heat pump, the flow rate of which was measured during the experiments. HP is used to cool the CPV/T system. The change of the electrical efficiency and the produced electric power of the CPV/T system with and without heat pump were studied.



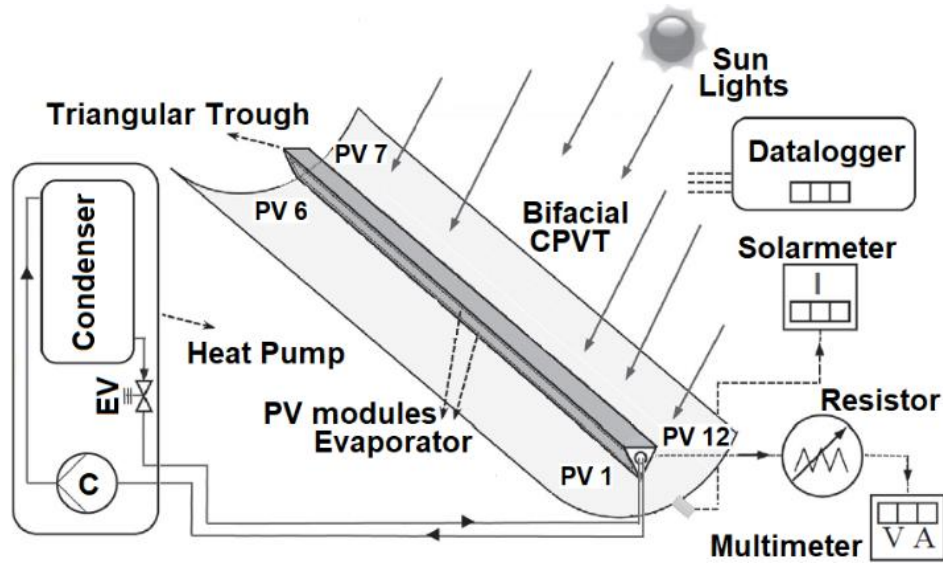


**Fig.4.8.** Schematic diagram of the CPVT system with heat pump

#### **4.4.2. Conducted research with PV/T installations**

##### **4.4.2.1. PV/T installation in TU Sofia, Plovdiv branch**

The experiments with the installation shown in Fig.4.6 were conducted for 2 days - May 26 and 27, 2010. Seven tests were performed, each of 15 minutes. The following parameters were measured: intensity of global solar radiation, ambient temperature, fluid flow rate, inlet and outlet temperature through the PV/T collector, electric power produced by the ordinary (PV) and combined (PV/T) panel. The heat flow rate produced by the PV/T collector, the ratio of the electrical power PV/T to the PV panel and the ratio of the heat flow rate to the electrical power of the PV/T panel are calculated.

##### **4.4.2.2. PV/T installation in PU „Paisii Hilendarski“, Plovdiv**

During the operation of PV/T panels in real conditions, the inlet fluid temperature varies widely. When the hot water buffer tank is cold (at the beginning of the water heating process), the inlet water temperature is about 15 °C. At the end of the process it can reach 60 °C. This leads to deterioration of the cooling conditions of the photovoltaic cells and even to their further heating. In the latter case, the panel is cooled only through its front side by the ambient air. Therefore, it is important to study the temperature range of the inlet fluid for which the power generation efficiency of the PV/T panel is higher than that of the PV panel.

##### **4.4.2.3. CPV/T system with heat pump at the University of Muğla/ Turkey**

The thermal efficiency of the HP-CPVT system is lower than that of the CPV/T system, as the PV/T is cooled by a heat pump. In addition, the electrical efficiency of HP-CPVT is higher than that of CPV/T. The photovoltaic modules

of the CPV/T are cooled with water, and those of the HP-CPV/T system by the refrigerant passing through the evaporator of the heat pump. The experiments were performed for a week. Data were processed on days when the values of radiation and ambient temperature in both systems were approximately the same.

The average power generation between 08:30 and 18:30 is 20,06 W and 19,83 W respectively for CPV/T with and without heat pump (Fig.4.9). The electrical efficiency of PV is 2,95% and 2,90% for CPVT with and without heat pump, respectively.

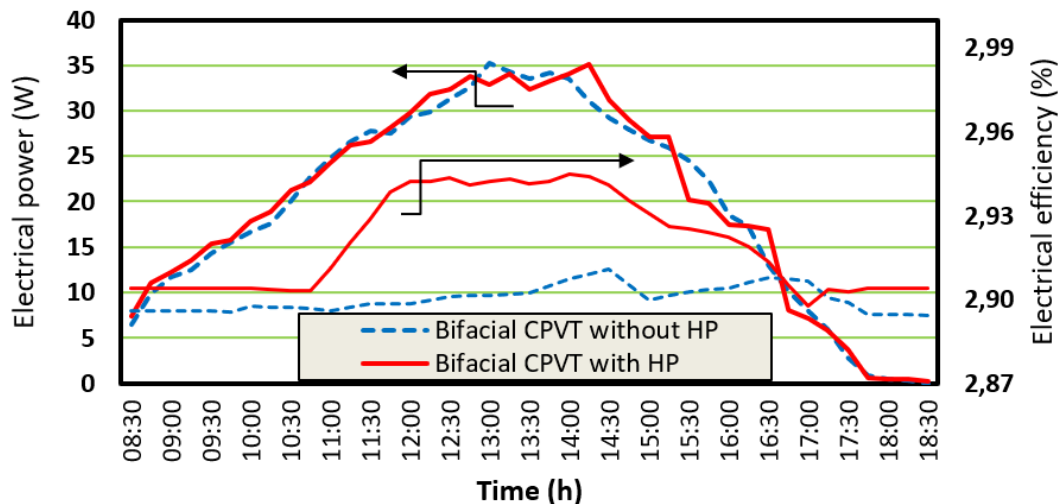


Fig.4.9. Time dependent change of electrical power and electrical efficiency

### Conclusions to Chapter 4.4.2.3

This study aims to examine the change in the electrical and thermal efficiency of a CPV/T system that is cooled by a refrigerant flowing through a heat pump evaporator and water. The power consumption of the HP compressor is higher than the power generation of the CPV/T. Although the electrical efficiency values are close to each other for the two systems, the thermal efficiency of CPV/T is higher than that of HP-CPV/T. Also, the overall efficiency of CPVT is higher than that of HP-CPV/T.

### **4.4.3. Processing of experimental results**

#### **4.4.3.1. PV/T installation in TU Sofia, Plovdiv branch**

The results of test 6 are presented in Fig.4.10, which shows the electric power produced by PV and PV/T panel on 27.05.10, starting at 10:55 h. It is obvious that the cooled PV/T panel produces more electricity. In addition, the coolant temperature rises.

### Conclusions to Chapter 4.4.3.1

Studies of two panels of the same size have been carried out, one of which is designed as a PV/T collector. Experiments show the following:

## *Evaluation of mixed installations with alternative energy sources*

- the PV/T panel, which is cooled by means of a fluid has higher efficiency than the other panel (Fig.4.10);
- a thermal power is gained in the PV/T panel (about 9 times more than the electrical power) in the temperature range of 20 to 50 °C;
- the effect of the better electrical production in the PV/T panel is relative stable in a long temperature interval;
- the cooled PV/T panel produces in the whole temperature interval about 3% more electricity than the PV panel;
- than lower the working temperature of the panel is, so higher the gained thermal power is.

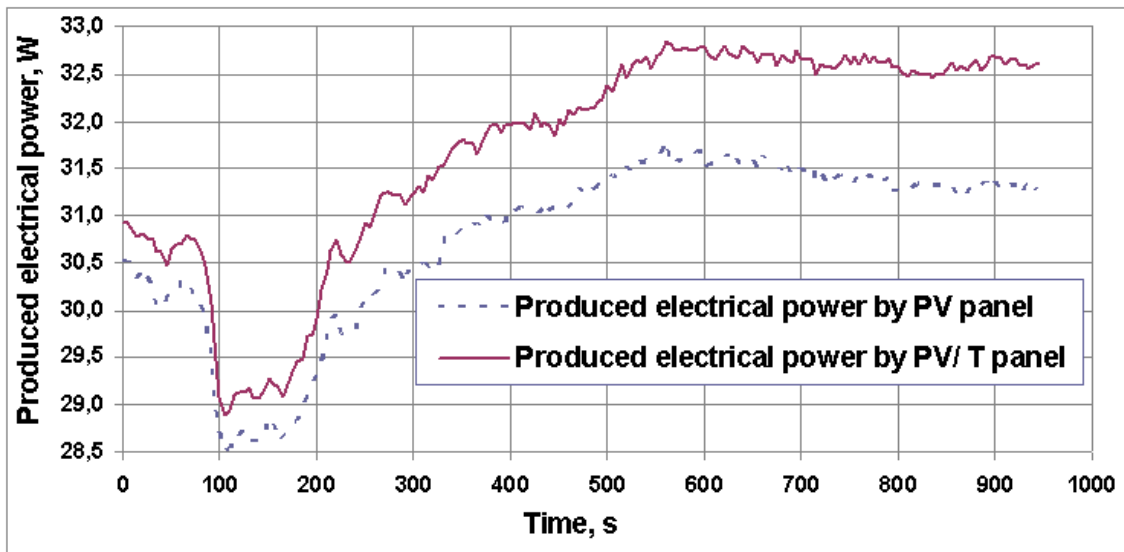


**Fig.4.10.** Produced electrical power by PV and PV/T panels on 27.05.10

### **4.4.3.2. PV/T installation in PU „Paisii Hilendarski“, Plovdiv**

The produced electric powers for each of the compared PV and PV/T panels are shown in Fig.4.11.

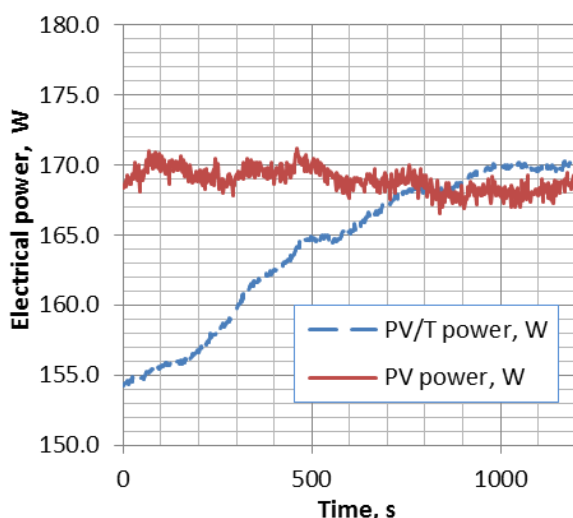


**Fig.4.11.** Comparison of PV and PV/T panel electrical power production

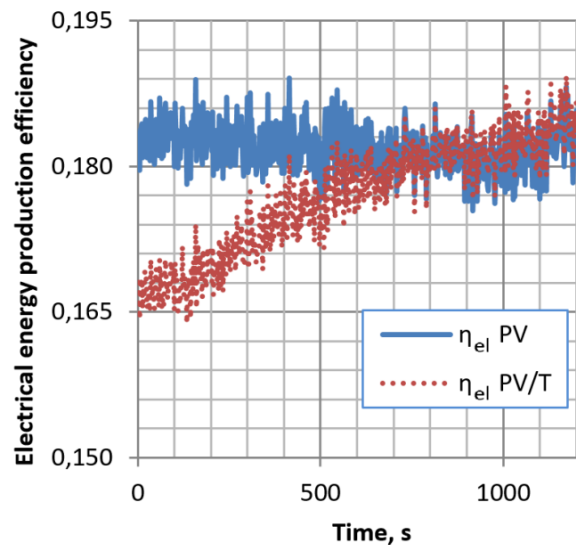


**Fig.4.12.** Change of the PV and PV/T panel's efficiencies

At the start of the test, the photovoltaic panel operates in a steady state and the cell temperature is almost constant, thanks to cooling with ambient air. On the other hand, the circulation of the liquid in the heat exchanger of the PV/T panel is switched on and the area of the cell is overheated due to the thermal insulation of the back panel. During this transition period, the sensible heat accumulated by the elements of the PV/T panel causes the production of a large heat flow rate, much greater than the incoming sunlight. The efficiency of both panels during the same test is presented in Fig.4.12. At the beginning of the test, the PV panel generates 15 W more than the PV/T panel. In the steady state, the efficiency of the PV/T panel is about 1% higher than the efficiency of the PV panel.

### **Conclusions to Chapter 4.4.3.2**

The following conclusions can be drawn from the research:

- Several tests have been performed to measure some characteristics of the constructed PV/T panel. As a result of experiments, it was found that the efficiency and electrical power of each photovoltaic cell decreases with increasing temperature. In the first stage of the test, when the PV/T is not well cooled (PV cell temperature 75,6 °C), its electrical efficiency and electrical power are lower than those of the PV panel, which is cooled to 60,3 °C from the surrounding air;

- As a result of the tests, poor thermal contact was found between the tube and the back of the cell plate. The conclusion is that it is necessary to change the design of the panel to reduce the thermal resistance of the contact between the pipe and the plate.

- At higher temperatures, the heat transfer in the PV/T panel deteriorates and the energy power of the PV panel becomes better. So PV/T panels (in the thermal part) should not be connected in series due to poor operating conditions of the panel at the highest temperature. Parallel connection is preferable.

## **4.5. GROUND SOURCE HEAT PUMP (GSHP) SYSTEM WITH SOLAR COLLECTORS (SC)**

### **4.5.1. Construction of a GSHP system with solar collectors**

An experimental system consisting of a ground source heat pump system and solar collectors has been built at the Technical University of Sofia, Plovdiv branch (Fig. 4.13). It consists of the following main parts:

- Three flat-plate solar collectors (SC) connected in parallel (each with an area of 2,15 m<sup>2</sup>);
- Hot water tank (200 dm<sup>3</sup>) with additional electric heater with a power of 3 kW;
- Insulated water thermal storage made of stainless steel (300 dm<sup>3</sup>);
- Water-to-water heat pump HWW-A / WP 15 (manufactured by Maxa);

- Heat-insulated buffer tank - 150 dm<sup>3</sup>;
- Fan coil Sabiana Carisma CRC type "air-water";
- Two borehole heat exchangers (BHE) are located at ground level (they are single and double loop).

Prior to the study of the system, Thermal response tests (TRT) were carried out to assess the thermal conductivity of the soil  $\lambda$  and the thermal resistance of the BHE  $R_b$ .

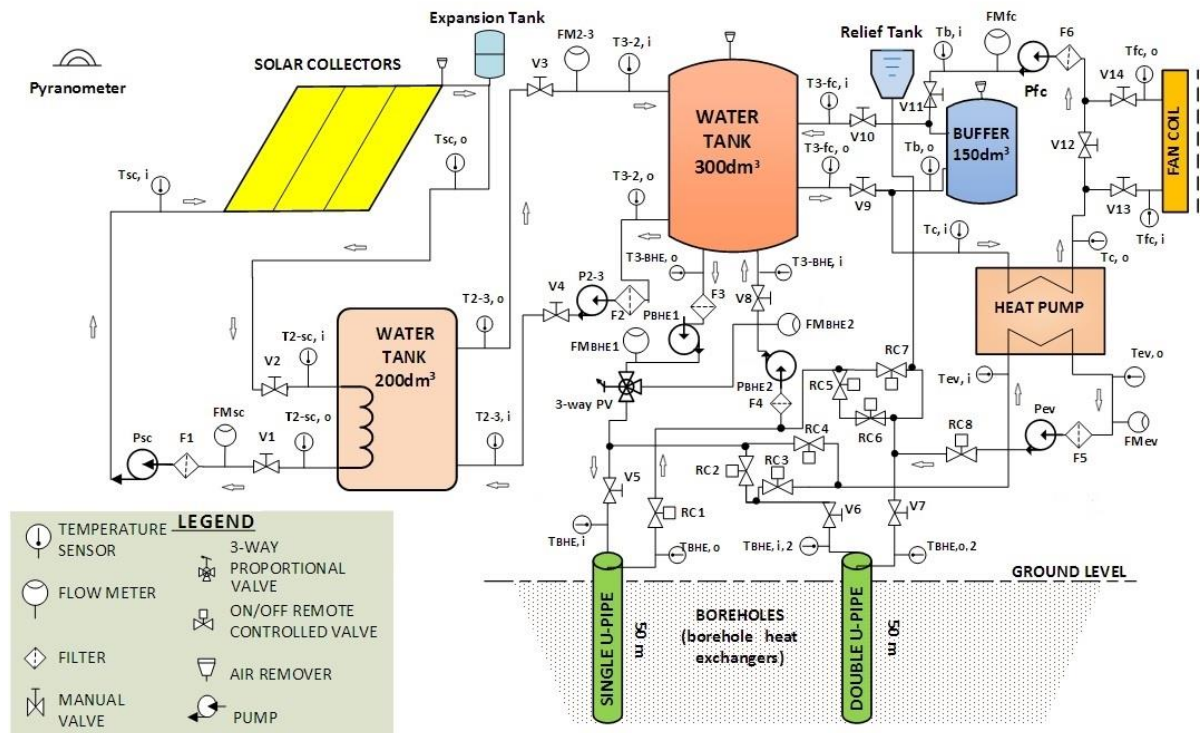


**Fig.4.13.** Schematic diagram of mixed GSHP installation with solar collectors

#### 4.5.2. Investigation methods of a mixed GSHP system with solar collectors

##### 4.5.2.1. Efficiencies of the mixed system at different operational modes

##### Charging mode of the water storages with thermal energy from the solar collectors

The system efficiency is to be determined in this mode as a ratio of stored thermal energy in the water accumulators to global solar insolation in the plane of the solar collectors plus electrical power of the circulation pumps during the test period:

$$(4.1) \quad \eta_{s,1} = \frac{\dot{m}_{st} \cdot c_{st} \cdot (t_{st,end} - t_{st,in})}{\sum_{i=1}^n \int_0^{\tau_i} (I_{sc} \cdot A_{ab} + N_{sc}) d\tau + \int_0^{\tau_{end}} N_{2-3} \cdot d\tau}$$

##### Charging mode of BHE with thermal energy from the solar collectors

The system efficiency is to be determined in this mode as a ratio of thermal energy injected to the BHE to global solar insolation in the plane of the solar collectors plus electrical powers of the circulation pumps during the test period:

$$(4.2) \quad \eta_{s,2} = \frac{\int_0^{\tau_{end}} \dot{m}_{BHE} \cdot c_{BHE} \cdot (t_{BHE,i} - t_{BHE,o}) d\tau}{\sum_{i=1}^n \int_0^{\tau_i} (I_{sc} \cdot A_{ab} + N_{sc}) d\tau + \int_0^{\tau_{end}} N_{2-3} d\tau + \int_0^{\tau_{end}} N_{BHE} d\tau}.$$

### Direct solar heating mode

The system efficiency is to be determined in this mode as a ratio of thermal energy supplied to the air convector to global solar insolation in the plane of the solar collectors plus electrical powers of the circulation pumps during the test period:

$$(4.3) \quad \eta_{s,3} = \frac{\int_0^{\tau_{end}} \dot{m}_{fc} \cdot c_{fc} \cdot (t_{fc,i} - t_{fc,o}) d\tau}{\sum_{i=1}^n \int_0^{\tau_i} (I_{sc} \cdot A_{ab} + N_{sc}) d\tau + \int_0^{\tau_{end}} (N_{2-3} + N_{fc}) d\tau}.$$

### Heating mode with ground source heat pump (GSHP)

The system efficiency is to be determined in this mode as a ratio of thermal energy supplied to the fan coil and thermal energy extracted from the BHE plus electrical powers of the heat pump and the circulation pumps during the test period:

$$(4.4) \quad \eta_{s,4} = \frac{\int_0^{\tau_{end}} \dot{m}_{fc} \cdot c_{fc} \cdot (t_{fc,i} - t_{fc,o}) d\tau}{\int_0^{\tau_{end}} N_{fc} \cdot d\tau + \sum_{j=1}^m \int_0^{\tau_j} \{ \dot{m}_{BHE} \cdot c_{BHE} (t_{BHE,o} - t_{BHE,i}) + N_{BHE} \} d\tau + \sum_{k=1}^m \int_0^{\tau_k} N_{hp} \cdot d\tau}.$$

### Heating mode with solar assisted heat pump (SAHP)

The system efficiency is to be determined in this mode as a ratio of thermal energy supplied to the fan coil to global solar insolation in the plane of the solar collectors plus electrical powers of the heat pump and the circulation pumps during the test period:

$$(4.5) \quad \eta_{s,5} = \frac{\int_0^{\tau_{end}} \dot{m}_{fc} \cdot c_{fc} \cdot (t_{fc,i} - t_{fc,o}) d\tau}{\sum_{i=1}^n \int_0^{\tau_i} (I_{sc} \cdot A_{ab} + N_{sc}) d\tau + \sum_{l=0}^p \int_0^{\tau_l} N_{AES} d\tau + \int_0^{\tau_{end}} (N_{2-3} + N_{fc} + N_{ev}) d\tau + \sum_{f=0}^q \int_0^{\tau_f} N_{hp} d\tau},$$

where:  $m_{st}$  is the water mass in the storages, kg;

$\dot{m}_{BHE}$ ,  $\dot{m}_{fc}$ ,  $\dot{m}_{ev}$ ,  $\dot{m}_{sc}$  - average fluid mass flow rate through BHE, fan coil, evaporator and solar collectors, kg/s;

$c$  - average fluid mass specific heat capacity, J/kgK;

$t_{st,end}$ ,  $t_{st,in}$  - end and initial water temperatures in the storage, °C;

$t_{BHE,i}$ ,  $t_{BHE,o}$  - inlet and outlet fluid BHE temperatures, °C;

$t_{fc,i}$ ,  $t_{fc,o}$  - inlet and outlet fluid fan coil temperature, °C;

$t_{ev,i}$ ,  $t_{ev,o}$  - inlet and outlet fluid evaporator temperatures, °C;

$A_{ab}$  - solar collector absorber area, m<sup>2</sup>;

$I_{sc}$  - intensity of the global solar radiation in plane of the solar collectors, W/m<sup>2</sup>;

## *Evaluation of mixed installations with alternative energy sources*

$N_{SC}$ ,  $N_{2-3}$  - momentary power of the solar circuit pump and the power of the pump between the 200 dm<sup>3</sup> and 300 dm<sup>3</sup> tanks, W;

$N_{BHE}$  - momentary power of the BHE circuit pump, W;

$N_{fc}$  - momentary power of the fan coil water circuit pump, W;

$N_{hp}$  - momentary electrical power of the heat pump during 1st operation period, W;

$N_{ev}$  - momentary electrical power of the evaporator circuit pump, W;

$N_{AES}$  - momentary electrical power of the additional energy source (AES), in the case - electrical heater, W;

$n$  - activity period number of the solar circuit pump,-;

$\tau_i$  -  $i$ -th time period of the solar circuit pump operation, s;

$\tau$  - time (it is 0 at the experiment start), s;

$\tau_{end}$  - time at the experiment's end, s;

$m$  - activity period number of the heat pump and the BHE circuit pump in GSHP operation mode,-;

$\tau_j$  -  $j$ -th time period of the BHE circuit pump operation, s;

$\tau_k$  -  $k$ -th time period of the heat pump operation in GSHP operation mode,

s;

$\tau_l$  -  $l$ -th time period of the AES operation (electrical heater), s;

$p$  - activity period number of the AES,-;

$q$  - activity period (cycles) number of the heat pump operation in SAHP mode,-;

$\tau_f$  -  $f$ -th time period of the heat pump operation in SAHP mode, s.

### **4.5.2.2. Investigation procedure**

The measurements are made under quasi-stationary conditions:

- all parameters are measured simultaneously every minute during the measuring period;

- the tested solar collectors are oriented towards the sun and tilted to the horizon at an angle ( $\varphi - \delta$ ), where  $\varphi$  is latitude, and  $\delta$  - declination.

### **4.5.2.3. Accuracy of the measured parameters**

The acceptable deviations of the directly measured parameters are as follows:

- intensity of the global solar radiation -  $\pm 2\%$ ;
- temperatures -  $\pm 2\%$ ;
- volume flow rates -  $\pm 2\%$ ;
- electrical powers -  $\pm 5\%$ .

The acceptable deviations of the indirectly measured parameters are as follows:

- condenser heat flow rate of the heat pump -  $\pm 6\%$ ;
- solar collector heat flow rate -  $\pm 6\%$ ;
- solar collector efficiency -  $\pm 6\%$ ;



- coefficient of performance of the heat pump (COP) -  $\pm 6\%$ ;
- system efficiency by different operation modes -  $\pm 6\%$ .

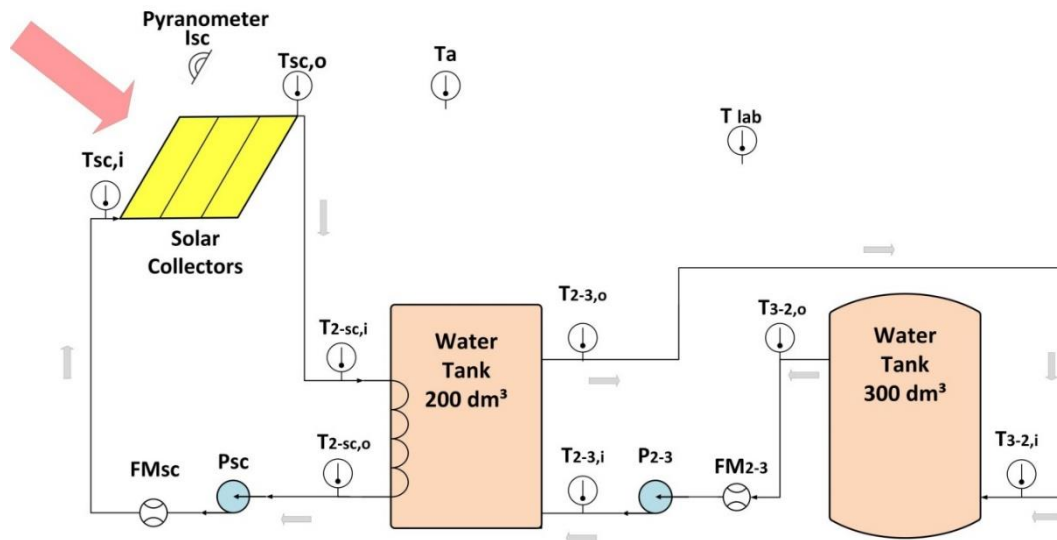


Fig.4.14. Working scheme of the mixed installation in CWT mode

### 4.5.3. Experimental results

#### 4.5.3.1. Operation modes

The mixed installation (Fig.4.13) has been tested in 5 different operation modes depending on the seasonal conditions and the needed load as follows:

1. Charging of water tanks with thermal energy from solar collectors (CWT mode): solar collectors charge a water storage with thermal energy.
2. Charging of borehole thermal energy storage (BTES) with thermal energy from solar collectors (CBTES mode): solar collectors charge the boreholes with thermal energy.
3. Direct solar heating (DSH mode): a thermal energy from water tank is delivered directly to the consumer.
4. GSHP heating (GSHPH mode): heat is delivered to the heat pump evaporator from the boreholes.
5. Heating with SAHP (SAHPH mode): heat is delivered to the heat pump evaporator from the solar collectors.

#### 4.5.3.2. Charging of water tanks with thermal energy from solar collectors (CWT mode)

The simplified working scheme of the mode is presented in Fig.4.14.

An experiment was performed on the installation in CWT mode (Fig.4.14). The energy flows between the system components in this mode are shown in Fig.4.15. All the presented values are calculated on the basis of data obtained during the experiment.



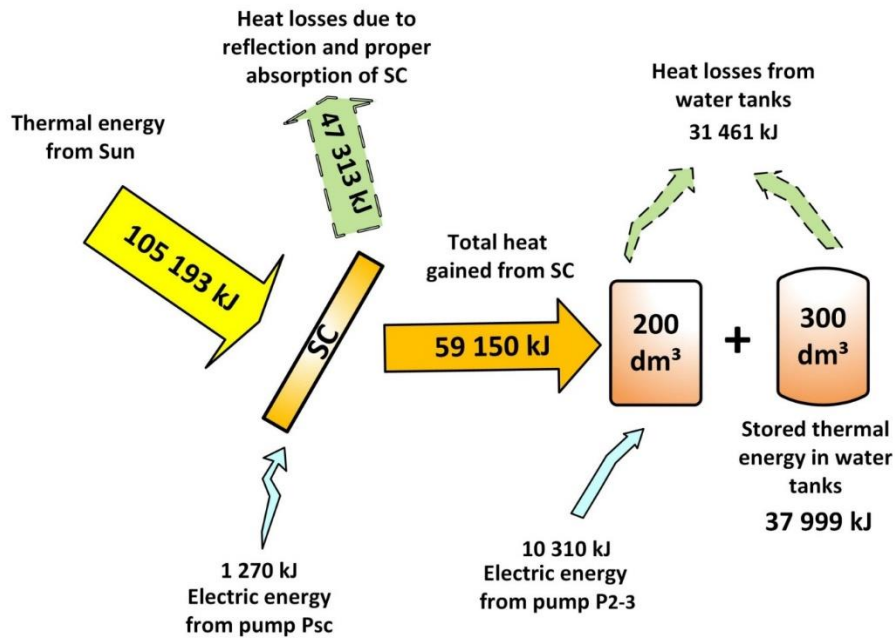


**Fig.4.15.** Energy diagram of CWT mode

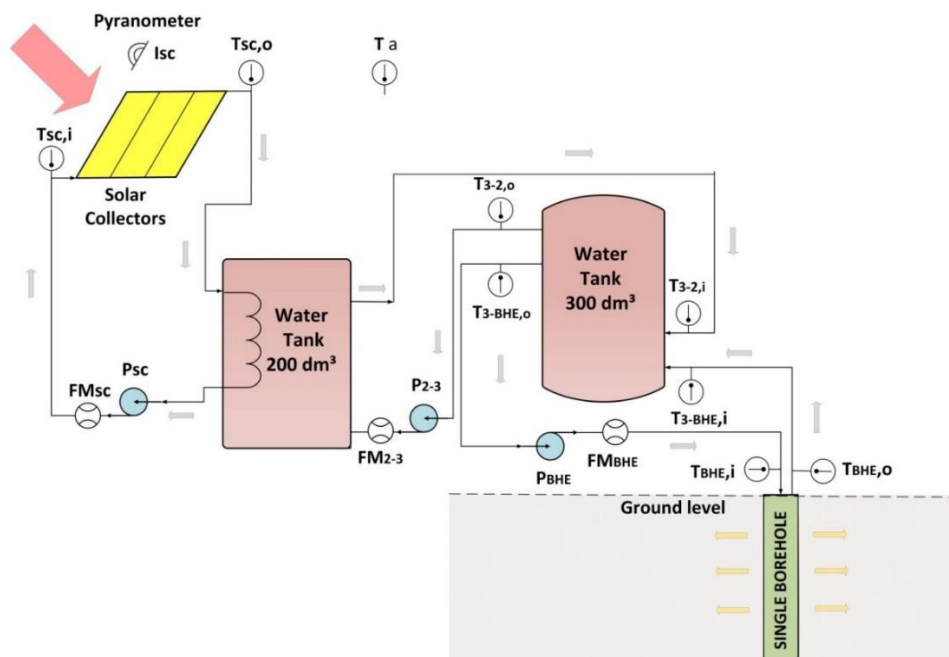


**Fig.4.16.** Working scheme of the mixed installation in CBTES mode

**4.5.3.3. Charging of BHE with thermal energy from solar collectors (CBTES mode)**

The simplified working scheme of the mode is presented in Fig.4.16.

An experiment was performed on the installation in CBTES mode (Fig.4.16). The energy flows between the system components in this mode are shown in Fig.4.17. All the presented values are calculated on the basis of data obtained during the experiment.

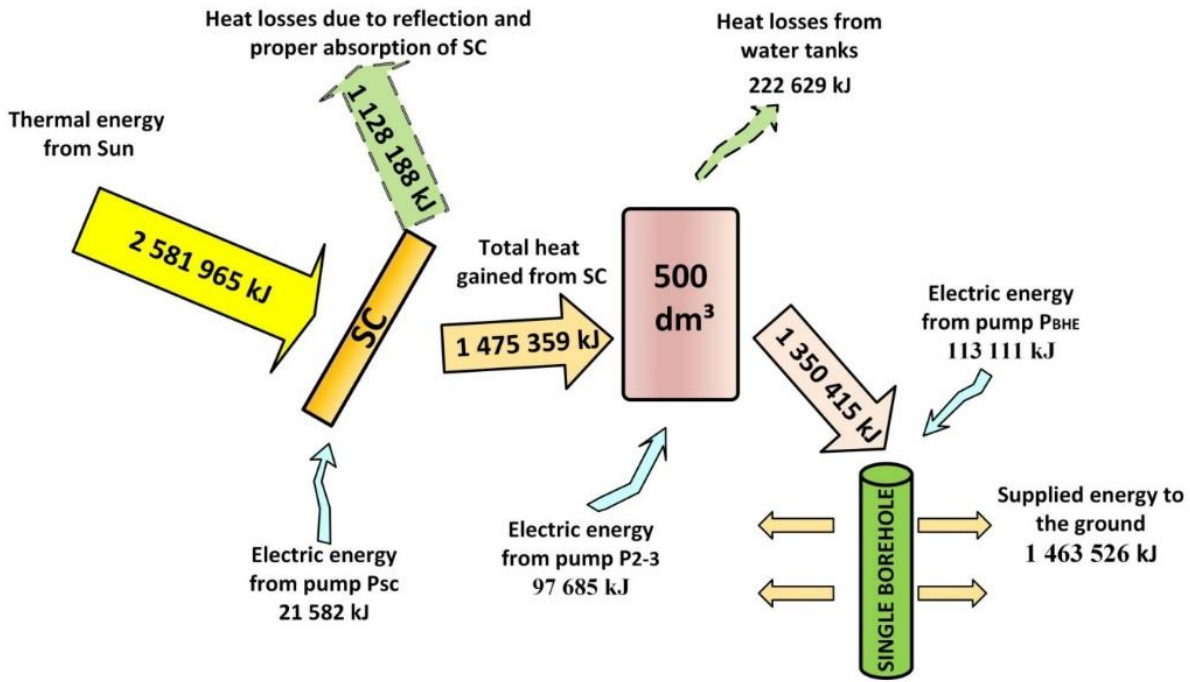


Fig.4.17. Energy diagram of CBTES mode

#### 4.5.3.4. Direct solar space heating (DSH mode)

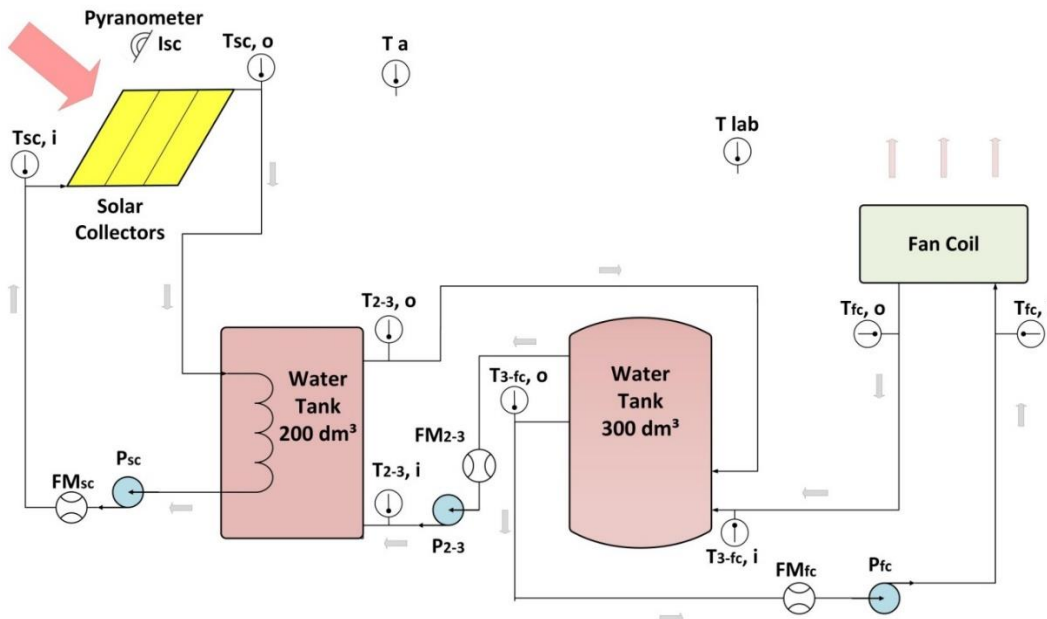
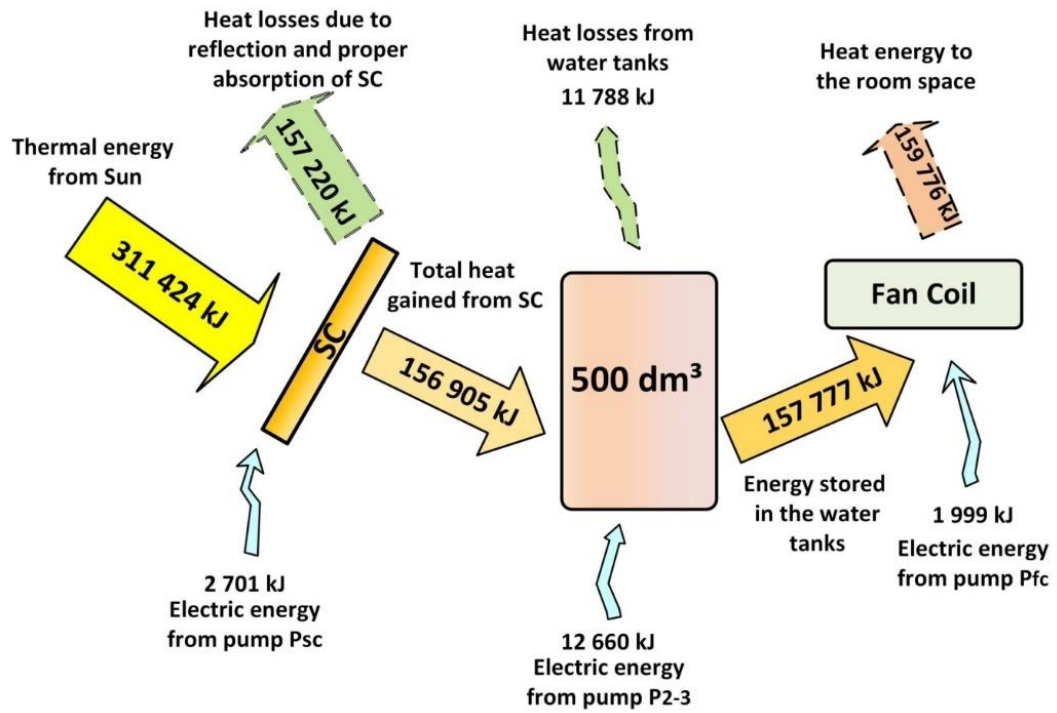


Fig.4.18. Working scheme of the mixed installation in DSH mode

The simplified working scheme of the mode is presented in Fig.4.18.

An experiment was performed on the installation in DSH mode (Fig.4.18). The energy flows between the system components in this mode are shown in Fig.4.19. All the presented values are calculated on the basis of data obtained during the experiment.



**Fig.4.19.** Energy diagram of DSH mode

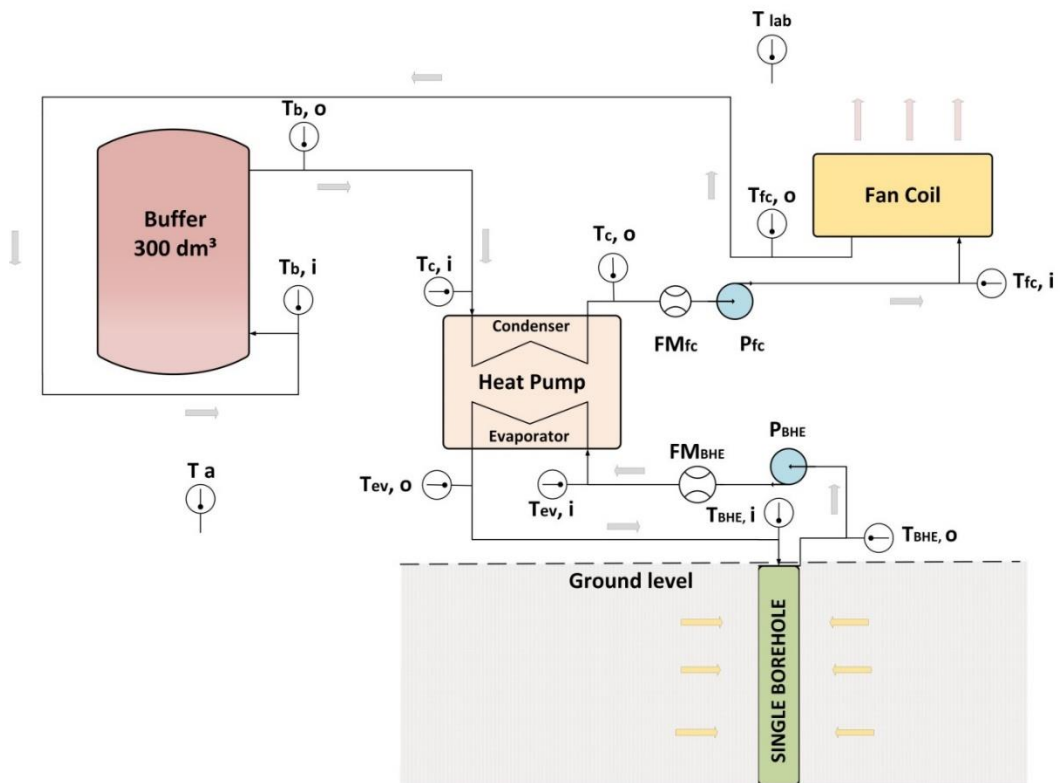


**Fig.4.20.** Working scheme of the mixed installation in GSHPH mode

**4.5.3.5. Ground source heat pump space heating (GSHPH mode)**

The simplified working scheme of the mode is presented in Fig.4.20.

An experiment was performed on the installation in GSHPH mode (Fig.4.20). The energy flows between the system components in this mode are shown in Fig.4.21. All the presented values are calculated on the basis of data obtained during the experiment.

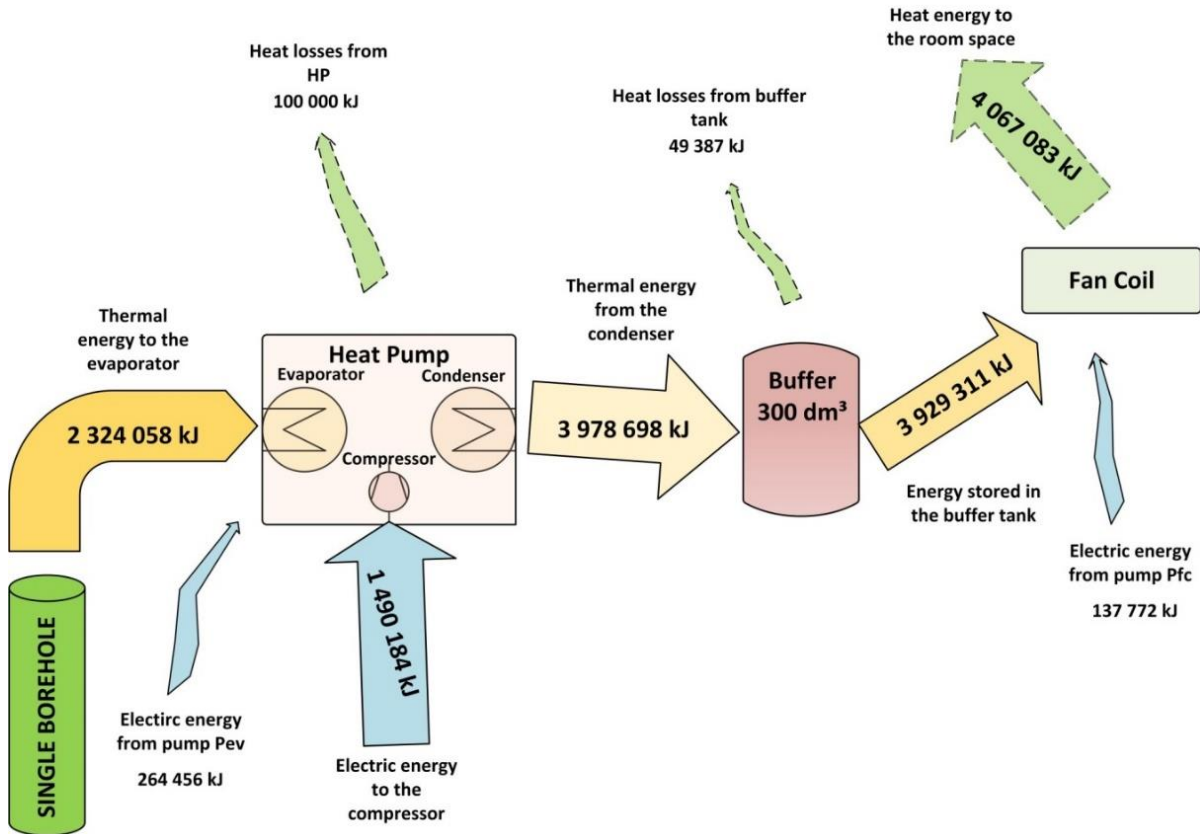


Fig.4.21. Energy diagram of GSHPH mode

#### 4.5.3.6. Solar assisted heat pump heating (SAHPH mode)

The simplified working scheme of the mode is presented in Fig.4.22.

An experiment was performed on the installation in SAHPH mode (Fig.4.22). The energy flows between the system components in this mode are shown in Fig.4.23. All the presented values are calculated on the basis of data obtained during the experiment.

#### 4.5.3.7. Error analysis

There are three types of errors, which can occur during an experiment: systematic, occasional and dynamic errors. There were no systematic errors during the tests because all the measuring instruments were calibrated recently before starting the measurements. Dynamic errors during the experiment were not present for the following reasons:

- the measuring equipment was used in the acceptable working condition limits of the instruments;
- the installation operated for more than an hour before starting the reading.

## Evaluation of mixed installations with alternative energy sources

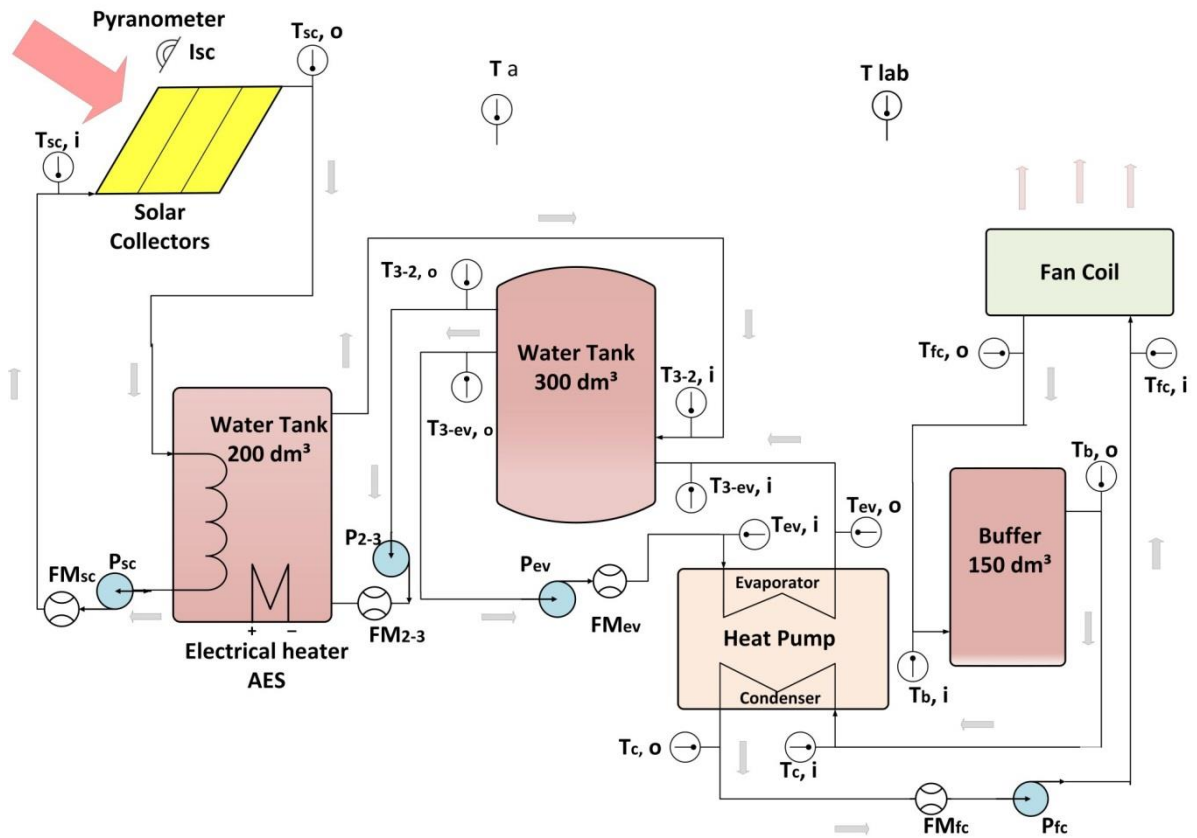


**Fig.4.22.** Working scheme of the mixed installation in SAHPH mode

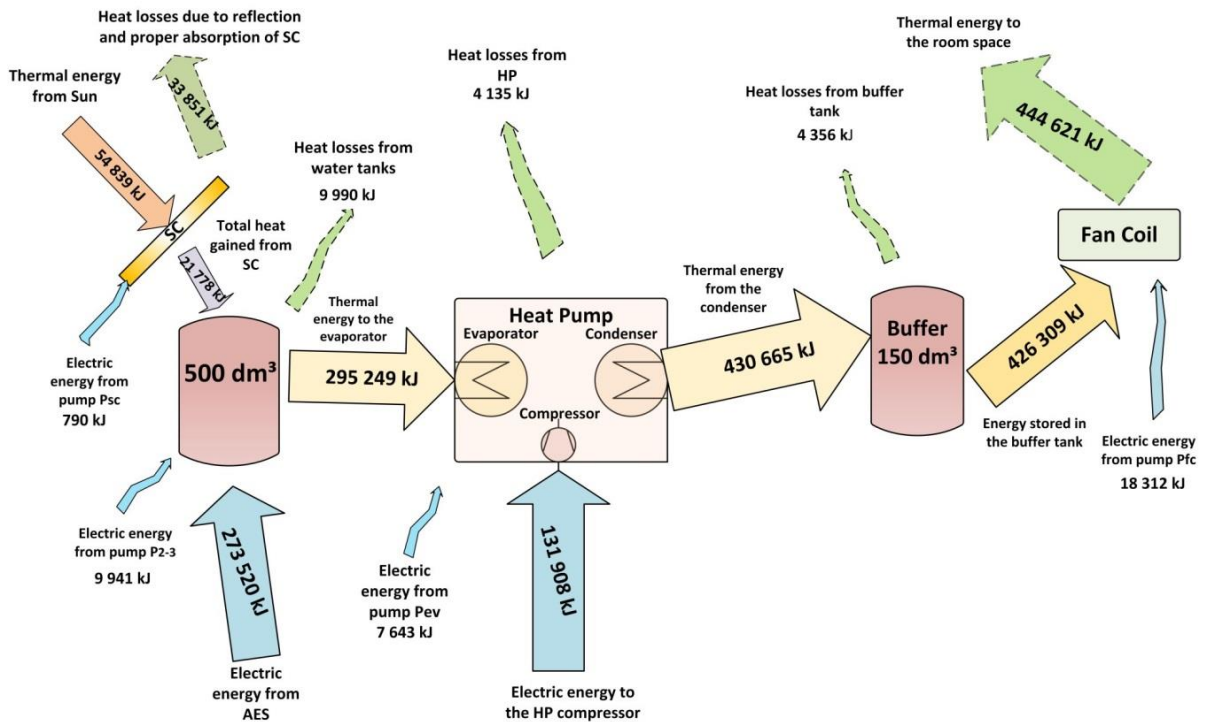


**Fig.4.23.** Energy diagram of SAHPH mode

The occasional errors were evaluated by means of regression analysis. Seven linear models were created for the solar collector efficiency  $\eta_{sc}$ , the coefficient of performance of the heat pump  $COP_{hp}$  and the five system efficiencies  $\eta_{s,1}$ ,  $\eta_{s,2}$ ,  $\eta_{s,3}$ ,  $\eta_{s,4}$ ,  $\eta_{s,5}$  as a function of several factors (global solar insolation intensity, some temperatures, fluid mass flow rate, and electrical powers). The relative errors of the measured parameters are less than the accuracy presented above in the Investigation methods.

The coefficient of multiple correlation  $R$  and the maximum absolute error were used as adequacy criteria of the model evaluations. The obtained values for the parameters of all the tests satisfy fully the requirements of the Investigation methods.

### **Conclusions to Chapters 4.5.1-4.5.3**

A mixed thermal system with ground source heat pump and solar collectors (SC) was studied experimentally in five working modes. The following conclusions can be drawn:

1) The measured values of the intensity of the solar radiation falling on the SC exceeded the normal values for Plovdiv in the summer period at about 25%. This is because of the large roof panel with a height of about 4m. Thus the roof plays the role of a nonimaging concentrator. It is recommended to use similar building roofs where the solar radiation in the plane of the collectors will be increased.

2) From the results obtained for the temperatures in the two water reservoirs (200 dm<sup>3</sup> and 300 dm<sup>3</sup>) it can be concluded that the temperatures are the same. There is no stratification observed and they can be considered as one water storage tank with a volume of 0,5 m<sup>3</sup>.

3) The ground temperature increased by 1 to 2 °C during the charging CBTES mode (experiment duration of about 1 month). The measurements show a decrease of the ground temperature by 1,25 to 1,85 °C during the GSHPH mode (similar experiment duration). This proves the necessity of BHE charging with thermal energy from the sun during the summer to avoid the ground thermal depletion.

4) The system energy efficiencies of the three heating modes have been calculated – 48,59% by the DSH mode, 96,46% by the GSHPH mode and 97,95% by the SAHPH mode. The results show bigger effectiveness of the HP modes. Otherwise the SAHPH mode is applicable for short term usage because of the high needs of thermal energy from the SC (which leads to big capital investments and a need of a huge area for installation). Thus there is an obvious advantage of the GSHPH mode compared with the other two heating regimes.



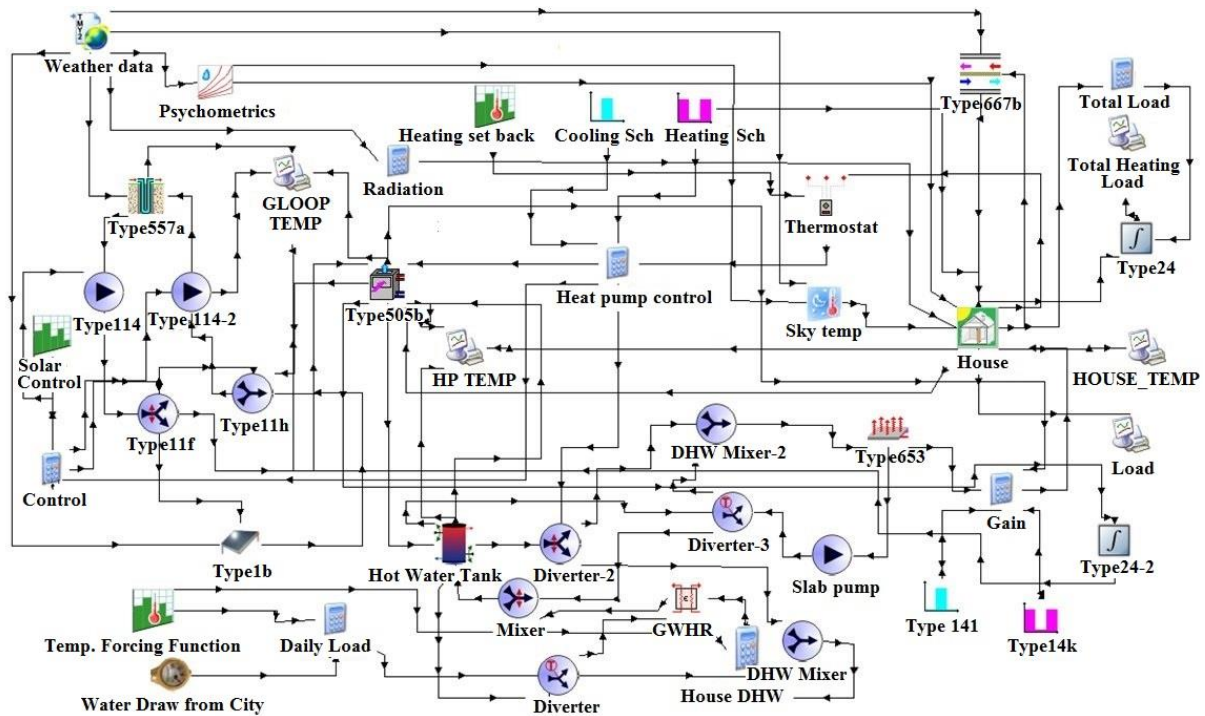


**Fig.4.24.** The structure of the model in TRNSYS Simulation Studio

#### **4.5.4. TRNSYS simulations of a house powered by GSHP with solar collectors**

##### **4.5.4.1. Modeling in “TRNSYS studio”**

A simulation model of a hybrid system for heating and cooling, consisting of solar collectors, borehole heat exchangers and a heat pump, has been created. The model of the system is built in the simulation environment of "TRNSYS studio" and allows to study different operation modes and to analyze the influence of system parameters on the performance characteristics.

TRNSYS commercial software was used to simulate the system. When studying the various systems, the following parameters had to be determined: heat extraction from the ground; the use of electricity; the lowest and average temperatures of the fluid supplied to the evaporator; electrical energy saving; the seasonal coefficient of efficiency (SCE) of the system and the coefficient of performance (COP) of the heat pump. Fig.4.24 shows the complete model of the mixed system compiled in "TRNSYS Studio".

##### **4.5.4.2. Simulation of the heat demands of a house powered by GSHP and solar collectors**

In this study, energy simulations are performed in the presence of fixed solar collectors and GSHP. The model of the house describes four zones: basement (volume of the area 201 m<sup>3</sup>), 1st floor (volume of the area 464 m<sup>3</sup>), 2nd floor (volume of the area 350 m<sup>3</sup>) and attic (volume of the area 240 m<sup>3</sup>). The main part of the heating power is spent on two zones: 1st floor and 2nd floor. The attic is not heated. The basement is heated, but at lower temperature settings of the thermostat.

The total heat consumption for the house is calculated by integrating the power in the different zones and then by additional summing. The approximate annual values are shown in Fig.4.25. An annual amount of 19,5 MJ is needed to heat the house. The annual consumption for cooling of the first, second floor and the basement has been calculated, and the reported values are 5,8 MJ, 3,6 MJ and 2,2 MJ, respectively.

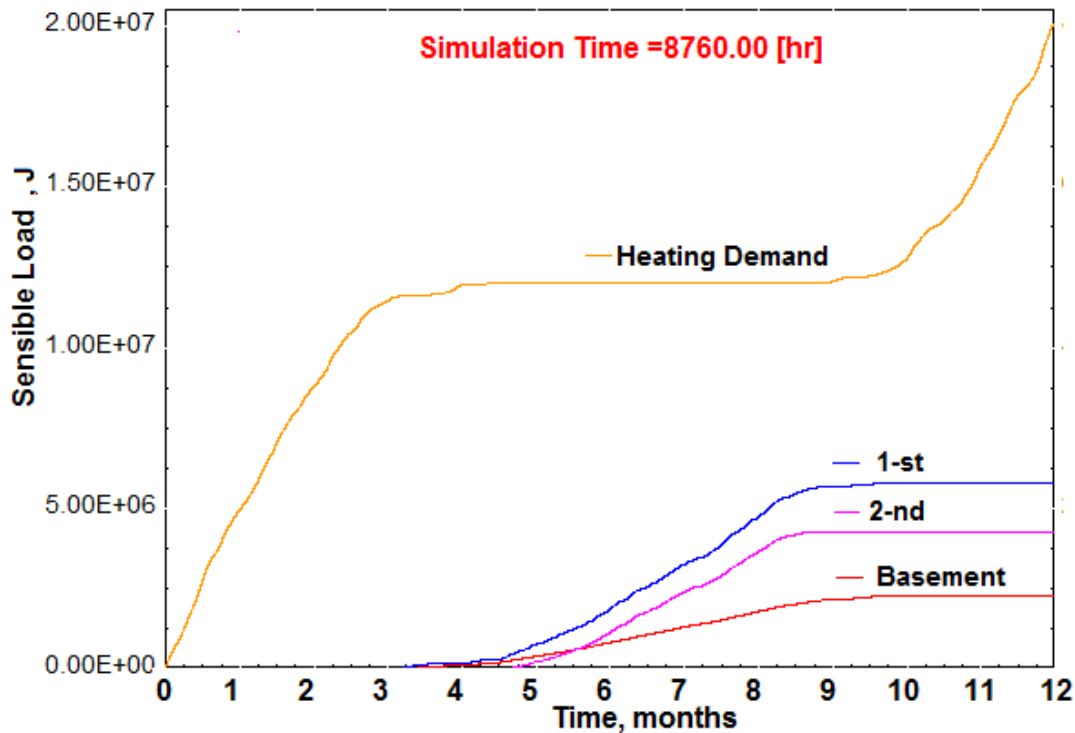


**Fig.4.25.** Simulated annual total heating and cooling demands

#### **Conclusions to Chapter 4.5.4**

A mixed ground source heat pump (GSHP) system with solar thermal collectors was constructed at the Technical University of Sofia, Plovdiv Branch. A simulation model of such systems has been developed in TRNSYS Simulation Studio. The following conclusions have been made:

1. The developed model could be a useful tool in hybrid heating and cooling system design process. Simple procedure needed to adopt model to any different system size and components parameters. The designer has only to change: the building plane and requirements; the type, size and parameters of the solar collectors, boreholes; heat pump; and the weather data.

2. A thermal response test (TRT) has to be previously performed for the purpose of validation of the borehole model parameters.

3. Additional experimental works in each design case are needed to validate model parameters.

4. System energy simulations carried out by the model allow the designer to optimize system components size and to reduce the costs.



#### **4.6. GROUND SOURCE HEAT PUMP (GSHP) INSTALLATION USING PHASE CHANGE MATERIALS (PCM)**

It is proposed to connect materials with change of phase change (PCM) and ground heat exchangers (GHE) in order to analyze the potential benefits for energy savings in the problem of non-stationary heat transfer of GSHP in space heating and cooling. Micro-encapsulated paraffin and water are taken as PCM, which are mixed directly with the filling material surrounding the GHE.

In the 2D area, it is assumed that a GHE with flat panel works in accordance with the hourly loads for heating and cooling of a simplified model of a building equipped with GSHP. The change in air temperature as a function of time is obtained according to the on/ off schedule of the heat pump to approach a realistic case.

##### **4.6.1. Model domain**

The model domain considers a cross section that includes a layer with PCM and a wide surrounding part of the soil. The PCM layer (as described above) is a mixture of microencapsulated paraffin, water and soil with certain mass ratios. A symmetrical approach was considered so that half of the area could be analyzed to reduce the finite element calculation. It is assumed that GHE is a flat panel with a high heat transfer coefficient. This is easy to reproduce in the 2D approach, which is why the flat panel is introduced as a boundary condition of the numerical area.

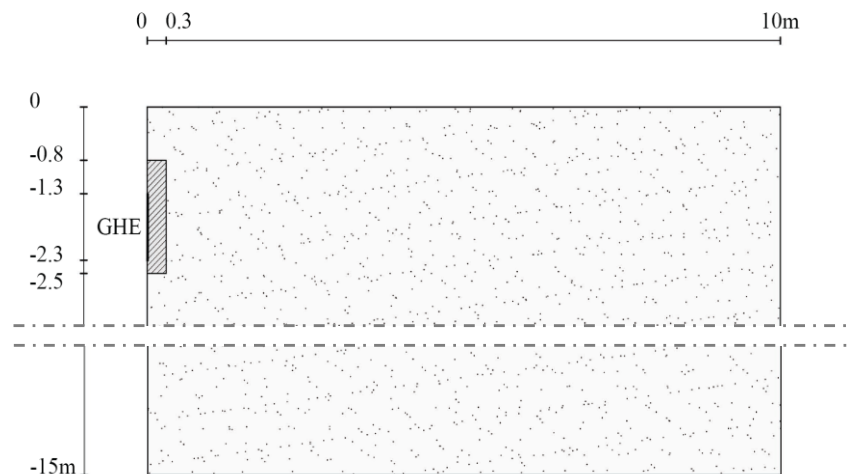


**Fig.4.26.** Sketch of the one-half symmetric model domain of a GHE

Fig.4.26 shows the dimensions of the considered area (half of the real one) - width 10 m and depth 15 m. GHE is 1 m high and is located at a depth of between 1,3 and 2,3 m. The PCM layer is placed between 0,8 and 2,5 m deep. It is assumed that its thickness is equal to 0,30 m, and the resulting volume of PCM layer for each meter per unit length of flat panel is 0,45 m<sup>3</sup>. The dimensions were chosen to be similar to those of the field experience being

tested in the Department of Architecture at the University of Ferrara, Italy, in order to compare modeling with experimental results.

#### 4.6.2. Simulations

In order to compare the impact of PCM on the temperature field of the soil and then on the temperature of the working fluid in the GHE, the cases with and without PCM were solved for a simulation period of two years. The second year was performed to check the seasonal periodic fluctuations and to assess the thermal deviation caused by the GHE. In fact, the heat flux fixed on the soil surface does not take into account the thermal impact of the GHE operation, as it is additionally (conversely) calculated with a model based on a fixed temperature on the surface. Therefore, it should be expected that the annual final temperature of the temperature field may be different from the initial one. However, if the same temperature difference occurs in the second year of simulation, it can be concluded that the model is in a steady trend.

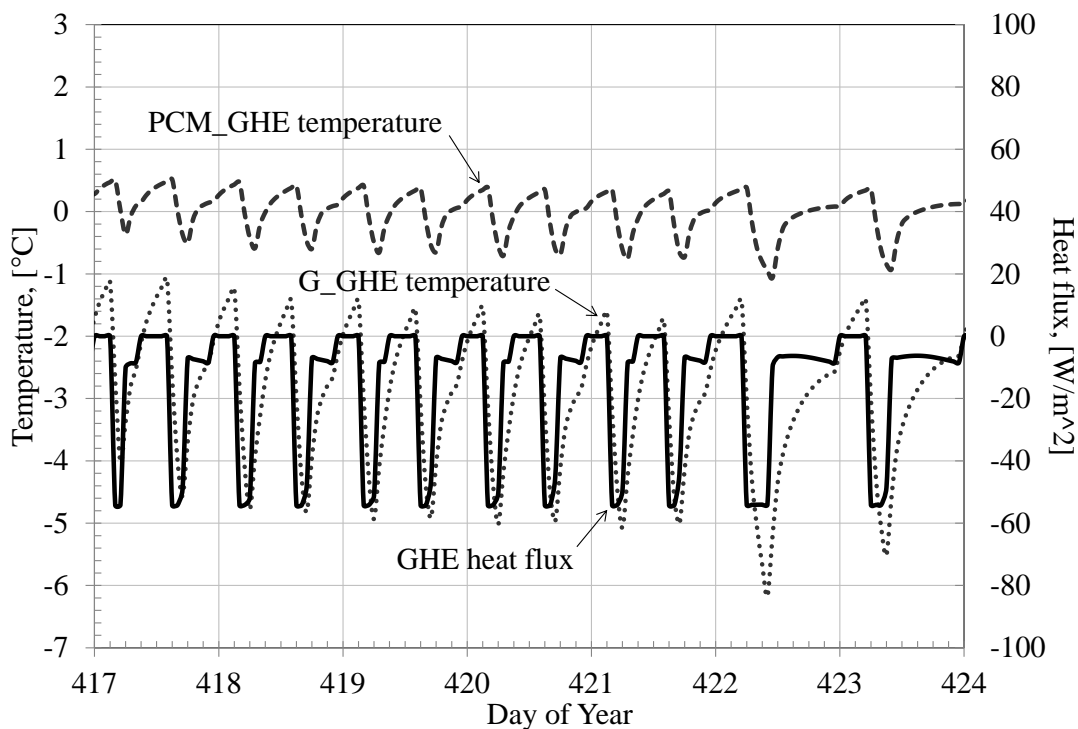


Fig.4.27. Simulated time series temperatures and heat flux for one week in wintertime

It has been verified that the soil temperature at a depth of 1,8 m and 10 m from the GHE changes by 0,3 °C both at the end of the first year and at the end of the second year (solely due to the operation of the GHE). With this approximation, the results of the simulation are discussed as shown below.

As shown in Fig.4.27, the results of the simulation for one week were chosen to show the daily changes in temperatures as a function of time on the wall of the GHE in both cases, as well as the corresponding heat flux. Here the different behaviors are described in detail as in winter, with evidence of the most

## *Evaluation of mixed installations with alternative energy sources*

difficult week in terms of temperature. The case of PCM shows average temperatures on the GHE wall with up to 5K higher than the case without GHE during the week (422 and 423 DOY). This corresponds to a very different operation of the heat pump and can allow the use of water as a working fluid without the addition of glycol.

### **Conclusions to Chapter 4.6**

As a result of the conducted research the following conclusions can be made:

- Compared to the case without PCM, the surface temperatures of GHE (combined with PCM) could be several degrees higher in winter or lower in summer. This means a potential increase in the coefficient of performance of the heat pump. In addition, there is the interesting effect of smoothing the temperature curve caused by the operation of the heat pump (reduction of sharp fluctuations in heating or cooling of the ground heat exchanger).

- The presented idea shows a new opportunity for horizontal shallow GHE. In contrast to the vertical and deep GHEs, it is considered inappropriate to attempt underground storage of thermal energy with shallow GHEs, as the soil around it is more strongly influenced by the environment during the different seasons.

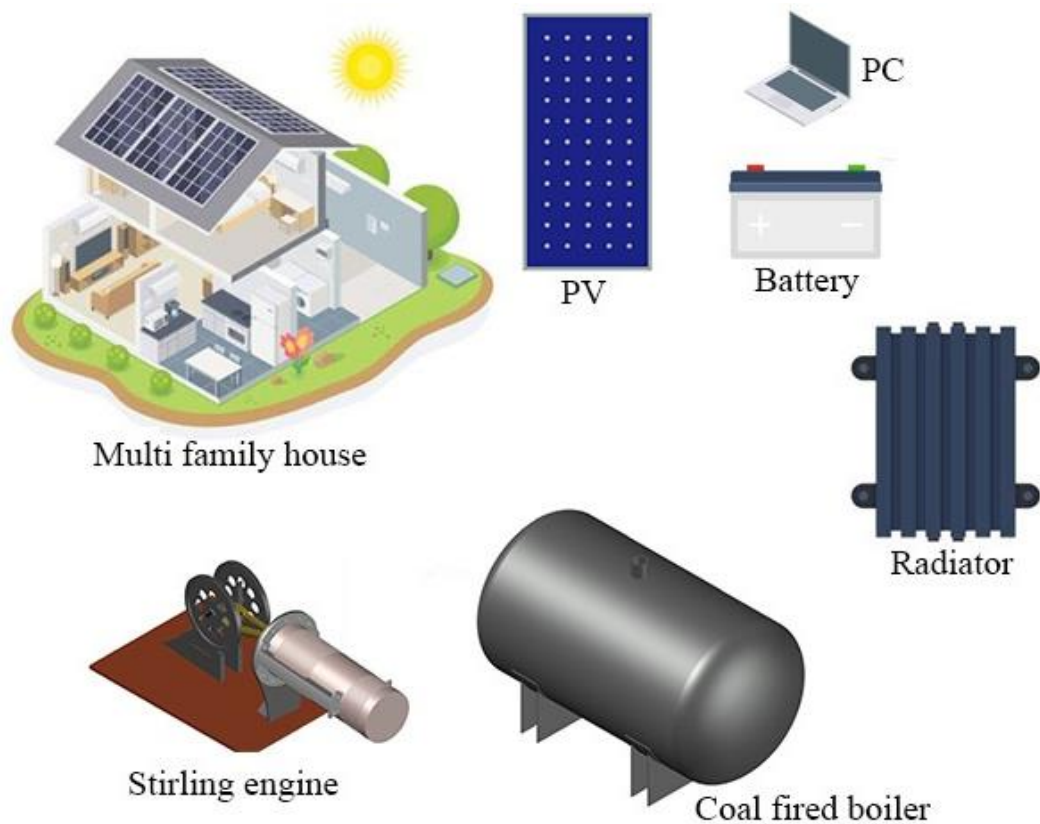


**Fig.4.28.** Schematic representation of PV assisted micro-CHP system

#### 4.7. MIXED MICRO-COGENERATION SYSTEM WITH PHOTOVOLTAIC PANELS AND STIRLING ENGINE FOR LOCAL HEATING

The micro-cogeneration system is a very suitable technology as a system for the production of heat and electricity, mainly for rural and remote areas. The simultaneous operation of a Stirling engine and photovoltaic (PV) panels for the production of electricity from a central heating system on solid fuel is considered. The thermodynamic characteristics of the mixed system were studied experimentally (Fig.4.28). It aims to fulfill its main purpose of a central heating system and at the same time to satisfy the electricity consumption of the boiler or to supply the home with electricity. The mechanical energy provided by the Stirling engine in the boiler is converted into electrical energy with an alternator and is prepared for use by accumulating in a battery along with the energy coming from the photovoltaic panels.

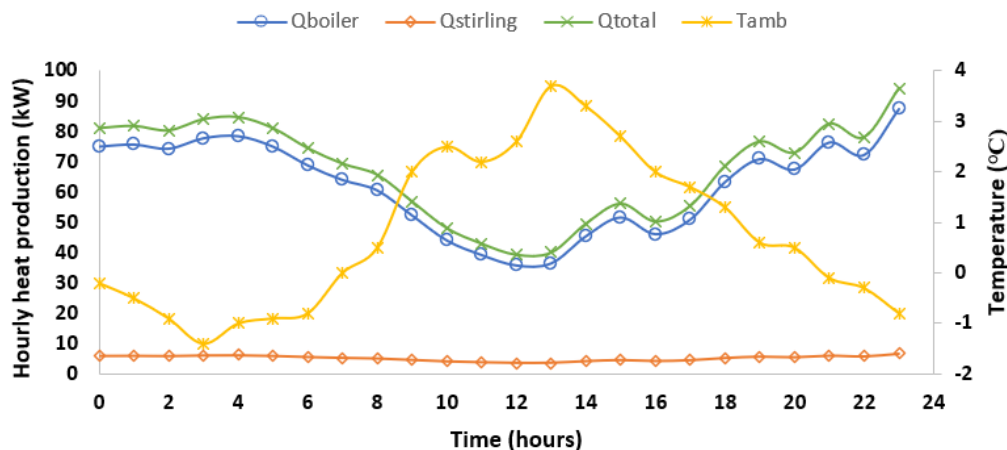


Fig.4.29. Change in heat production and ambient temperature as a function of time, h

Heat production from the coal boiler, Stirling engine, micro-cogeneration system and ambient air temperature as a function of time (in hours) are presented in Fig.4.29. The daily heat production from the coal boiler, Stirling engine and micro-cogeneration system is 1489,8, 124,2 and 1614 kW, respectively. When the ambient temperature rises, the difference in water temperature at the inlet and outlet of the heating system decreases.  $Q_{boiler}$  decreases due to the decrease in the temperature difference between the outlet water temperature of the building heating system  $T_2$  and the outlet water temperature from the boiler  $T_1$ . The daily production of electricity from the Stirling engine and PV panels is 3,6 kW and 0,36 kW, respectively.

#### Conclusions to Chapter 4.7

The following conclusions can be drawn from the research:

## *Evaluation of mixed installations with alternative energy sources*

- The total electricity production from the PV panel and the Stirling engine varies between 121,3 and 244,6 W;
- Heating of a building with cogeneration system is offered for rural and remote areas where there is no electricity. The generated electricity is stored in batteries to meet the electricity needs of the auxiliary system equipment;
- The micro-cogeneration system was combined with a PV module, aiming to increase its own electricity production for the needs of the installation.

### **5. GENERAL CONCLUSIONS**

The conclusions of the research are reflected in the appropriate places in Chapters 3 and 4. Here are discussed the general conclusions related to the evaluation of the various mixed installations with Alternative Energy Sources (AES).

In the dissertation some types of mixed installations with AES, as well as their components were considered. Here are the most important features of the presented mixed installations:

1. Vacuum solar collectors with heat pipe in combination with water thermal storage:

- The outlet fluid temperature from this installation can reach temperatures above 100 °C and thus be a source of heat for generators of absorption refrigeration machines, for example.

2. Refrigeration installation with built-in solar collectors and thermal storage:

- Implementation of a heat pump increases the efficiency of a solar installation that can work in winter;

- The system is suitable for use in food, pharmaceutical, biotechnology, etc. industries where both heating and cooling are needed.

3. Borehole thermal energy storage (BTES) with solar collectors:

- BTES is almost universal and independent of the environment;

- Charging BTES from solar collectors (or waste heat) leads to the use of the ground not only as a source of energy but also as a thermal accumulator.

4. Photovoltaic-thermal (PV/T) installations:

- Installation in places where the area is limited (this leads to a reduction in installation costs);

- Elementary conversion of PV into PV/T panel leads to the production of electricity and heat, as the production of electricity increases with the cooling;

- Concentrating PV (CPV) devices increase the incident solar radiation on the PV surface and reduce the photovoltaic material per receiver unit.

5. Ground source heat pump (GSHP) system with solar collectors:

- Ground source heat pump (GSHP) systems use the earth as a huge heat source, with the heat pump helping to transfer heat to a higher level;

- Through the GSHP, both heating and production of domestic hot water, and cooling can be achieved;

- TRNSYS and EED commercial software are useful tools in the design process.

6. Ground source heat pump (GSHP) installation using phase change materials (PCM):

- Mixing PCM directly with the soil in combination with GSHP leads to smoothing of the temperature curve caused by the operation of the heat pump.

7. Mixed micro-cogeneration system with photovoltaic panels and Stirling engine for local heating:

- Micro-cogeneration systems (providing heat and electricity at the same time) with photovoltaic panels and Stirling engine (producing electricity for own needs) for local heating are suitable for powering individual buildings located in rural or remote areas.

Two systems are emerging as the most promising technologies:

Systems using **PCM** because:

- Are suitable for application in both chemical and biochemical technologies;

- They are extremely convenient due to the wide variety of melting points.

**GSHP** systems because:

- The heat pump delivers energy to a higher level than the original - the efficiencies of heating with a solar assisted heat pump (SAHPH) and heating with GSHP (GSHPH) are much higher than that of direct solar heating (DSH);

- Earth is an endless source of heat when used as an accumulator;

- The comparison between the Solar Assisted Heat Pump (SAHP) and the GSHP leads to the conclusion of an obvious advantage of the GSHP given both its long-term use and the lack of large capital costs and the need for a huge area for installing solar collectors (available in the SAHP system).

The combination of these two systems is extremely attractive (already shown in item 6 above).

Here are the most important conclusions about mixed heating systems with AES:

1. The correct choice of components leads to a well-designed mixed heating system.

2. It is necessary to select new and more efficient materials in the elements of the system.

3. The creation and validation of mathematical models allow the simulation of various mixed systems and modes of operation, helping the more correct design.

4. The optimization of the regime of the already known mixed systems with regard to the different climatic conditions leads to the correct choice of the specific mixed system.

## **6. MAIN CONTRIBUTIONS**

The main contributions of the author in the dissertation are presented. They are divided into three sections - SCIENTIFIC, SCIENTIFIC-APPLIED or APPLIED.

### **6.1. SCIENTIFIC CONTRIBUTIONS**

1. A vacuum solar collector with a heat pipe was studied in detail (by experiment and mathematical modeling). Subsequently, the computer program was created, with which simulations were performed in different modes.

2. Experimental tests of a mixed water storage with stratification of the working fluid have been performed. With the selected mathematical model, a computer program was created, which facilitates its verification on the basis of the conducted experiments.

3. An industrial water storage with two separate coils has been studied experimentally and a mathematical model describing its operation has been selected. The verification of the model is done with the help of the created computer program.

4. Three different installations have been built (one stationary in Chile, one mobile with an electric heater in Bulgaria and one with a heat pump in Spain) to conduct the new effective Thermal response test (TRT). Borehole heat exchangers (BHE) have been built in Valparaiso, Chile and Plovdiv, Bulgaria, where TRTs have been carried out to determine the thermal properties of the soil. The obtained results are processed by various mathematical methods. Simulations were made with the commercial software TRNSYS, comparing the calculated values with the experimental data. It is planned to create a cadaster in Bulgaria to be used in future geothermal projects.

5. Latent storage using phase change materials (PCM) is designed and built in TU Sofia, Plovdiv branch, which is equipped with a specialized autonomous measuring system developed by the research team in Plovdiv. Several types of paraffin were studied, whose thermal properties were studied in detail. Mathematical modeling and simulation of storage processes was performed in two different ways - by the finite element method based on Comsol multiphysics and by the enthalpy porosity technique used in ANSYS Fluent.

### **6.2. SCIENTIFIC AND APPLIED CONTRIBUTIONS**

1. A mixed installation containing vacuum solar collectors with a heat pipe and a water thermal storage with a four turn pipe windings has been tested experimentally. The created general mathematical model, describing the joint work of the two elements, has been programmed and verified on the basis of conducted experiments.

2. The Chilean installation constructed for implementation of TRT has been redesigned to conduct natural experiments on solar energy charging and

discharging of underground storages. Long-term experiments were performed under the two mentioned regimes. A comparison was made between the calculated values with the commercial product TRNSYS and the measured values during the charging and discharging process, and the results showed a good match.

3. A solar thermal system combined with photovoltaic panels has been designed and manufactured. A new set of virtual tools has been developed and proven, providing on-line or off-line calculation of the error when performing experiments. The experiments performed characterized the energy efficiency of the cheap construction of PV/T panel and helped to verify the proper operation of the developed virtual tools.

4. The ground source heat pump (GSHP) system was experimentally tested in the following five operating modes of the system: charging of water tanks (CWT), Charging of borehole thermal energy storage (CBTES), direct solar heating (DSH), heating with GSHP (GSHPH) and heating by solar assisted heat pump (SAHPH). A detailed energy analysis was performed for the mentioned regimes, taking into account all energy sources and calculating the respective losses and system coefficients of energy efficiency for each regime.

5. During the construction of the BHE of the GSHP system, temperature sensors were installed every 10 m in depth to monitor the change of the temperature field. Diagrams were obtained confirming the heating (when charging - CBTES mode) and cooling (when heating – GSHPH mode) of the soil layer over time. The temperature field was also measured after the end of the two modes in the so-called natural relaxation.

6. A model was created, built in the simulation environment of "TRNSYS studio", which allows to study different modes of operation of the GSHP system and to analyze the impact of system parameters on the performance characteristics. Attention was paid to the following elements of the system: solar collector, water storage, heat pump, ventilation and house. With the model thus created, a simulation of a house heated by this installation was made.

7. Numerical modeling is presented, evaluating a new type of construction for the application of PCM in underground horizontal heat exchangers (GHE), integrated with ground source heat pumps (GSHP). PCM is mixed directly with the soil around the GHE - this is a new approach, not yet studied for horizontal ground heat exchangers. The results show that the merging of PCM with GHE effectively meets the heat loads of GSHP and reduces the sharp fluctuations in heating or cooling of the ground heat exchanger. The conducted simulations are for cases with and without PCM, solved for a simulation period of two years.

### **6.3. APPLIED CONTRIBUTIONS**

1. It is proposed to increase the efficiency of a solar installation, which will work in the winter, by implementing a heat pump unit. A methodology for



calculating the parameters of the system has been created, with which sample calculations have subsequently been performed.

2. An existing photovoltaic (PV) panel has been converted into a photovoltaic-thermal (PV/T) panel. Comparative experiments of the mixed installation (consisting of two different panels) were performed, proving the advantage of the combined PV/T element, producing both more electricity and additional heat energy during cooling.

3. A concentrating photovoltaic-thermal (CPV/T) system has been created, which is connected to the heat pump evaporator (HP) - the PV modules are cooled by the refrigerant passing through the HP evaporator. The installation is designed for heating of buildings. A theoretical and experimental study was conducted, showing the efficient production of electricity and heat with the described system.

4. A new construction of a mixed ground source heat pump (PSP) system has been created, consisting of two borehole heat exchangers, three flat-plate solar collectors (SC), a reversible heat pump (HP) and a fan coil. A methodology for determining the thermal characteristics in the following five modes of operation has been developed: CWT, CBTES, DSH, GSHPH and SAHPH.

5. The simultaneous and experimental operation of a Stirling engine and photovoltaic (PV) panels for the production of electricity from a central heating system on solid fuel, aimed at both heating buildings and satisfying the boiler's electricity consumption or supplying the home with electricity, has been studied theoretically and experimentally. The heating capacity of a multi-family house in Mugla, Turkey was provided with a micro-cogeneration system, and the experiment was carried out within three months.

## **7. AUTHOR'S PUBLICATIONS IN FULL TEXT ON THE DISSERTATION**

- [1] Георгиев, А., М. Джауад. Пресмятане температурното поле на флуида в смесителен акумулатор със стратификация. Изв. на ВМЕИ – София, 43, 1989, № 3, с. 47 – 52.
- [2] Картелов, Г., А. Георгиев. Повишаване ефективността на хладилна инсталация чрез вграждане на системата слънчеви колектори – топлоакумулатор. Теор. и прил. механика: Докл. VI нац. конгр. по теор. и прил. механика, Варна 1990: Кн.3. 3 секция, Хидродинамика, топло- и масообмен, стр. 117-120.
- [3] Георгиев, А., С. Бързилова, Я. Картелов. Конструкция на мобилна инсталация за измерване топлинни свойства на земята. Топлотехника за бита, № 5/6, 2007, стр. 26 – 30.

- [4] Georgiev, A. Mathematisches Modell eines Vakuumsolarkollektors mit Wärmerohr und Flachabsorber. BWK. Brennstoff, Wärme, Kraft, 1993, N° 12, p. 527-534 (**IF: 0,62**).
- [5] Georgiev, A. Mathematische Modellierung eines Warmwasserspeichers mit vierfachen Rohrwendeln. Elektrowärme international. Part A, ETA, 1995, N° 3, p.132-134 (**int. journal**).
- [6] Georgiev, A. Bestimmung der Hilfsparameter des mathematischen Modells eines Warmwasserspeichers mit vierfachen Rohrwendeln. J. of the Technical Univ. at Plovdiv, 4, 1996, p. 263-271.
- [7] Georgiev, A. Experimentelle Untersuchung eines Vakuumsolarkollektors mit Wärmerohren und Flachabsorber. J. of the Technical Univ. at Plovdiv, 4, 1996, p. 273-278.
- [8] Georgiev, A. Versuchsaufbau und Untersuchung einer Anlage von Vakuumsolarkollektoren mit Wärmerohren und Warmwasserspeicher. J. of the Technical Univ. at Plovdiv, 5B, 1997, p. 40-49.
- [9] Georgiev, A. Mathematical modelling of a System Vacuum Solar Collectors – Warm Water Storage. J. of the Technical Univ. at Plovdiv, 5B, 1997, pp.71-80.
- [10] Ortiz, A., Georgiev, A., Roth, P. (2002). Ground Thermal Properties Study for BTES Applications - World and Chilean Review. Proceedings of Int. Solar Energy Congress "Sun at the End of the World", Chile, Valparaíso, 28 - 31 October, 2002 (**int. congress**).
- [11] Busso, A., A. Georgiev, P. Roth. Underground Thermal Energy Storage - First Thermal Response Test in South America. Proc. of the Int. Congress "RIO 3 - World Climate and Energy Event", 1 - 5 December 2003, Rio de Janeiro, Brazil, p. 189 – 196 (**int. congress**).
- [12] Roth, P., A. Georgiev, A. Busso, E. Barraza. First In-situ Determination of Ground and Borehole Thermal Properties in Latin America. Renewable Energy, 2004, V. 29 (12) p. 1947-1963 (**IF: 0,607**).
- [13] Busso, A., A. Georgiev, P. Roth. Operating Experience with Vertical Borehole Heat Exchanger for Underground Thermal Energy Storage Applications in Chile and Argentina. Proc. of the World Geothermal Congress 2005, 24-29 April 2005, Antalya,Turkey, 1446.pdf (**int. congress**).
- [14] Georgiev, A. Simulation and experimental results of a vacuum solar collector system with storage. Energy Conversion and Management, 2005, V. 46 (9-10) p. 1423-1442 (**IF: 1,244**).
- [15] Georgiev, A., A. Busso, P. Roth. Shallow Borehole Heat Exchanger: Response test and Charging - Discharging test with solar collectors. Renewable Energy, 2006, V. 31 (7) p. 971-985 (**IF: 0,85**).

- [16] Georgiev, A., R. Popov, S. Stavrev. Borehole for Implementing of Thermal Response Test in the Technical University Sofia, branch Plovdiv. Proc. of the 4th Int. Scientific Conference “Energy Efficiency and Agricultural Engineering”, 1-3 October, 2009, Rouse, Bulgaria, p. 525 – 530 (**int. conference**).
- [17] Urchueguia, J.F., P. Atanasov, A. Georgiev. A Mobile Thermal Response Test Facility for Heat Injection and Extraction at the Polytechnic University of Valencia. J. of Fundamental Sciences and Applications, Vol. 15, 2009, Proc. of the Int. Scientific Conf. „Advanced Manufacturing Technologies”, AMTECH’09, pp. 297-303 (**int. conference**).
- [18] Georgiev, A., R. Popov, I. Valkov, N. Kaloferov. Utilization of the thermal energy potential in photo voltaic solar panels. Proceedings of the World Renewable Energy Congress-XI, 2010, Abu Dhabi, United Arab Emirates, 25-30 September 2010, 199.pdf (**int. congress**).
- [19] Toshkov, E., A. Georgiev, R. Popov. Measuring system of a hybrid installation with ground source heat pump and solar collectors. J. of the Technical Univ. Sofia, branch Plovdiv, “Fundamental Sciences and Applications”, Vol. 20, 2014, pp. 33-38.
- [20] Bottarelli, M., M. Bortoloni, Y. Su, C. Yousif, A. A. Aydin, A. Georgiev. Numerical Analysis of a Novel Ground Heat Exchanger Coupled with Phase Change Materials. Applied Thermal Engineering, Vol. 88, 2015, pp. 369-375, <https://doi.org/10.1016/j.applthermaleng.2014.10.016> (**IF: 3,043**).
- [21] Toshkov, E., A. Georgiev, R. Popov, N. Vassileva. Investigation methods of hybrid Ground Source Heat Pump system with solar collectors. Proc. of the Union of scientists, Ruse. 6th Int. Conference “Energy Efficiency and Agricultural Engineering”, Ruse, Bulgaria, November 11-12, 2015, ISSN 1311-9974, p. 55 – 62 (**int. conference**).
- [22] Georgiev, A. Installation of Ground Source Heat Pump systems in Bulgaria - yes or no? Proc. of the 15th Int. Scientific Conf. “Renewable energy & Innovative technologies”, 10 - 11 June, Smolyan, 2016, Bulgaria, Vol. 1, pp. 21-26 (**int. conference**).
- [23] Georgiev, A. Preconditions for cadastre preparation using ground thermal properties. Proc. of the 15th Int. Scientific Conf. “Renewable energy & Innovative technologies”, 10 - 11 June, Smolyan, 2016, Bulgaria, Vol. 1, pp. 27-32 (**int. conference**).
- [24] Amanzholov, Tannur, Bakytzhan Akhmetov, Aleksandar Georgiev, Aidarkhan Kaltayev, Rumen Popov, Daniela Dzhonova-Atanasova, Rustem Manatbayev, Madina Tungatarova. Installation for thermal response test implementation. Proc. of the 15th Int. Scientific Conf. “Renewable energy

- & Innovative technologies”, 10 - 11 June, Smolyan, 2016, Bulgaria, Vol. 1, pp. 164-168 (**int. conference**).
- [25] Georgiev, A.G. Long term experience and research on hybrid thermal systems. Bulgarian Chemical Communications, Vol. 48, Special Issue E, 2016, pp. 7-18 (**IF: 0,238**).
- [26] Georgiev, A.G., R. K. Popov, E. T. Toshkov, In-situ measurements of ground thermal properties around borehole heat exchangers in Plovdiv, Bulgaria. Bulgarian Chemical Communications, Vol. 48, Special Issue E, 2016, pp. 19-26 (**IF: 0,238**).
- [27] Akhmetov, B., A. G. Georgiev, A. Kaltayev A. A. Dzhomartov, R. Popov M. S. Tungatarova, Thermal energy storage systems – review. Bulgarian Chemical Communications, Vol. 48, Special Issue E, 2016, pp. 31-40 (**IF: 0,238**).
- [28] Vassileva, N. D., A. G. Georgiev, R. K. Popov, Simulation study of hybrid ground-source heat pump system with solar collectors. Bulgarian Chemical Communications, Vol. 48, Special Issue E, 2016, pp. 71-76 (**IF: 0,238**).
- [29] Lishev, S. N., R. K. Popov, A. G. Georgiev, Specialized measuring system for analysing thermal fields in hybrid systems. Bulgarian Chemical Communications, Vol. 48, Special Issue E, 2016, pp. 96-101 (**IF: 0,238**).
- [30] Amanzholov, T., B. Akhmetov, A. G. Georgiev, A. Kaltayev, R. K. Popov, D. B. Dzhonova-Atanasova, M. S. Tungatarova, Numerical modelling as a supplementary tool for Thermal Response Test. Bulgarian Chemical Communications, Vol. 48, Special Issue E, 2016, pp. 109-114 (**IF: 0,238**).
- [31] Seitov, A., B. Akhmetov, A. G. Georgiev, A. Kaltayev, R. K. Popov, D. B. Dzhonova-Atanasova, M. S. Tungatarova. Numerical simulation of thermal energy storage based on phase change materials. Bulgarian Chemical Communications, Vol. 48, Special Issue E, 2016, pp. 181-188 (**IF: 0,238**).
- [32] Dzhonova-Atansova, D. B., A. G. Georgiev, R. K. Popov, Numerical study of heat transfer in macro-encapsulated phase change material for thermal energy storage. Bulgarian Chemical Communications, Vol. 48, Special Issue E, 2016, pp. 189-194 (**IF: 0,238**).
- [33] Georgiev, A., Rumén Popov, Emil Toshkov. Investigation of a hybrid system with ground source heat pump and solar collectors: Charging of thermal storages and space heating. Renewable Energy, March 2020, V. 147, Part 2, pp. 2774-2790, <https://doi.org/10.1016/j.renene.2018.12.087> (**IF: 6,274**).
- [34] Popov, R., Nikolay Paunkov, Vania Rangelova, Aleksandar Georgiev. Study of hybrid thermal system with photovoltaic panels using virtual instruments. Renewable Energy, Vol. 154, July 2020, Pages 1053-1064, <https://doi.org/10.1016/j.renene.2020.03.024> (**IF: 6,274**).

*Evaluation of mixed installations with alternative energy sources*

- [35] Kiloglu, B., G. Karaca Dolgun, O. V. Güler, A. Keçebas, Aleksandar Georgiev. Thermodynamic performance of a heat pump based concentrating parabolic trough photovoltaic thermal system for a micro CHP. Proc. of “Alternative Energy Sources, Materials & Technologies, AESMT’21”, Vol. 3, 2021, 14 - 15 June, 2021, Ruse, Bulgaria, ISSN 2603-364X, pp. 11-12.
- [36] Incili, V., G. Karaca Dolgun, A. G. Georgiev, A. Keçebas, N. S. Çetin. Performance evaluation of a hybrid micro-CHP integrated PV-Stirling engine for local heating system. Proc. of “Alternative Energy Sources, Materials & Technologies, AESMT’21”, Vol. 3, 2021, 14 - 15 June, 2021, Ruse, Bulgaria, ISSN 2603-364X, pp. 27-28.